SOLID STATE PHYSICS II
(DPHY24)
(MSC PHYSICS)

ACHARYA NAGARJUNA UNIVERSITY

CENTRE FOR DISTANCE EDUCATION

NAGARJUNA NAGAR,

GUNTUR

ANDHRA PRADESH

DIELECTRIC PROPERTIES OF INSULATORS

Objective of the lesson

To introduce the basic definitions in the theory of dielectrics like dipole, dipole moment, polarization, polarizability and sources of polarization etc. To give the classification of polarisations and to discuss the theory of orientation polarisation

Structure of the lesson

1.1.1. Introduction

1.1.2. Sources of Polarizability:

1.1.1. Introduction

Dielectrics are insulators i.e., non-conductors of electricity.   The function of any insulator is to prevent the flow of electricity through it when a potential difference is applied across its ends.   These materials prevent the leakage of electrical charges in electrical devices. Substances like bakelite, PVC used in electrical wiring and pipes, polymer materials etc., come under this category. Dielectrics possess high resistivity values in the range 10^6 Ω-m to 10^{16} Ω-m. Under high voltage bias, they allow very little current (10^{-6} A to 10^{-14} A). They withstand very high voltages. The conduction phenomenon in dielectrics is mostly associated with ionic motion through defects or hopping of charges. They have no free charges. They consist of positively and negatively charged particles bound together. The fundamental action of the electrical field is to separate positive and negative charges of the entire volume of the dielectric, causing what is known as the polarization of the dielectric. Fig.1.1.1 shows the effect of polarization in a dielectric when external field E_0 is applied on a dielectric. We see that the net polarization charges produced at the faces of the dielectric, a positive charge on the right and a negative on the left; inside the medium there is no excess charge in any given volume element. The medium as a whole remains neutral, and the positive charge on the right is equal in magnitude to the negative charge on the left. These induced charges create their own electric field E_p called polarization field that is directed to the left, and thus oppose the external field E_0. When we add this polarization field E_p to the external
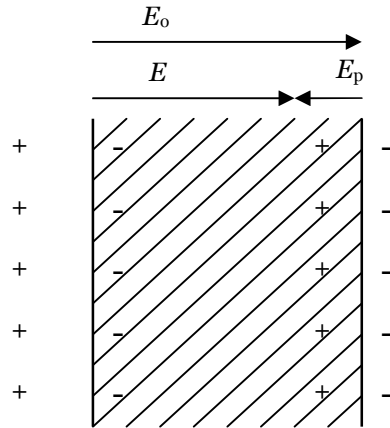
Fig.1.1.1 Effect of polarization in a dielectric.

field E_0, so as to obtain the effective field E, we find that $E < E_0$. Therefore, effect of introducing insulating substance (i.e., dielectric) results in reduction in applied field or reduction in surface charge density. Thus, the polarization of the medium reduces the electric field in its interior. During the polarization the charges in the dielectric are displaced from their equilibrium positions by distances that are considerably less than atomic diameter. There is no transfer of charge over macroscopic distances such as occur when a current is set up in a conductor.

Dielectrics: Dielectrics are the insulating materials having electric dipoles permanently or temporarily by inducement during the application of electric field.

Electric Field Strength or Intensity (E): The space around the charged body, up to where its influence felt is called Electric Field. Suppose an additional infinitesimal test charge q_0 is brought into the electric field and at a certain point in it, it experiences an electrostatic force **F**. The electric field strength or intensity **E** at the point is a vector and defined by

$$\mathbf{E} = \frac{F}{q_0} \qquad \text{volt/metre} \tag{1.1.1}$$

Electric Field Induction (or) Flux density (or) Displacement Vector (D): Consider a charge q at the centre of a sphere of radius r. The charge q will send q lines of force and this will be received by surface area $4\pi\, r^2$. The number of electric lines of force received by a unit area is called flux density or electric displacement **D**.

i.e., $D = \dfrac{q}{4\pi r^2} = \dfrac{q}{A}$; where A is the surface area of the sphere,

The unit of electric flux density is coulomb/metre^2.

Electric dipoles: The system of two equal and opposite charges separated by certain distance is called electric dipole.

-q   - - - - - -p ⟶   +q
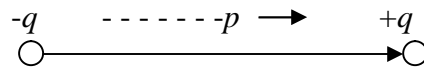
Fig.1.2.1 An electric dipole

Electric Dipole moment: The product of any one of two charges of dipole and the separation between them is called electric dipole moment.

Let the two charges are +q and –q separated by a distance r. The moment of this dipole is defined as

$$p = qr \tag{1.1.2}$$

The dipole moment is therefore equal to the magnitude of the one of the charges times the distance between them. The unit of electric dipole moment is esu-cm   (10^{-18} esu-cm = 3.3 x 10^{-30} C-m = 1 debye)

Polarization (P): The process of producing electric dipoles out of neutral atoms and molecules is known as polarization. Polarization **P** in a solid is defined as the total dipole moment per unit volume:

$$P = \sum_n p_i \;\; = \;\; \dfrac{\sum_n q_i r_i}{V} \tag{1.1.3}$$

Here P is the total dipole moment (including the induced and permanent) and n is the number of dipoles per unit volume. Polarization P has the same units as the surface charge density (C-m^{-2}). This equivalence is substantiated by the fact that electric field induces charges on the surface of the dielectric and the density of charges is a measure of the extent of polarization.

Dielectric Constant: Dielectric constant or relative permittivity is defined as the ratio of permittivity of the substance to the permittivity of the free space,

Consider a parallel plate capacitor consisting of two plane parallel plates of area A and separation d, charged with a surface charge density σ. If the space between the plates is vacuum and if d is small compared with the dimensions of the plates, there will result an electric field between the plates, whose strength is given by

$$E_{vac} = 4\pi\sigma$$

in esu. The potential difference between the plates is equal to

$$V_{vac} = E_{vac}\, d$$

and the capacitance of the capacitor is defined by

$$C_{vac} = \frac{A\sigma}{V_{vac}}.$$

Suppose now that the space between the plates is filled with an insulating substance the charge on the plates being kept constant. The new potential difference V is lower than V_{vac} and the capacitance is increased.

The **static dielectric constant** ε is then defined by

$$\varepsilon = \frac{V_{vac}}{V} = \frac{C}{C_{vac}}$$

Thus, the field strength is reduced from the value E_{vac} to the value E, where

$$\frac{E_{vac}}{E} = \varepsilon$$

or $E_{vac} = D = \varepsilon E$ (1.1.4)

or, in other words, the effective surface charge density on the plates is now changed from $\sigma = $

$\dfrac{E_{vac}}{4\pi}$ to $\sigma^1 = \dfrac{E}{4\pi}$.

The effect of introducing the insulating substance is thus to reduce the surface charge density by an amount

$$\sigma - \sigma^1 \quad = \quad \frac{E_{vac}}{4\pi} - \frac{E}{4\pi} \quad = (\varepsilon - 1)\frac{E}{4\pi} \qquad (1.1.5)$$

Since the charge on the plates is being kept constant, the positive plate thus acquires a negative induced surface charge density ($\sigma - \sigma^1$) and vice versa; whole of the dielectric becomes a single dipole of moment ($\sigma - \sigma^1$)Ad. Under this condition, and using equation (1.1.3) we see that ($\sigma - \sigma^1$) = P. Thus, the quantity on the left hand side of the of equation (1.1.5) is the *polarization* of the dielectric and we can write

$$P = (\varepsilon - 1)\ \frac{E}{4\pi} \qquad\qquad (1.1.6)$$

The above explanation of the induction of charges at the surface of the dielectric is in accordance with that considered earlier.

From equations (1.1.5) and (1.1.6) we may write

$$D = E + 4\pi\ P = \varepsilon E \qquad\qquad (1.1.7)$$

Dielectric constant expresses the properties of the medium: all dielectric and optical properties of the medium are contained in this constant.

Susceptibility (χ):   It is defined as polarization per unit electric field.

$$\chi\ = \frac{P}{E}\ ;$$

It measures the amount of polarization a given field produces. In empty space P=0, χ = 0, ε = 1.

Polarizability (α):   The strength of the induced dipole moment an atom acquires is directly proportional to the strength of the external applied field

$$\text{i.e., } p \propto\ E$$

$$p = \alpha E$$

where α is known as dielectric polarizability. We can relate polarizability α, which is an atomic property to the macroscopic property polarization P. It has the dimensions of volume.

## 1.1.2 Sources of polarizability:

Polarization occurs due to several microscopic mechanisms. Polarization is a consequence of the fact that when an electric field acts on a molecule/atom, its positive charges (nuclei) are displaced along the field while the negative charges (electrons) in a direction opposite to that of the filed. The opposite charges are thus pulled apart and the molecule is polarized. The displacements of electrical charges result the formation of dipoles. Particularly in d.c. electric fields, the macroscopic polarization vector P is created by three types of mechanisms and hence polarization can be broadly classified into three types:

1.   Electronic Polarization
2.   Ionic Polarization
3.   Orientational Polarization

1.1.2 (a) Electronic polarization: Electronic polarization is due to displacement of charge centers of electron cloud (negative charge center) and nucleus (positive charge center) of an atom in the presence of an applied electric field.

Although we are interested in the dielectric properties of solids, it will be useful to consider first the much simpler problem of the behaviour of free atoms and molecules in an external field.

Consider an atom of a dielectric material such that its atomic number is equal to 'Z' and atomic radius 'r'. The centers of gravities of charges of electron cloud and positive nucleus are at the same point and hence there is no displacement. Suppose if the atom is placed in a d.c. electric field of strength 'E', the nucleus and the electron cloud experiences Lorentz forces of magnitude "ZeE" in opposite directions. i.e., nucleus and electron cloud are pulled apart, therefore an attractive coulomb force develop between them. When the Lorentz force and coulomb attractive forces are equal and opposite, there is a new equilibrium between the nucleus and the electron cloud of the atom and hence dipole is formed. Let the distance of separation between the centers of the displaced nucleus and electron cloud is 'd'.
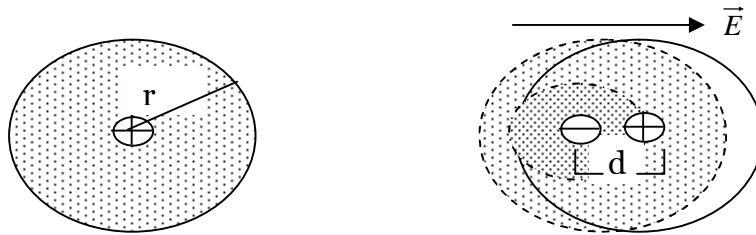
Fig. 1.1.3 An atom without any field and with field.

The negative charge enclosed in the sphere of radius 'r' is equal to $\dfrac{4}{3}\pi \, d^3 \rho$

Where 'ρ' is the charge density of electron cloud, and is equal to $\left[\dfrac{-Ze}{\dfrac{4}{3}\pi r^3}\right]$

Therefore charge enclosed in the sphere of radius, d is,

$$= \frac{4}{3}\pi d^3 \left[\frac{-Ze}{\dfrac{4}{3}\pi r^3}\right] \qquad = \left[\frac{-Zed^3}{r^3}\right]$$

Therefore, Coulomb force of attraction, F_c

$$= \frac{Ze.[\text{charge enclosed in the sphere of radius } d]}{d^2}$$

$$F_c = \frac{-Ze.Zed^3}{d^2 r^3} = \frac{-Z^2 e^2 d}{r^3}$$

Lorentz force of repulsion experienced by the electron due to applied field 'E' is

$$F_L = -ZeE$$

In equilibrium condition,

$$\frac{-Z^2 e^2 d}{r^3} = -ZeE$$

$$E = \frac{Zed}{r^3}$$

$$d = \frac{r^3}{Ze} E$$

$$\Rightarrow \qquad d \propto E$$

i.e., the separation between the two charge centers is proportional to the applied field 'E'.

The induced electric dipole moment,

$$p = Zed = r^3 E, \tag{1.1.8}$$

and the induced polarizability

$$\alpha_e = \frac{p}{E} = r^3 \tag{1.1.9}$$

Hence, α_e has the dimensions of a volume. It is also evident that in general atoms with many electrons tend to have a larger polarizability than those with few electrons. Electrons in the outer electronic shells will contribute more to α_e than do electrons in the inner shells, because the former are not so strongly bound to the nucleus as the latter. Positive ions therefore will have relatively small polarizabilities compared with the corresponding neutral atoms: for negative ions the reverse is true. Few examples of α_e are given in Table 1.1.1.

Table 1.1.1 Electronic Polarizabilities of some atoms and ions.

Atoms	α_e $(10^{-24} cm^3)$	Positive ions	α_e $(10^{-24} cm^3)$	Negative ions	α_e $(10^{-24} cm^3)$
He	0.29	Li^+	0.02	F^-	0.85
Ne	0.39	Na^+	0.22	Cl^-	3.00
Ar	1.62	K^+	0.97	Br^-	4.13
Kr	2.46	Rb^+	1.50	I^-	6.16
Xe	3.99	Cs^+	2.42		

1.1.2 (b) Ionic polarization: Ionic polarization is due to the displacement of positive ion and negative ion of a molecule in the presence of an applied electric field and occurs in ionic crystals. One might suppose that an ionic crystal would possess polarization even in the absence of an electric field, since each ion pair constitutes an electric dipole. But this is not so, because the lattice symmetry ensures that these dipoles cancel each other every where. So, the polarization in ionic crystals arises due to the fact that the ions are displaced from their equilibrium positions by the force of the applied electric field.

Consider an ionic compound composed of positive and negative ions separated by inter atomic distance, r_0, then the dipole moment is 'er_0' in the absence of applied field. When the field E_0 is applied to the molecule, the positive ion is displaced in the direction of field and negative ion is displaced in opposite direction until ionic bonding forces stop the process. Thus the dipole moment increases.

(a)

(b)
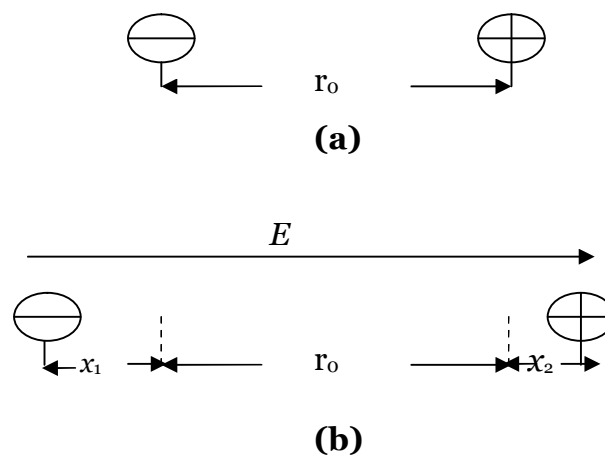
Due to the ionic displacement the resultant dipole moment increases and is given by

$$p = e (x_1 + x_2)$$

where x_1 is the shift of positive ion and x_2 is the shift of negative ion with respect to their equilibrium position.

Due to the application of static electric field $\mathbf{E_0}$, the force produced may be taken as $\mathbf{F}$ newtons and the restoring force on positive ion is $\beta_1 x_1$ and the restoring force on negative ion is $\beta_2 x_2$. Here β_1 and β_2 are restoring force constants which depend upon the mass of ion and angular frequency of the molecule in which ions are present.

Therefore, under equilibrium

$$F = \beta_1 x_1 = \beta_2 x_2$$

$$x_1 = \frac{F}{\beta_1} = \frac{eE_0}{m\omega_0^2} \tag{1.1.10}$$

where m is the mass of the positive ion and

$$F = eE_0 \text{ and } \beta_1 = m\omega_0^2$$

Similarly, for negative ion

$$x_2 = \frac{eE_0}{M\omega_0^2} \tag{1.1.11}$$

where M is the mass of negative ion.

Therefore, $(x_1 + x_2) = \dfrac{eE_0}{\omega_0^2}\left(\dfrac{1}{m} + \dfrac{1}{M}\right)$ \hfill (1.1.12)

And dipole moment

$$p = e(x_1 + x_2) = \frac{e^2 E_0}{\omega_0^2}\left(\frac{1}{m} + \frac{1}{M}\right) \tag{1.1.13}$$

Therefore, ionic polarizability

$$\alpha_i = \frac{p}{E_0} = \frac{e^2}{\omega_0^2}\left(\frac{1}{m} + \frac{1}{M}\right) \tag{1.1.14}$$

Thus ionic polarizability α_i is inversely proportional to the square of the natural frequency of the ionic molecule and to its reduced mass where reduced mass

$$\left(\frac{1}{m} + \frac{1}{M}\right)^{-1}$$

1.1.2(c) Orientational Polarization: Orientation polarization is due to the alignment of dipoles of polar molecules in the presence of applied electric field. Polar molecules have permanent dipole moments even in the absence of an electric field. These polar molecular dipoles are randomly distributed in space in the absence of an electric field and hence the net dipole moment of the dielectric is zero. But when dielectric is kept under electric field, the field produces a torque in individual dipoles and there is a tendency for the field to align dipole with the field and a net dipole moment per unit volume is originated in the dielectric. If the field is strong enough, the dipoles may completely be aligned along the field direction. The polarization due to the orientation, i.e, orientational polarizability 'α_o'.

E=0 $\vec{E}$

(a)   (b)

dipoles in the   dipoles in the

absence of '*E*'   presence of '*E*'
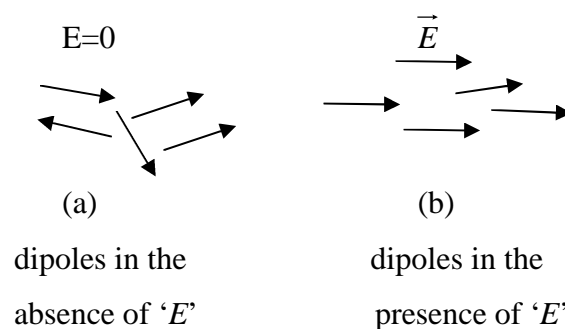
Fig. 1.1.5 Orientational polarization.

Consider for example, a gas containing a large number of identical molecules, each with a permanent dipole moment p. Without an external field, the dipoles will be oriented at random and the gas as a whole will have no resulting dipole moment. An external field E will exert a torque on each dipole and will tend to orient the dipoles in the direction of the field.

+e

eE

θ

E

eE

-e
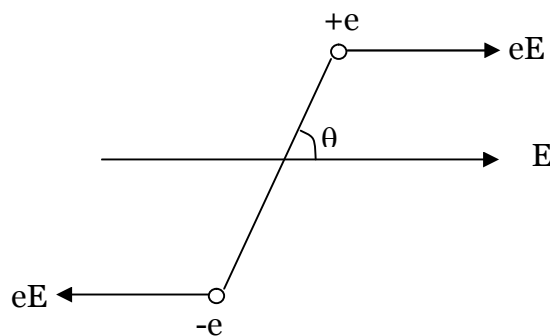
Fig. 1.1.6 Torque applied by a field on a dipole.

On the other hand, the thermal motion of the dipoles will counteract this ordering influence of the external field. Therefore, an equilibrium state will reach in which different dipoles will make zero to π radian angles with the field direction, producing a net polarization in the direction of the field. It is this polarization that we are going to calculate.

Let us define the potential energy of a dipole making a 90^0 angle with the external field as zero. The potential energy corresponding to an angle θ between p and E is equal to

$$-p\,E\,\cos\theta = p.E$$

According to statistical mechanics, the probability for a dipole to make an angle between θ and θ+dθ with the electric field is then proportional to

$$2\pi \sin\theta\, d\theta\, \exp[(pE \cos\theta)/kT]$$

where $2\pi \sin\theta\, d\theta$ is the solid angle between θ and θ+dθ. The number of dipoles having their orientation between θ and θ+dθ is also proportional to this probability. Now a dipole of moment p making an angle θ with the field direction contributes to the polarization a component p cos θ. Hence the contribution made by the above number of dipoles is

$$p \cos\theta . \, 2\pi \sin\theta\, d\theta\, \exp[(pE \cos\theta)/kT]$$

and the average contribution per dipole $\bar{p}$ is given by

$$\bar{p} = \frac{\int\limits_{0}^{\pi} p\cos\theta\, 2\pi \sin\theta\, d\theta\, \exp[(pE \cos\theta)/kT]]}{\int\limits_{0}^{\pi} 2\pi \sin\theta\, d\theta\, \exp[(pE \cos\theta)/kT]} \qquad (1.1.\ 15)$$

(θ = 0 corresponds to parallel alignment and θ = π corresponds to anti parallel alignment of dipoles).

Dividing numerator and denominator by 2π and letting

$$a = \frac{pE}{kT}\ , \qquad\qquad x = a \cos\theta\ , \qquad\qquad dx = \text{-}a \sin\theta\, d\theta,$$

equation (1.1.15) can be written as

$$\overline{p} = \frac{p \int\limits_{a}^{-a} x\, e^{x}\, dx}{a \int\limits_{a}^{-a} e^{x}\, dx}$$

$$\frac{\overline{p}}{p} = \frac{e^{a} + e^{-a}}{e^{a} - e^{-a}} \;-\; \frac{1}{a} = \text{coth a} - \frac{1}{a} = \text{L(a)} \qquad\qquad (1.1.16)$$

The function L(a) is called the Langevin function, since this first derived by Langevin in connection with the theory of paramagnetism.   In Fig. 1.1.7 L(a) has been plotted as a function of a = pE/kT. As a increases, the function continues to increase, approaching the saturation value unity as a → ∞. This situation corresponds to complete alignment of the dipoles in the field direction.
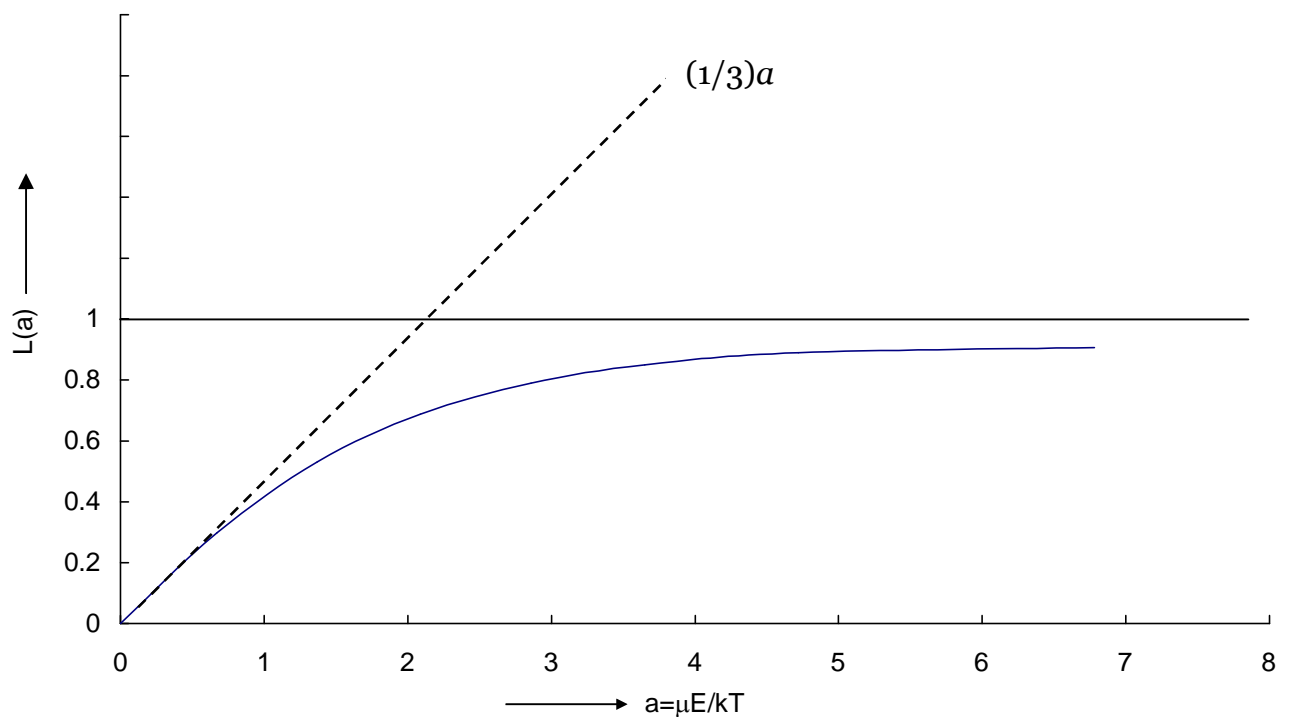
Fig. 1.1.7. Langevin function L(a) verses a

As long as the field strength is not too high and the temperature is not too low, the situation may be strongly simplified by making the approximation a<<1 or $\dfrac{pE}{kT}$ <<kT. Under these circumstances the Langevin function L(a) = a/3, so then from equation (1.1.16)

$$\frac{\overline{p}}{p} = L(a) = \frac{a}{3} = \frac{pE}{3kT}$$

$$\overline{p} = \frac{p^2}{3kT} E \qquad\qquad (1.1.17)$$

Hence, orientational or dipolar polarizability

$$\alpha_o = \frac{\overline{p}}{E} = \frac{p^2}{3kT} \qquad\qquad (1.1.18)$$

Hence, orientational polarizability α_o decreases with temperature. Since higher is the temperature, greater is the thermal agitation and lower is 'α_o'

A large number of molecules have polarizability, yet not all the molecules. The deciding factor for its existence is simply whether or not the molecules have a permanent moment. The existence of a permanent moment is purely a matter of molecular geometry. For example, CO_2 has no permanent moment at all, because its atoms are in line. On the other hand different geometry of H_2O molecule gives p=1.87 Debye units to it.

It may be noted that equation (1.1.18) is actually applicable to liquids and gases, because only in these substances the molecular dipole moment may rotate as continuously and freely as has been assumed in its derivation. In solids, a dipole may hop back and forth between certain discrete orientations in a manner which depends on the temperature and the electric field. Yet the dipolar polarizability for solids has been found to be of the same form as the result (1.1.18), expect for a numerical factor.

1.1.3 Summary

Physical quantities involved in the theory of dielectrics are defined. Various sources of polarization are discussed. Details of three types of polarizations are discussed at in depth.

1.1.4 Key-Terminology

Dielectrics-dipole-dipole moment—polarization-polarizability-dielectric constant-sources of polarization.

1.1.5 Self-Assessment Questions

1. What do you mean by polarization of a solid? Explain polarizability of atoms and molecules. Discuss different sources.

2. Obtain expressions for electronic, ionic and dipolar polarizability of a dielectric material.

3. Discuss the classification solids on the basis of dielectric polarization.

1.1.6 Reference Books

1. Solid State Physics- A.J.Dekker (Macmillan India Limited).

2. Elements of Solid state Physics- J.P.Srivastava (Prentice-Hall of India, New Delhi).

UNIT –I

LESSON-2

DIELECTRIC PROPERTIES –STATIC ELECTRIC FIELD

Objective of the lesson

- To discuss Dielectric constant of gases with examples.

- To give the reasons for the arise of local field and its calculation.

- To Discuss static dielectric constant of gases and solids

- To derive Classius –Mossotti equation

Structure of the lesson

1.2.1 Introduction

1.2.2 Static Dielectric Constant of Gases

1.2.3 Internal Field or Local Field

1.2.4 The Clausius-Mossotti Relation

1.2. 5 The static dielectric constant of solids

1.2.1 Introduction

In this chapter how the internal field influences the dielectric constant is described in detail. The Classius –Mossotti relation that connects dielectric constant with the polarizabilities is also derived

1.2.2 Static Dielectric Constant of Gases

We are now in a position to give an atomic interpretation of static dielectric constant of a gas. It will be assumed that the number of molecules per unit volume is small enough so that the interaction between them may be neglected. In that case, the field acting at the location of a particular molecule is to a good approximation equal to the applied field E. Suppose the gas contains N molecules per unit volume; the properties of the molecules will be characterized by an electronic polarizability α_e, an ionic polarizability α_i, and a permanent dipole moment p. From the discussion in the preceding two sections it follows that, as a result of the external field E, there will exist a resulting dipole moment per unit volume:

$$P= N(\alpha_e + \alpha_i + p^2/3kT)E \qquad\qquad (1.2.1)$$

Note that only the permanent dipole moment gives a temperature dependent contribution, because α_e and α_i are essentially independent of T. If the gas fills the space

between two capacitor plates of area A and separation d, the total dipole moment between the plates will be equal to

$$M = PAd$$

This simple relation shows immediately that the same total dipole moment would be obtained by assuming that the dielectric acquires an induced surface charge density P at the boundaries facing the capacitor plates, as discussed in section 1.1.1. Hence the quantity P introduced in moment per unit volume is identical with the quantity P introduced in section 1.1.1, where it represented the induced surface charge density at the dielectric-plate interface. Therefore, combination of (1.2.1) and (1.1.6) leads immediately to the **Debye formula** for the static dielectric constant of gas.

$$P = (\varepsilon - 1) \frac{E}{4\pi} \quad = N(\alpha_e + \alpha_i + p^2/3kT)E$$

$$(\varepsilon-1) = 4\pi P/E = 4\pi N(\alpha_e + \alpha_i + p^2/3kT) \qquad (1.2.2)$$

As an example of an application of this formula, the temperature dependence of some organic substances in the gaseous state is shown in Fig.1.2.8. The values of $(\varepsilon - 1)$ versus the reciprocal of absolute temperature have been plotted, leading to straight lines, in agreement with formula (1.2.20). From the slope of the lines and knowledge of the number of molecules per unit volume, the dipole moment p may be obtained. Also, form the extrapolated intercept of the lines with the ordinate, one can calculate $(\alpha_e + \alpha_i)$. The determination of dipole moments has contributed a great deal to our knowledge of molecular structure. For example, CCl_4 and CH_4, according to Fig. 1.2.8, do not possess permanent dipole moments (indicated by zero slope), in agreement with the symmetric structure of these molecules. Similarly, the fact that H_2O has dipole moment of 1.84 Debye units, whereas CO_2 has no dipole moment, indicates that CO_2 molecule has a linear structure, whereas in H_2O the two OH bonds must make an angle different from 180^0 with each other.

### 1.2.3 Internal Field or Local Field

In solids a molecule or atom experiences not only the external field, but the fields produced by the dipoles as well. As a result of the long range of Coulomb forces, the later contribution cannot be neglected. This resultant field is called the *local field*, and is responsible for polarizing individual molecules or atoms of solids.

To calculate the local field, we follow the method suggested by Lorentz. According to this method, we select a small spherical region from the dielectric with the atom for which the local field must be calculated at the centre. The radius of the sphere is chosen large enough to consider the region outside the sphere as a continuum whiles the region inside the
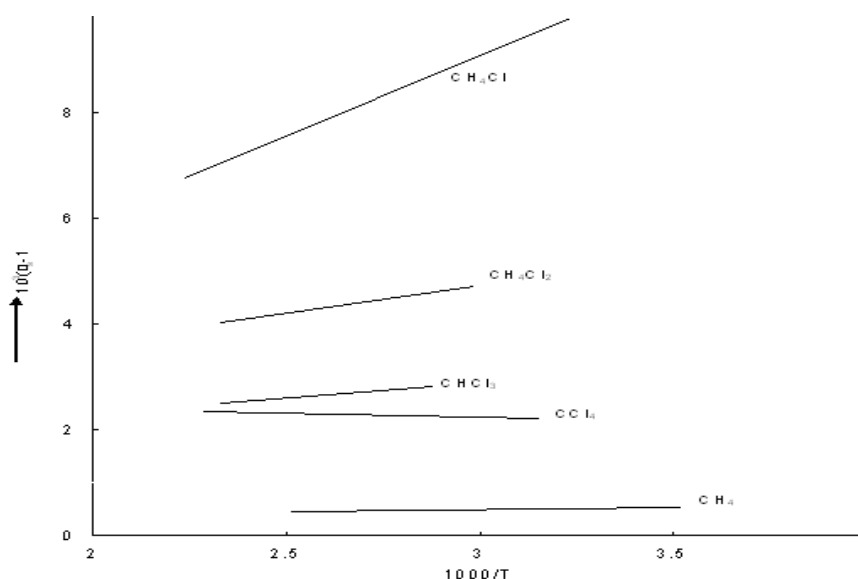
Fig 1.2.1 Temperature variation of the static dielectric constant of some vapours.

sphere as the actual structure of the substance. We suppose that, placing it in a uniform electric field between two oppositely charged parallel plates has uniformly polarized the given dielectric.
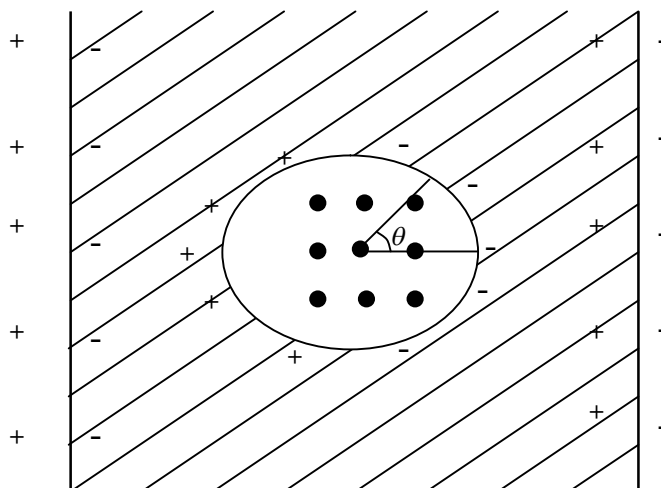
Fig. 1.2.2 Illustrating the calculation of the internal field as described in the text

Now, since the part of the dielectric external to the sphere may be replaced by a system of charges induced at the spherical surface as shown in Fig. 1.2.1, the electric field at the center of the sphere may be written as

$$E_{loc} = E_0 + E_p + E_s + E_m \qquad (1.2.3)$$

Here E_0 is the primary electric field due to the charge on the plates, E_p is the field due to the polarization charges at the plate-dielectric interface, E_s is the field due to the charges induced at the spherical surface and E_m due to all the dipoles of the atoms inside the spherical region. Now we know that $E_0 + E_p = E$, the macroscopic electric field inside dielectric. Hence,

$$E_{loc} = E + E_s + E_m \qquad (1.2.4)$$

Further, if we are considering crystals of high symmetry (such as cubic crystals) $E_m = 0$. This is because E_m is due to all the dipoles inside the spherical surface, and in such crystals these are randomly distributed in position.

We may then write

$$E_{loc} = E + E_s \qquad (1.2.5)$$

It must be remembered that equation, (1.2.5) is not applicable to anisotropic materials, as the assumption $E_m = 0$ is not rue for them.

To determine the E_s we proceed as follows:
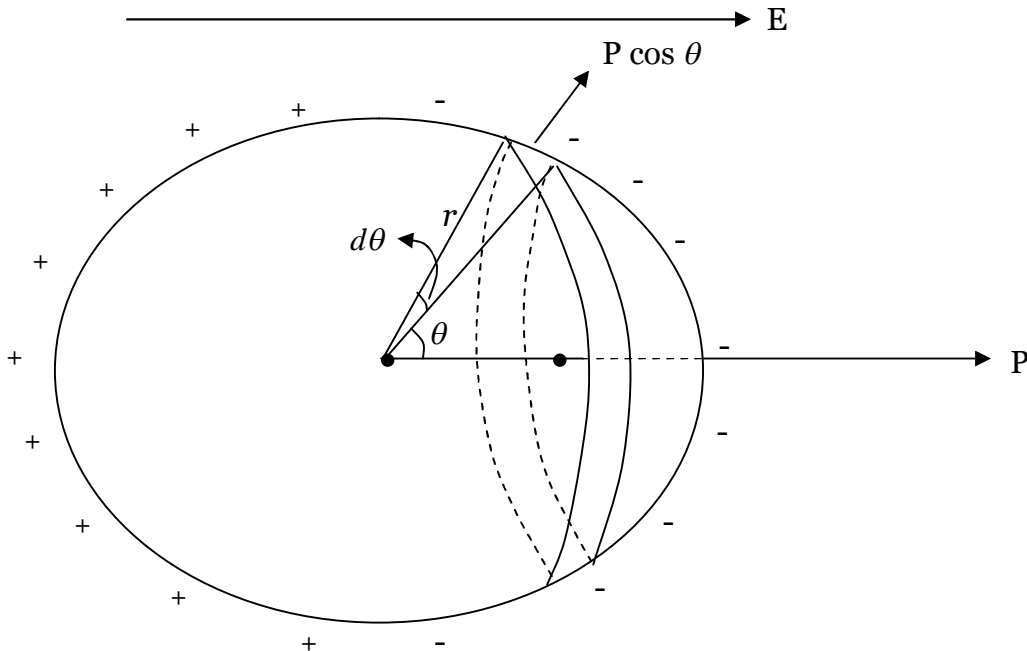
Fig. 1.2.3 Enlarged view of the sphere.

Fig.1.2.3 shows an enlarged view of the sphere shown in Fig.1.2.2. The charge element on a surface element dS of the sphere is equal to the normal component of the polarization times

the surface element, that is, -P cosθ dS. According to Coulomb's law, this charge element produces a force, given by

$$dF = q_1 q_2 / r^2 = -\frac{qP \cos\theta\, dS}{r^2}$$

acting on a test charge q assumed at the centre of the sphere in this direction of r. Hence, the field dE, at the centre due to this charge element is

$$dE_s = dF/q = -\frac{P \cos\theta\, dS}{r^2} \qquad (1.2.6)$$

Now resolving dE_s into components parallel and perpendicular to the direction of P, we can see a perpendicular component will be cancelled due to an equal contribution from another symmetrically situated surface element. Thus only the component of dE_s along the direction of P will contribute to the integral of equation (1.2.6) over the entire surface. Thus,

$$E_s = \int \frac{P \cos^2\theta\, dS}{r^2} \qquad (1.2.7)$$

Now the appropriate surface element dS in this case is the ring shown in Fig.1.2.10 so that dS = 2π r sinθ r dθ = 2π r² sinθ dθ, and the limits of integration with respect to θ are from 0 to π. Thus,

$$E_s = \int_0^\pi \frac{P \cos^2\theta}{r^2}\, 2\pi\, r^2 \sin\theta\, d\theta,$$

$$= 2\pi P \int_0^\pi \cos^2\theta \, \sin\theta\, d\theta,$$

This integral can be evaluated directly by making the substitution

z = cosθ and dz = -sinθ dθ,

so that

$$E_s = -2\pi P \int_1^{-1} z^2\, dz = -2\pi P \left[\frac{z^3}{3}\right]_1^{-1}$$

$$= \frac{4\pi P}{3} \qquad (1.2.8)$$

from equation (1.2.23) , we get

$$E_{loc} = E + \frac{4\pi P}{3} \qquad (1.2.9)$$

This equation is called Lorenz relation. This shows that E_{loc} is indeed different from E, as it is expected. The former field is larger than latter, so the molecules are more effectively polarized.

Substituting value of P from (1.1.6) we get

$$E_{loc} = \frac{\varepsilon + 2}{3}.\qquad\qquad (1.2.10)$$

This field is referred as Lorentz field.

The assumption Em = 0 is valid for simple cubic lattice. It is also valid for f.c.c. and b.c.c. lattices and for crystals such as NaCl. It does not hold for all cubic crystals. For example, in barium titanate, which has cubic symmetry E_m does not vanish.

Each type of atom in a given crystal has its own internal field because the environment of the different atoms is generally different. Thus the internal field at the location of atoms of type 1, 2, etc. may be written in the form

$$E_{loc1} = E + \gamma_1 P;\qquad E_{loc2} = E + \gamma_2 P, \text{ etc} \qquad\qquad (1.2.11)$$

where the γ's are the internal field constants. Only if Em = 0 do we have $\gamma = 4\pi/3$.

1.2.3 The Clausius-Mossotti Relation

Now we are in a position to relate the microscopic and macroscopic quantities defined above. The dipole moment p of a single atom is proportional to the local field, that is,

$$p = \alpha\, E_{loc}$$

Where α is the electrical polarizability of the atom. If there are different types of atoms, the polarizabilities are additive and the total polarization of an insulator containing N types is

$$P = \sum_{i=1}^{N} n_i\,\alpha_i\, E_{loc} \;=\; E_{loc} \sum_{i=1}^{N} n_i\,\alpha_i$$

Where n_i is the number of i atoms per unit volume having polarizabilities α_i and acted on by local field E_{loc} . Substituting the Lorentz field (1.2.9) then gives

$$P = (E + \frac{4\pi P}{3}\,) \sum_{i=1}^{N} n_i\,\alpha_i$$

or, after rearranging terms

$$\frac{P}{E} \;=\; \frac{\sum_{i}^{N} n_i \alpha_i}{1 - \left(\dfrac{4\pi}{3}\right)\sum_{i}^{N} n_i \alpha_i} \qquad\qquad (1.2.12)$$

Further, equation (1.1.6) can be rewritten as to give

$$\frac{P}{E} = \frac{\varepsilon - 1}{4\pi} \tag{1.2.13}$$

Thus, combining equations (1.2.13) and (1.2.12) we get

$$\frac{\varepsilon - 1}{4\pi} = \frac{\sum_{i}^{N} n_i \alpha_i}{1 - \left(\frac{4\pi}{3}\right)\sum_{i}^{N} n_i \alpha_i}$$

$$\frac{\varepsilon - 1}{\varepsilon + 2} = \frac{4\pi}{3}\sum_{i} n_i \alpha_i \tag{1.2.14}$$

If all the atoms i are the same, then $\sum_{i} n_i \alpha_i = n\alpha$ and $n = \dfrac{\rho N_a}{M}$, where ρ = density, N_a is Avogadro number, and M is molecular weight. So, equation (12.14) can be written in this case as

$$\frac{\varepsilon - 1}{\varepsilon + 2} = \frac{4\pi}{3}\frac{\rho N_a}{M}\alpha$$

or

$$\frac{M}{\rho}\frac{\varepsilon - 1}{\varepsilon + 2} = \frac{4\pi}{3}N_a\alpha \tag{1.2.15}$$

Equation (12.14) or (1.2.15) is called the Clausius-Mossotti equation. It can be used to determine the polarizabilities of the atoms if the dielectric constant is known. Further, the dielectric constants of new materials can be predicted from knowledge of the polarizabilities. This equation thus provides the necessary relation between the microscopic and macroscopic quantities.

1.2. 4 The static dielectric constant of solids

From the discussions in the preceding sections it is evident that in general the dielectric polarization P may be considered the sum of three contributions,

$$P = P_e + P_i + P_o \tag{1.2.16}$$

where the subscripts e, i and o refer, respectively, to electric, ionic and orientation polarization. This provides a basis for the classification of dielectrics into three classes:

(i) Substances for which $P_i = P_o = 0$ so that $P = P_e$

(ii) Substances for which $P_o = 0$ and $P = P_e + P_i$

(iii) Substances for which all three contributions are different from zero.

Although the calculation of internal field is usually complicated by the fact that the Lorentz expression (1.2.10) does not apply, some remarks may be made about each of these classes in so far as they apply to solids.

(i)   Substances for which the static polarization is entirely due to electronic displacements are necessarily elements, such as diamond. If we assume for the internal field an expression of the type (1.2.10), one obtains from the relation

$$P_e = N\alpha_e E_{loc} = (\varepsilon - 1)E/4\pi \tag{1.2.17}$$

The following expression for the dielectric constant:

$$\varepsilon - 1 = 4\pi N \alpha_e/(1-N\gamma\alpha_e) \tag{1.2.18}$$

Where N represents the number of atoms per unit volume. In the particular case for which the Lorentz expression for the internal field (1.2.18) is valid, $\gamma = 4\pi/3$. The resulting expression is then usually written in the form of Clausius-Mossotti formula, which may be obtained by substitution of (1.2.18) into (1.2.13):

$$(\varepsilon - 1)/ (\varepsilon + 2) = (4\pi/3)N\alpha_e \tag{1.2.19}$$

the main experimental test of the correction of either (1.2.17) or (1.2.18) is provided by measurements of the dielectric constant as function of the number of atoms per unit volume. It has therefore been applied mainly to gases. For solid elements one would have to vary the temperature in order to vary N and the possible range of N values is of course very limited.

It may be noted that for this class of substances under consideration, the dielectric constant is equal to the square of the index of refraction, $\varepsilon = n^2$. The reason is, that α_e is constant even for frequencies in the visible spectrum. This relationship has been confirmed experimentally for diamond and the dielectric constant of diamond is 5.68 ± 0.03.

(ii)   In general, solids containing more than one type of atom, but no permanent dipoles, exhibit electronic as well as atomic or ionic polarization. Of particular interest in this respect are the crystals, such as the alkali halides. Consider, for example, a NaCl crystal in an external static field E. Apart from the electronic displacements in the ions relative to the nuclei, the positive ion lattice will tend to move as a whole relative to the negative ion lattice. Consequently, a considerable contribution to the total polarization may be expected to arise from the ionic displacements (P_i). That this is indeed the case, becomes apparent from a comparison of the values of the static dielectric constant defined by

$$P_e + P_a = (\varepsilon - 1) E/4\pi \tag{1.2.20}$$

and the "high-frequency dielectric constant" ε_0 defined by

$$P_e = (\varepsilon_0 - 1) E/4\pi \tag{1.2.21}$$

(The high-frequency dielectric constant is equal to the square of the index of refraction for visible light; at such frequencies the ionic displacements cannot follow the field

variations and consequently $\varepsilon_0 = n^2$ is a measure only of P_e). By way of illustration values for ε and ε_0 for alkali halides are given in Table 1.2.1.

Table 1.2.1 Static and High – frequency Dielectric constant for some Alkali Halides

	ε	$\varepsilon_0 = n^2$
LiF	9.27	1.92
Nacl	5.62	2.25
LiCl	11.056	2.75

Hence P_i is about two or three times P_e in these compounds. In non-ionic compounds, on the other hand, P_i is usually a relatively small fraction of P_e.

The observed difference between the static and high- frequency dielectric constants is because of the difficulties involved in calculating quantitatively the internal field.

It may be noted that the force constant and the masses of the positive and negative ions determine the infrared frequency associated with the lattice vibrations. It is therefore possible to express the difference $(\varepsilon_s - \varepsilon_0)$ in terms of infrared absorption frequency of the lattice.

(iii) In substances composed of molecules which bear permanent electric dipole moments, the total polarization is made up of three contributions,

$$P = P_e + P_i + P_o \qquad\qquad (1.2.22)$$

Were P_o corresponds to the dipolar contribution. There exists no general quantitative theory for dipolar solids because first of all the same difficulties arises in evaluating the internal fields as in class (ii), and further more, the dipoles in such solids may not able to rotate at all or only to some extent. The discussion must therefore be limited to some qualitative remarks. As an example of a dipolar solid which behaves in a relatively manner, the dielectric constant measured as function of temperature for $C_6H_5NO_2$(nitrobenzene) is shown in Fig. 1.2.11. It is observed that at the melting point there is large increase in dielectric constant. This is interpreted as an indication that in the solid the dipoles cannot rotate freely and P_o is essentially zero; in the liquid, alignment of the dipoles in the field direction is possible, so that the increase in ε is determined by the now freely rotating dipoles. The subsequent slow decrease in ε is a consequence of the thermal motion

of particles, as may be understood from equation (1.2.17). In other cases, the behaviour may be more complicated, as illustrated by Fig. 1.2.12, in which ε versus T has been plotted for H_2s. the melting point of H_2S is 187.7_0K. in this case, the dipoles are apparently "frozen in" at temperature below 103.5^0K;at this temperature the structure changes in such a manner that the dipolar groups become mobile; as the temperature is further increased, the dielectric constant decreases as a result of increased thermal motion. The other changes evidently affect essentially the density of the material, i.e., N is reduced at these transition points.

1.2.5 Summary of the lesson

The local internal field in a dielectric has been calculated. The Classius-Mosetti relation that governs the relation between the dielectric constant and various polarizabilities has been derived.. The description of the static dielectric constant of gasses and solids has also been presented.

1.2.6   Key -Terminology

Local field, Clausius-Mossotti relation, static dielectric constant of gases and solids.

1.2.7 Self-Assessment Questions

1.   Obtain an expression for the local field that is responsible for polarizing atoms or molecules of a substance.

2.   Set-up Clausius-Mossotti relation between polarizability and dielectric constant of a solid.

3.   Discuss the static dielectric constant of gases and solids

1.2.8   Reference Books

1.   Solid State Physics- A.J.Dekker (Macmillan India Limited).

2.   Elements of Solid state Physics- J.P.Srivastava (Prentice-Hall of India, New Delhi).

Unit-I

Lesson –3

DIELECTRIC PROPERTIES -ALTERNATING FIELDS

Objective

In this lesson we study the behaviour of dielectrics in alternating electric fields. This study gives rise to complex dielectric constant and dielectric losses. We also study the frequency dependency of dielectric constant and measurement of dielectric constant.

Structure of the lesson

1.3.1 Introduction

1.3.2 The complex dielectric constant and Dielectric Losses

1.3.3 Dielectric Losses and Relaxation time

1.3.4 The classical theory of electronic polarization and optical absorption

1.3.5 Measurement of Dielectric constant

1.3.1 Introduction

We now take up the study of the behaviour of dielectrics in alternating electric fields. Here again we make use of the same basic atomic models used earlier and study the behaviour of this model in alternating electric field. This study reveals that the dielectric constant under these conditions is a complex quantity. The imaginary part of this complex dielectric constant determines the dielectric losses of the material.

In the macroscopic theory of isotropic dielectrics under static fields, the electric flux density D is proportional to the electric filed intensity E, so the D = ε E, where ε is a constant defined as the electric permittivity and is a property of the dielectric.

When a dielectric material is subjected to an alternating field the orientation of the dipoles, and hence the polarization, will tend to reverse every time the polarity of the field changes. As long as the frequency remains low ($<10^6$ c/s) the polarization follows the alternations of the field without any significant lag and the permittivity is independent of the frequency and has the same magnitude as in static field. When the frequency is increased the dipoles will no longer be able to rotate sufficiently rapidly so that their oscillations will begin to lag behind those of the field. As the frequency is further raised the permanent dipoles, if

present in the medium, will be completely unable to follow the field and the contribution to the static permittivity from this molecular process, the orientation polarization ceases; this usually occurs in the radio frequency range (10^6-10^{11} Hz) of the electromagnetic spectrum. At still higher frequencies, usually in the infra-red (10^{11}-10^{14} Hz) the relatively heavy positive and negative ions cannot follow the field variations so that the contribution to the permittivity from the atomic or ionic polarization ceases and only the electronic polarization remains.

The above effects lead to fall in the permittivity of a dielectric material with increasing frequency, a phenomenon which is usually referred to as **anomalous dielectric dispersion**.

Dispersion arising during the transition from full atomic polarization at radio frequencies to negligible atomic polarization at optical frequency is usually referred to as **resonance absorption.**

Dispersion arising during the transition from full orientational polarization at zero or low frequencies to negligible orientational polarization at high radio frequencies is referred to as **dielectric relaxation.**

It should be possible to explain the frequency dependence of the dielectric constant directly in terms of the electronic structure. It is known that the refractive index varies with the wavelength of light in the optical region the phenomenon being known as dispersion. Dispersion can be explained on the basis of classical theory which assumes that atom contains electrons vibrating at certain natural frequencies characteristic of the atom and that the application of an alternating field sets such electrons into forced vibration. Since the molecules in a dielectric are represented as dipoles on bound charges, there must be equal number of positive charges and negative charges because the dielectric is a neutral medium. When an electromagnetic wave impinges on this bound charge, it is caused to oscillate and therefore to radiate. If the frequency of the wave is not equal to the natural frequency of the bound charge the forced oscillation will have small amplitude and the radiation is very weak. This corresponds to molecular scattering. If the frequency of the wave is equal to the natural frequency of the bound charge, there is resonance and a much larger energy form the wave goes into the charge. In solid, liquid or gas at high pressure there is strong intermolecular action and friction type forces cause heavy damping with the result that the dipole energy is quickly dissipated. This corresponds to true absorption. In a gas at low pressure there is no damping and the dipole radiate strongly. This is resonance radiation. The absorption of an

electromagnetic wave by a conducting medium is easily explained because the conduction has a large number of free electrons. When the wave arrives its energy makes the charge move. The moving charge constitutes current and the usual dissipation of energy by the current explains the absorption of energy.

At optical frequencies the permittivity is almost entirely due to the electronic polarization. To determine the dependence of the electronic polarizability on the frequency of the applied field we shall use the classical model of an electron elastically bound to the atom.

1.3.2 The complex dielectric constant and Dielectric Losses

When a dielectric is kept between a capacitor plates is subjected to an alternating field the polarization P also varies periodically with time and so does the displacement D. In general however P and D may lag behind in phase relative to E so that for example if

$$E = E_o \cos\omega t \tag{1.3.1}$$

we have

$$D = D_0 \cos(\omega t - \delta) \tag{1.3.2}$$

$$= D_0 \cos \delta \cos \omega t + D_0 \sin \delta \sin \omega t$$

$$= D_1 \cos\omega t + D_2 \sin \omega t$$

where δ is the phase angle,

$$D_1 = D_0 \cos \delta \quad \text{and} \quad D_2 = D_0 \sin \delta. \tag{1.3.3}$$

For most dielectric D_o is proportional to E_o but the ratio (D_o/E_o) is generally frequency dependent. To describe this situation one may thus introduce two frequency dependent dielectric constants,

$$\varepsilon^{\mathrm{I}} = \frac{D_1}{E_o} = \frac{D_o}{E_o} \cos\delta$$

$$\varepsilon^{\mathrm{II}} = \frac{D_2}{E_0} = \frac{D_0}{E_0} \sin\delta \tag{1.3.4}$$

It is frequently convenient to sum these two constants into a single complex dielectric constant,

$$\varepsilon^* = \varepsilon^{\mathrm{I}} - i\varepsilon^{\mathrm{II}} \tag{1.3.5}$$

Thus $\qquad D = \varepsilon^* E_0 e^{i\omega t} = \varepsilon^* E_0 (\cos \omega t + i \sin \omega t)$ (1.3.6)

Also we see that

$$\tan \delta = \frac{\varepsilon^{''}}{\varepsilon^{'}}$$ (1.3.7)

Because both $\varepsilon^{'}$ and $\varepsilon^{''}$ are frequency dependent the phase angle δ is also frequency dependent. We shall now show that the energy dissipated in the dielectric in form of heat is proportional to $\varepsilon^{''}$.

The current density in the capacitor is equal to $\dfrac{d(D)}{dt}$.

Thus $\qquad J = \dfrac{d}{dt}(\sigma) = \dfrac{1}{4\pi}\dfrac{dD}{dt}$

$$= \frac{\omega}{4\pi}\left(- D_1 \sin \omega t + D_2 \cos \omega t\right)$$ (1.3.8)

using equations (1.1.4) and (1.3.2). Where, σ is the surface charge density on the capacitor plates.

The energy dissipated or absorbed per second in the dielectric is given by

$$W = \left(\frac{\omega}{4\pi}\right)\int_0^{2\pi/\omega} JE\, dt$$ (1.3.9)

Substituting for J and E, from (1.3.8) and (1.3.1) one gets

$$W = \frac{\omega}{4\pi}\left[\int_0^{2\pi/\omega}\omega\left(- D_1 \sin \omega t + D_2 \cos \omega t\right)E_o \cos \omega t\, dt\right]$$

$$W = \frac{\omega}{4\pi}\left[-\omega \int_0^{2\pi/\omega} E_0 D_1 \sin \omega t \cos \omega t\, dt + \omega \int_0^{2\pi/\omega} E_o D_2 \cos^2 \omega t\, dt\right]$$

The value of integral containing D_1 is equal to zero and we are left with

$$W = (\frac{\omega}{8\pi})D_2 E_o = \frac{\omega}{8\pi}E_0^2 \varepsilon^{''}$$ (1.3.10)

Equation (1.3.10) tells that the amount of energy absorbed is proportional to $\sin\delta$ since $\varepsilon^{''} = (D_0/E_0) \sin \delta$. The energy so dissipated in the dielectric medium is referred to as the dielectric

loss. For this reason sinδ is called the loss factor and δ is the loss angle (but it is customary) to call tanδ as the loss factor; this is correct only for small values of δ because $\tan \delta \approx \sin \delta \approx \delta$. The dielectric loss at low frequencies is mainly due to d.c. resistivity. But at high frequencies the dielectric loss is mostly due to dipole rotations or to ionic transitions from the lower energy states to higher energy states. Because of the upward transition the energy is absorbed from the applied field. The losses associated with ions, the frequency of which fall in the infrared region, are usually referred to as optical infrared absorption. Similarly, the losses in the optical region, associated with the electrons, are referred to as optical absorption.

1.3.3 Dielectric Losses and Relaxation time

Let us consider a dielectric, for which the total polarization P_s in a static field is determined by three contributions,

$$P_s = P_e + P_i + P_o \qquad (1.3.11)$$

In general, when such a substance is suddenly exposed to an external static field, a certain length of time is required for P to be built up to its final value. In the present section it will be assumed that the values of P_e and P_i are attained instantaneously, i.e., we shall be concerned with frequencies appreciably smaller than infrared frequencies. The time required for orientational polarization, P_o to reach its static value may vary between days and 10^{-12} second, depending on temperature, chemical constitution of the material, and its physical state is called relaxation time.

To begin with we shall give a phenomenological description of the transient effects based on the assumption that a relaxation time can be defined; we can then proceed to consider the case of an alternating field. Let P_{os} denote the saturation value of P_o as function of the time after the field has been switched on is given by

$$P_o(t) = P_{os}(1 - e^{-t/\tau}) \qquad (1.3.12)$$

where τ is the relaxation time.

$$dP_o/dt = (1/\tau) [P_{os} - P_o(t)] \qquad (1.3.13)$$

For the decay occurring after the field has been switched off, this leads to a well–known proportionality with $e^{-t/\tau}$. In the case of an alternating field $E = E_0 e^{i\omega t}$, equation may employed if we make the following change: P_{os} must be replaced by a function of time $P_{os}(t)$

representing the saturation value which would be obtained in static field equal to the instantaneous value E(t). Hence for alternating fields we shall employ the differential equation

$$dP_o/dt = (1/\tau) [[P_{os}(t) - P_o(t)] \tag{1.3.14}$$

Now, our final goal is to express the real and imaginary parts of the dielectric constant in terms of the frequency ω and the relaxation time τ. For this purpose we shall define the "instantaneous" dielectric constant ε_{ei} by

$$P_e + P_i = (\varepsilon_{ei} - 1)/4\pi \quad E \tag{1.3.15}$$

We may then write

$$P_{os} = P_s - (P_e + P_i) = (\varepsilon_s - \varepsilon_{ei})/4\pi \quad E \tag{1.3.16}$$

Where ε_s is the static dielectric constant and εei is the dielectric constant arising due to electronic and ionic polarization. Substitution of P_{os} into (1.3.14) yields

$$dP_o/dt = (1/\tau)[(\varepsilon_s - \varepsilon_{ei})/4\pi \quad E_0 e^{i\omega t} - P_o] \tag{1.3.17}$$

Solving this equation, we obtain

$$P_o(t) = Ce^{-t/}\tau + 1/4\pi \quad (\varepsilon_s - \varepsilon_{ei})/(1+i\omega\tau) E_0 e^{i\omega t} \tag{1.3.18}$$

The first term represents a transient. The total polarization is now also a function of time and is given by $P(t) = P_e + P_i + P_o(t)$. Hence, for the displacement one obtains
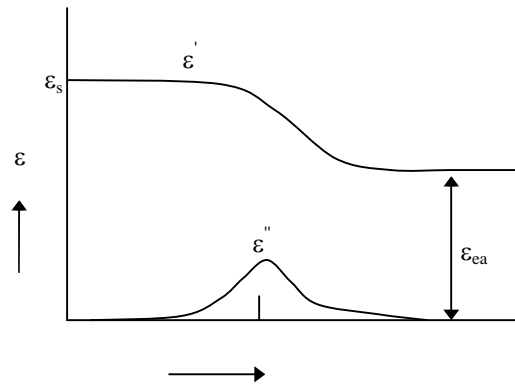
$$D(t) = \varepsilon^* E(t) = E(t) + 4\pi P(t) \tag{1.3.19}$$

where ε^* is the complex dielectric constant. From the last two equations and from the definition $\varepsilon^* = \varepsilon^1 - i \varepsilon^{11}$ the following expressions result:

$$\varepsilon^1(\omega) = \varepsilon_{ei} + (\varepsilon_s - \varepsilon_{ei})/(1+i\omega^2\tau^2) \tag{1.3.20}$$

$$\varepsilon^{11}(\omega) = (\varepsilon_s - \varepsilon_{ei}) \omega\tau/(1+i\omega^2\tau^2) \tag{1.3.21}$$

These equations are frequently referred to as the **Debye's equations**. In Fig. 1.3.1 the quantities ε^1 and ε^{11} are represented as functions of $\omega\tau$. It is observed that the dielectric

Fig. 1.3.1 Debye curves for ε' and ε'' as function of frequency for a dielectric with a single relaxation time

loss, which is proportional to ε'' according to (1.3.10), exhibits a maximum for $\omega\tau = 1$, i.e., for an angular frequency equal to $1/\tau$. Also, for frequencies appreciably less than $1/\tau$, the real part of the dielectric constant ε' become equal to the static dielectric constant. In this frequency range, therefore, the losses vanish and the dipoles contribute their full share to the polarization. On the other hand, for frequencies larger than $1/\tau$, the dipoles are no longer able to follow the field variations and the dielectric constant ε' approaches ε_{ei}.

Note that for this type of mechanism the relaxation time decreases with increasing temperature as so does the saturation polarization. It is of interest to observe that if the quantities ε' and ε'' are measured at a constant frequency but at different temperatures, the curves as indicated in Fig. 1.3.2 may be expected to result.
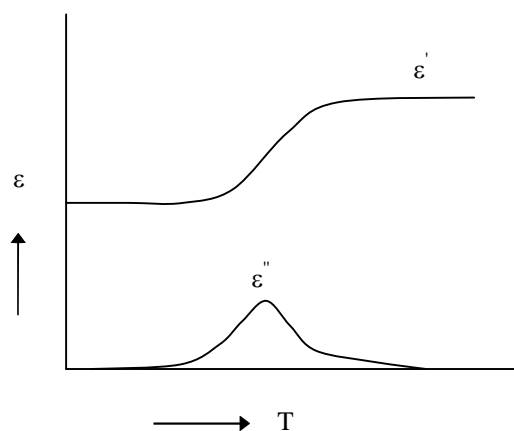
Fig. 1.3.2 The dielectric constant as a function of temperature at a given frequency, as predicted from the model discussed in the text

1.3.4 The classical theory of electronic polarization and optical absorption

In Lesson 1.1 the concept of the static polarizability due to elastic displacements of electrons and ions was introduced. In the present section the classical theory of this phenomenon in alternating fields will be discussed. We have seen that restoring force determining the displacement is in first approximation proportional to the displacement itself. The discussion is therefore based on the model of a displacement itself. The discussions is therefore based on the model of an elastically bound particle of charge e and mass m in an alternating field $E_0 e^{i\omega t}$ may be written

$$m\frac{d^2 x}{dt^2} + m\gamma\frac{dx}{xt} + m\omega_0^2 x = e\, E_0 e^{i\omega t} \qquad (1.3.22)$$

where ω_0 is the natural angular frequency of the particle; $\omega_0 = (f/m)^{1/2}$ where f is the restoring force constant ; the second term on the left – hand side is a damping term, which results from the fact that the particle emits radiation as a consequence of its acceleration and γ is the damping factor. The solution for this forced damped vibration is

$$x(t) = \frac{e}{m} \cdot \frac{E_0 e^{i\omega t}}{\omega_0^2 - \omega^2 + i\gamma\omega} \qquad (1.3.23)$$

We first of all note that in a static field, for $\omega = 0$, this reduces simply to

$$x = eE_0/m\omega_0^2 \text{ or } \alpha_s = ex/E_0 = e^2/m\omega_0^2 \text{ for } \omega = 0 \qquad (1.3.24)$$

Where α_s is static polarizability associated with the elastically bound particle. If we take for e and m the electronic charge and mass, this expression would correspond to the contribution of a particular electron to the electron polarizability. Now we have seen in Sec. **1.1.2** that the electronic polarizabilities are of the order of 10^{-24} cm^3; this gives a natural frequency $\nu_0 = \omega_0/2\pi \cong 10^{15}$ per second. Thus, even for frequencies corresponding to the visible spectrum, the electronic polarizability may be considered constant. If e and m refer to an ion, the natural frequencies are of the order of 10^{13} per second, corresponding to the infrared part of the spectrum.

The electronic polarizability is therefore

$$\alpha_e = \frac{ex}{E} = \frac{e^2}{m}\frac{1}{\omega_0^2 - \omega^2 + i\gamma\omega} \qquad (1.3.25)$$

The complex dielectric constant is then gieven by

$$\varepsilon(\omega) = 1 + \frac{4\pi \, Ne^2}{m} \cdot \frac{1}{\omega_0^2 - \omega^2 + i\gamma\omega} \tag{1.3.26}$$

where N is the number of electrons per unit volume. This follows by using P = Nex and ε = 1+4πP/E.

Now, from the definition of the complex dielectric constant $\varepsilon(\omega) = \varepsilon^{\text{I}}(\omega) - i\varepsilon^{\text{II}}(\omega)$

One finds

$$\varepsilon^{\text{I}}(\omega) = 1 + \frac{4\pi \, Ne^2}{m} \frac{\omega_{0-}^2 \omega^2}{(\omega_0^2 - \omega^2)^2 + \gamma^{\,2}\omega^2} \tag{1.3.27}$$

$$\varepsilon^{\text{II}}(\omega) = \frac{4\pi \, Ne^2}{m} \frac{\gamma\omega}{(\omega_0^2 - \omega^2)^2 + \gamma^{\,2}\omega^2} \tag{1.3.28}$$

It may be noted that $\varepsilon^{\text{I}}(\omega)$ gives us the value of the dielectric constant and from $\varepsilon^{\text{II}}(\omega)$ we get the power dissipated and hence the damping loss. The variation of $(\varepsilon^{\text{I}} - 1)$ and ε^{II} these with frequency is shown in Fig. 1.3.3. Note that ε^{II} has a
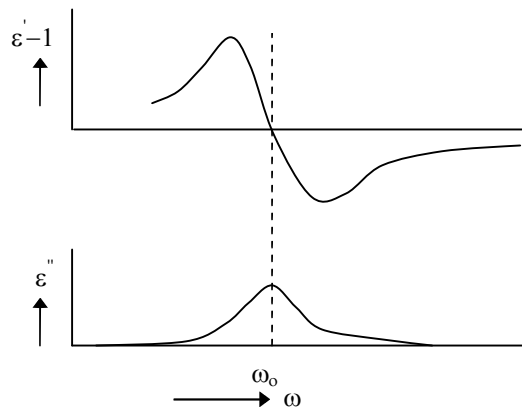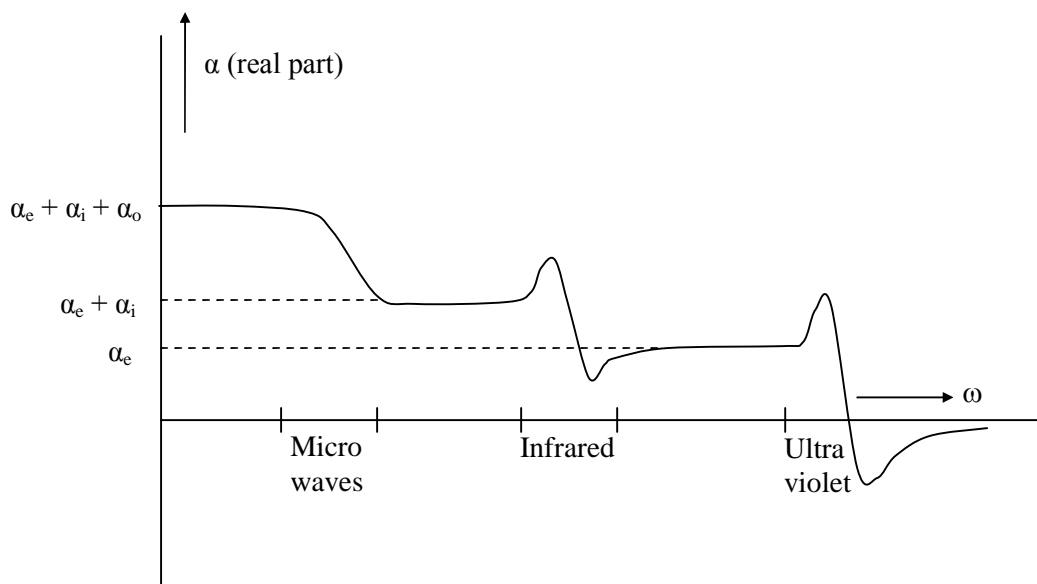

Fig. 1.3.3   Behaviour of $\varepsilon_o^{'}$ and $\varepsilon_o^{''}$ as function of frequency in the vicinity of the resonance frequency ω_o

maximum at $\omega = \omega_0$. The meaning of this maximum is that the material absorbs energy at the natural frequency; this type of absorption is called resonance absorption. In the absorption region, the dielectric constant ε^{I} depends on frequency and one speaks in this connection of **dispersion**. The region for which ε^{I} decreasing with frequency is referred to as the region of **anomalous dispersion**.

Total Polarizability

Let us now discuss the total polarizability $\alpha = \alpha_o + \alpha_i + \alpha_e$. It has been found that the total polarizability of a dielectric substance shows marked difference in behavior when studied as a function of frequency. To summarize the frequency-dependence of the polarizability we have represented, in Fig.1.3.4, $\alpha(\omega)$ for a dipolar substance. It is clear that as we go from the static to the optical region, the polarizability α decreases by a substantial amount. Speaking in terms of dielectric constant, the dielectric constant of water, for example is 81 at zero frequency while it is only 1.8 at optical frequencies. Moreover, the decrease in polarizability α is not uniform –remarkable decrease occurs only in the microwave, infrared and ultra-violet regions.

Fig. 1.3.4 Variation of total polarizability as a function of frequency.

The behaviour of polarizability can be understood from the various possesses and from the concept of the relaxation time for each process. When the frequency of the applied field is much greater than the inverse of the relaxation time for a particular polarization process, that particular polarization process fails and so it does not contribute to polarizability. Thus, the decrease of total polarizability with increase in frequency is due to the disappearance of α_o, α_i and α_e successively.

1.3.5 Measurement of Dielectric constant

Dielectric constant of a given substance is usually measured by comparing the capacity C_d of a condenser filled with the substance and the capacity C_0 of a the empty condenser . The ratio $\dfrac{C_d}{C_0} = \varepsilon$, is the dielectric constant. The capacities C_d and C_0 may be measured by resonance method as shown in the Fig 1.3.4.

Oscillator
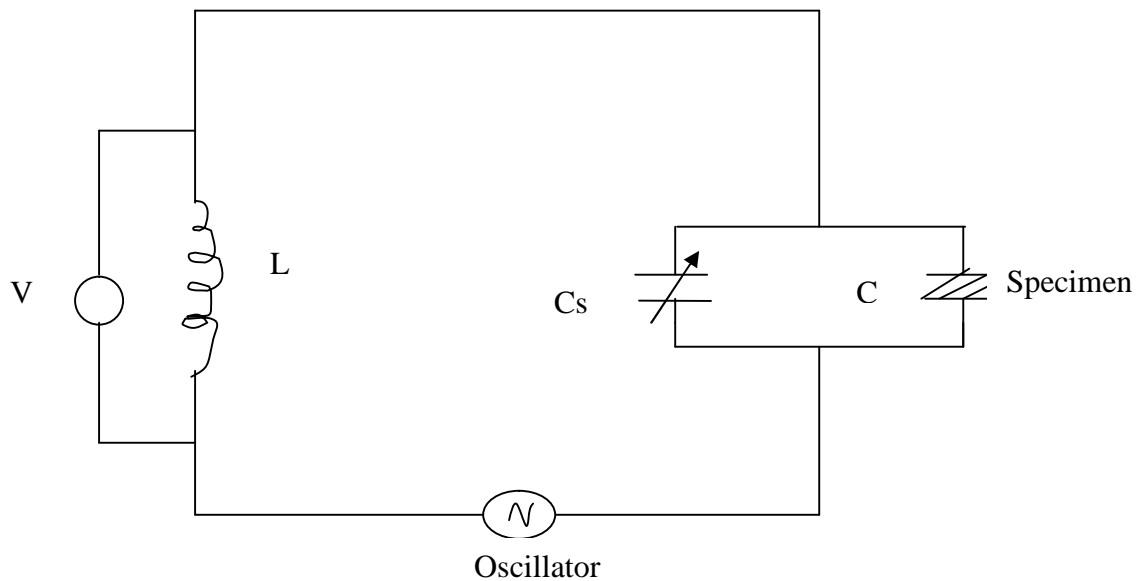
Fig. 1.3.5 Principle of the resonance method for measuring C_o and C_d.

In the figure, Cs is a calibrated variable condenser and C is the condenser in which the given substance which is taken in the form of a thin disc may be placed. By varying Cs so a sto keep the resonance frequency

$$\omega o = \frac{1}{\sqrt{[L(C_s + C)]}} \qquad (1.3.29)$$

constant when C is empdty and then filled, we may determine C0 and Cd, and hence ε. The voltmeter V measures the response of the resonant circuit.

This method is generally used to measure the dielectric constant up to frequencies 100 Mhz. At the microwave region ($\sim 10^3$ to $\sim 10^5$ Mhz) the frequencies are so high that the

dimensions of the apparatus are comparable with or greater than the wavelength, and the specimen hen can no longer be treated as if it were in quasi-static fields. Rather, it has to be treated as a medium for the propagation of electromagnetic waves. Here we may measure the dielectric constant of the specimen by measusring the wavelength of the microwave radiation in the specimen and using the relation

$$\frac{\lambda_{vvacuum}}{\lambda_{specimen}} = (\varepsilon\mu)^{1/2} \qquad\qquad (1.3.30)$$

where μ is the permeability; for non-magnetic materials, $\mu \approx 1$. For optical and infrared frequencies, ε can be measured by measuring the refractive index, n as

$$n^2 = \varepsilon\,\mu \; \approx \varepsilon$$

1.3.6 Summary of the lesson

When a dielectric material is subjected to an alternating field the orientation of the dipoles alter in accordance with the field changes. At higher frequencies dipoles will no longer be able to rotate sufficiently rapidly and unable to follow the field and the permittivity of the material decreases. The average time taken by the dipoles to orient in the field direction is known as relaxation time.

When a dielectric is subjected to an alternating field, the polarization and displacement vector also vary periodically with time and this gives rise to complex dielectric constant. Dielectric constant depends on the frequency of the applied electric field. When a dielectric is subjected to alternating field, the electrical energy is absorbed by the material and dissipated in the form of heat. This dissipation of energy is called dielectric loss. Debye's equations relating dielectric loss and relaxation time are

$$\varepsilon^{i}(\omega) = \varepsilon_{ei} + (\varepsilon_s - \varepsilon_{ei})/(1+i\omega^2\tau^2)$$

$$\varepsilon^{ii}(\omega) = (\varepsilon_s - \varepsilon_{ei})\;\omega\tau/(1+i\omega^2\tau^2)$$

The losses associated with ions, the frequency of which fall in the infrared region, are called as **optical infrared absorption** and the losses in the optical region, associated with the electrons, are referred to as **optical absorption**.

1.3.7 Key- Terminology

Complex dielectric constant-dielectric losses-optical infrared absorption- optical absorption-resonance absorption-relaxation time Debye's equations-measurement of dielectric constant

1.3.8 Self-Assessment Questions

1. Explain the behaviour of dielectrics in an alternating electric field.

2. Obtain the expression for the energy absorbed per second in dielectric material when an alternating electric field is applied.

3. Deduce Debye's equations relating dielectric loss and relaxation time.

4. Explain the phenomenon of optical absorption on the basis of classical theory.

5. Discuss the variation of total polarizability as a function of frequency.

6. Explain the method to determine dielectric constant of a substance.

1.3.9 Reference Books

1. Solid State Physics- A.J.Dekker (Macmillan India Limited).
2. Elements of Solid state Physics- J.P.Srivastava (Prentice-Hall of India, New Delhi).

Lesson-4

FERROELECTRIC   CRYSTALS

Objectives

- To present in detail the properties of ferroelectric crystals and their classification.

- To discussion on the ferroelectric transitions of $BaTiO_3$ based on thermodynamic theory

Structure of the lesson

1.4.1 Introduction

When the centre of a positive charge does not coincide with the centre of negative charge in a primitive cell, the primitive cell possesses an electric dipole moment even in the absence of applied electric field. Thus the crystal as a whole has a polarization implying that it is spontaneously polarized The shifting of positive charge from the centre of negative charge is exhibited in the lack of centre of symmetry in the crystal. Out of 32 crystal point groups, 21 point groups do not have a centre of symmetry. Except one point group, which is highly symmetric, the rest 20 point groups represent an extremely useful class of materials, known as piezoelectrics.

Piezoelectrics: Piezoelectric crystals show electric polarization on being externally strained and conversely, show deformation when placed under the influence of an applied electric field. This was discovered by French physicists Pierre curie and Paul-Jean Curie in the year 1980. If the crystal belongs to any one of the above 20 point groups, it can be predicted that the crystal would be piezoelectric. Ammonium phosphate, quartz, PZT (Lead Zirconate Titanate) are some examples of piezoelectric crystals.

Pyroelectrics: Among the class of 20 crystal point groups which lack centre of symmetry, 10 crystal point groups are spontaneously polarized. These spontaneously polarized dielectric crystals are called pyroelectric crystals. The polarization in pyroelectric crystals is

usually masked by surface charges that accumulate on the surface from the atmosphere and subsequently neutralize the layers of ions. But, when the temperature of the crystal is altered, the masking is no longer complete as the polarization changes because of thermal expansion or contraction of the crystal. Owing to the thermal effect on polarization, these crystals are named pyroelectric (pyro means fire). The thermal effect accompanying deformation thus supports the piezoelectric property of the crystals. This only confirms that all pyroelectric crystals are piezoelectric, though converse is not true.

While maintaining the crystalline properties, the symmetry operations of a pyroelectric crystal must preserve the direction of polarization P. This imposes severe restrictions on the point group symmetries as a result of which only 10 point groups are found to meet the conditions of pyroelectric crystals. The rotation is allowed about only one axis that is parallel to P and there cannot exist mirror planes perpendicular to this axis. The structural scrutiny of crystal groups reveals that only the following point groups meet the restrictions of pyroelectric crystals:

C_n, C_{nv} (n = 2,3,4,6), C_1 and C_{1h}

Thus the pyroelectric property too, like piezoelectricity, is solely determined by the symmetry properties of crystals.

Ferroelectrics: Ferroelectric crystals have additional property that the polarization in them can be changed and even reversed by an external electric field. On the other hand, this is not possible in pyroelectrics even with the maximum electric field that may be applied without causing electrical breakdown. The additional feature of ferroelectrics that distinguishes them as a special class of pyroelectrics does not follow from the characteristics of crystal structure. It is established only on the basis of dielectric measurement.

Furthermore, the additional feature of ferroelectrics mentioned above converts the usual linear relationship between polarization and applied electric field into a hysteresis loop. Since the dielectric behaviour of these materials is in many respects analogous to the magnetic behaviour of ferromagnetic materials, they are called ferroelectric solids, or ferroelectrics. The ferroelectric behaviour is observed only below a certain temperature, called the Curie point, T_c. A ferroelectric is spontaneously polarized, i.e., it is polarized in the absence of external field; the direction of the spontaneous polarization may be altered under influence of an applied electric field. In general, the direction of spontaneous polarization is not the same throughout a macroscopic crystal. Rather, the crystal consists of a number of domains; within each domain the polarization has a specific direction, but this direction varies from one domain to another.

1.4.2. Representative crystal types of ferroelectrics

In general the ferroelectric crystals may be broadly classified into four representative groups such as i) Ilmenites and Perovskites, ii) KDP type iii) TGS type and iv) Rochelle salt type as given in Table 1.4.1. The table gives the Curie point T_c and the spontaneous polarization P_s for a number of common ferroelectric crystals. The electric susceptibility χ in the paraelectric phase is related to temperature by the Curie- Weiss law: $\quad \chi = \dfrac{C}{T - T_c}$ .... (1.4.1)

where C is the Curie constant.

The ferroelectric crystals are also distinguished on the basis of oscillatory nature of the atomic displacements that destroy the ferroelectric dipole order above the Curie temperature. In the ferroelectric phase of some crystals, the atomic displacements can be viewed as oscillations about a **polar site**. In the paraelectric phase these oscillations take place about a **non-polar site**. The phase transition that brings about this transformation in the nature of oscillations is called a **Displacive phase transition**. These crystals are accordingly identified as **Displacive type**. The well-known examples of this class are ionic crystals with ilmenite and perovskite structures. The GeTe is the simplest ferroelectric crystal having the ilmenite structure (i.e., NaCl structure) and $BaTiO_3$ is the representative crystal of perovskites.

Table 1.4.1 Data on some representative ferroelectric crystals

Group	Crystal	T_c(K)	P_s $C/m^{-2} \times 10^{-2}$	At T (K)
Ilmenites and	GeTe	670	------	------
Perovskites	$LiNbO_3$	1480	71	296
	$KNbO_3$	710	30	600
	$BaTiO_3$	393	26	300
	$SrTiO_3$	32	3	4.2
KDP type	KH_2PO_4	123	4.7	100
	KD_2PO_4	213	5.5	100
	RbH_2PO_4	147	5.6	90
	KH_2AsO_4	97	5.0	78
TGS type	$(Nh_2CH_2COOH)_3.H_2SO_4$ 322		2.8	275
	(Triglycine sulphate)			
Rochelle	$NaKC_4H_4O_6.4H_2O$	296(upper)	0.25	275
Salt type	(Rochelle salt)	255(lower)		

There is another very interesting class of crystals in whose non-ferroelectric state the potential energy function around certain atomic sites is double-well or multiple-well shaped. On the transition to the ferroelectric state the atomic displacements about those sites are executed as oscillations in an ordered subset of the referred potential wells. It involves an order-disorder type of phase transition. Common examples of these crystals, classified as order-disorder type, are some

hydrogen bonded solids, namely KDP type crystals. The replacement of hydrogen by deuterium in KDP type crystals raises the Curie point in an amazing proportion. Though the increase in the molecular weight is less than 2 percent, the T_c rises from 123K to 213K in the deuterated KDP and from 96K to 162K in KD_2AsO_4.

For specific description, Rochelle salt and $BaTiO_3$ are chosen as the two representative compounds of ferroelectrics whose properties are uniquely different.

a. Rochelle Salt

The first solid which was recognized to exhibit ferroelectric properties is Rochelle salt, the sodium-potassium salt of tartaric acid; it has the chemical formula $NaKC_4H_4O_6.4H_2O$. It was first prepared in 1672 by a pharmacist Seignette who lived in Rochelle. It represents the tartaric group of salts whose other well known member are lithium ammonium tartrate and lithium tantalum tartrate. The most noteworthy characteristic of Rochelle salt is that it is ferroelectric between two temperatures (255K and 296K). On account of its two transition temperatures, Rochelle salt becomes a special and peculiar example of ferroelectrics.

The crystal structure of Rochelle salt is somewhat complex. Above 296K and bellow 255K the structure is orthorhombic (three mutually perpendicular axes a,b,c). It has a monoclinic symmetry in the ferroelectric phase such that the angle β(between the c- and a- axes) differs from 90^0 and the spontaneous polarization is along the original orthorhombic a- axis. Thus Rochelle salt has only one polar axis and two possible polarization directions (+ and – along the a- axis).

Halblutzel has measured the dielectric constant of Rochelle salt along the three crystal axes over the whole useful range of temperatures. Figure 1.4.1 gives a logarithmic plot of these values. The Curie-Weiss law applies above 296 K and below

255 K. With the help of the experimental data it is easy to confirm that the two regions have different values of Curie constants. The dielectric constant measured along the polar axis ε_a

peaks at both transition temperatures, assuming a value as high as 4000. The behaviour of spontaneous polarization as a function of temperature is shown in fig 1.4.2. The lower curve represents Rochelle salt and the upper curve belongs to the deuterated salt.
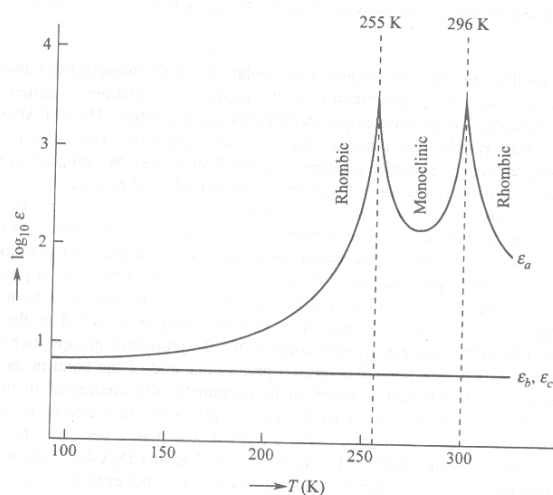

Fig. 1.4.1. Variation of dielectric constant of Rochelle salt with temperature.
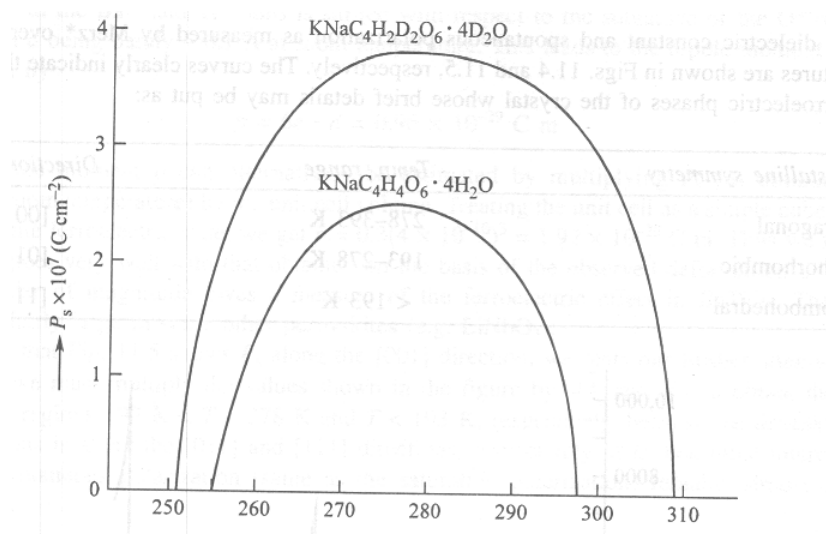

Fig. 1.4.2. Variation of the spontaneous polarization with change in temperature. The lower curve represents original Rochelle salt and the upper curve represents the deuterated salt.

b. BaTiO$_3$

The BaTiO$_3$ is the most important and most completely investigated representative of the perovskites type ferroelectrics. In the non-ferroelectric state (i.e. above 393 K) it has cubic symmetry as shown in Fig.1.4.3 (a). The Ba^{2+} ions are positioned at the corners, O^{2-} ions at the centre of the faces and the Ti^{4+} ion is located at the centre of the cube. It has an

arrangement of highly polarizable oxygen ions in the form of an octahedron with a small titanium ion at the centre [Fig 1.4.3(b)].
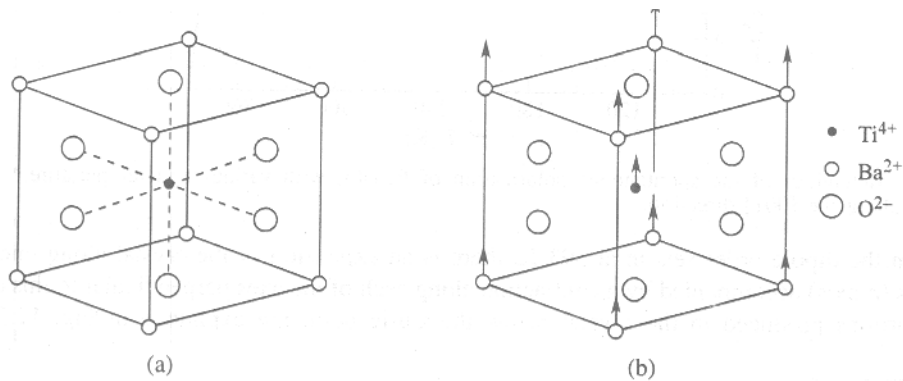

Fig. 1.4.3. a) Unit cell of $BaTiO_3$ (perovskite structure) b) Main distortion in $BaTiO_3$ Unit cell that gives rise to ferroelectricity.

The dielectric and spontaneous polarization over a range of temperatures are shown in figs. 1.4.4 and 1.4.5, respectively.
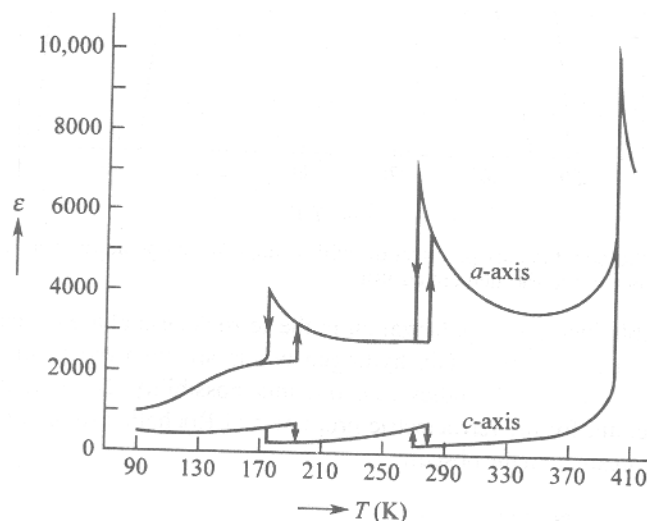

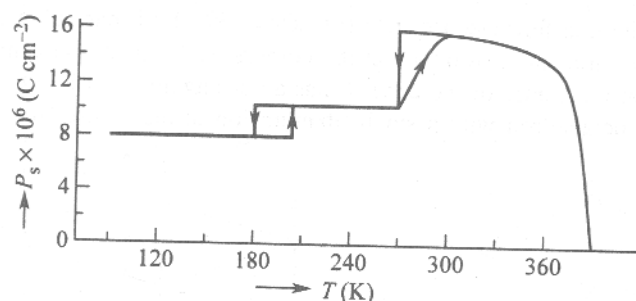Fig.1.4.4. Variation of the dielectric constant $BaTiO_3$ with change in temperature.

Fig. 1.4.5. Behaviour of the spontaneous polarisation of $BaTiO_3$ with variation in temperature.

The curves clearly indicate that there are three ferroelectric phases of crystal whose brief details may be put as:

Temperature range	Direction of P_s	Crystalline symmetry
278-393 K	[001]	Tetragonal
193-278 K	[011]	Orthorhombic
< 193 K	[111]	Rhombohedral

When the dipole order sets in at 393 K, there is an expansion of the crystal along one pseudo-cubic axis(c-axis) accompanied by a contraction along each of the axes perpendicular to this direction. The distortions produced in the crystal below the Curie point are explained in fig. 1.4.3(b). The sub-lattice of all the Ba^{2+} and Ti^{4+} ions is shifted with respect to the sub-lattice of the O^{2-} ions, the displacement d being barely ~0.1 A^0 at room temperature. This leads to the dipole moment per unit cell p, given by

$$p = 6e \cdot d = 0.96 \times 10^{-29} \text{ C m}$$

The dipole moment p can alternatively be estimated by multiplying P_s (as obtained from Fig.1.4.5 at room temperature) by the unit cell volume. Treating the unit cell as a simple cube of edge 4 A^0 even in the ferroelectric state, we get $p = 0.3(4 \times 10^{-10})^3 = 1.92 \times 10^{-29}$ C m. Thus we find this value agrees very well with that obtained on the basis of the observed deformation of the unit cell. The order of magnitude gives a measure of the ferroelectric effect in $BaTiO_3$. The effect, however, is fairly large in some other perovskites (e.g. $LiNbO_3$).

The fact that Fig.1.4.5 shows P_s along the [001] direction, warrants our further attention. This implies that we must multiply the values shown in the figure by $\sqrt{2}$ and $\sqrt{3}$ to obtain the actual values in the regions 193 K < T < 278 K and T<193K, respectively, because the direction of P_s in these regions is along the [011] and [111] directions, respectively. It is then quite interesting to note that spontaneous polarization (same as the saturation polarization) remains almost constant below 300K.

1.4.3. Theory of the ferroelectric displacive transitions

The theory that gives a good account of transitions in perovskites type crystals merits a separate treatment on account of having stood the test of vast experimental data. These crystals generally undergo a displacive transition at the Curie point. We can follow two approaches for finding interpretation to a displacive transition. One approach is the **polarization catastrophe** and the other one is the **soft mode approach**.

The polarization catastrophe refers to an unusual situation in which the polarization becomes infinitely large. In this condition the force exerted by the local electric field is greater than the elastic restoring force. This produces an asymmetric shift in the positions of positive and negative ions. The shift is, however, limited to a finite displacement by the anharmonic restoring forces.

In the soft mode approach a transverse optical (TO) mode is frozen, i.e. its frequency vanishes at some point in the Brillouin zone below the Curie temperature. This TO mode is known as a soft mode. When $\omega_T = 0$, the crystal becomes unstable because of the absence of an effective restoring force.

Polarization Catastrophe

The Clausius-Mossotti relation (1.2.14) can be rearranged in the form

$$\varepsilon = 1 + \frac{3(N_i\alpha_i + N_e\alpha_e)}{3\varepsilon_0 - (N_i\alpha_i + N_e\alpha_e)} \qquad (1.4.2)$$

where

N_i and N_e are the density of polarizable ion pairs and electrons, respectively and

α_i and α_e are the ionic and electronic polarizabilities, respectively.

When

$$(N_i\alpha_i + N_e\alpha_e) = 3\varepsilon_0 \qquad (1.4.3)$$

the dielectric constant becomes infinite [from 1.4.2], giving the state of polarization catastrophe.

Further,

$$P = (N_i\alpha_i + N_e\alpha_e)\, E_{loc}$$

$$= (N_i\alpha_i + N_e\alpha_e) \left[E + \frac{P}{3\varepsilon_0} \right] \qquad (1.4.4)$$

for a cubic crystal (using Lorentz expression for E_{loc}).

If E = 0, then from (1.4.4) we have

$$P\left(\frac{N_i\alpha_i + N_e\alpha_e}{3\varepsilon_0} - 1\right) = 0 \qquad (1.4.5)$$

But, when the polarization catastrophe occurs, the quantity within the brackets equals zero [from (1.4.3)].

This requires that

$$P \neq 0 \qquad (1.4.6)$$

for (1.4.5) to be true.

This result (1.4.6) is true only when applied field is zero.

In order to understand the above situation, let us consider a highly polarizable ionic crystal of cubic symmetry. Let α be the total polarizability and p the dipole moment of an ion pair. Let us assume that some transient stray field starts polarizing the ion pairs. The ion pairs will keep on polarizing until some resistance develops to stop the process. The resistance that finally stops the process of polarization exists in the form of anharmonic restoring forces. The dipole moment of a single ion pair with ion separation x is

$$P = q.x = \alpha \; E_{loc} = \left(\frac{\alpha F}{q}\right) \qquad (1.4.7)$$

where F is the restoring force that tends to bring the positive and negative ions together and q is the charge on each ion.

The work required to create N such dipoles in the unit volume of the crystal is

$$E_1 = N \int F.dx = \frac{Nq^2}{\alpha} \int x.dx = \frac{Np^2}{2\alpha} \; \text{(using 1.4.7)} \qquad (1.4.8)$$

$$= \frac{P^2}{N2\alpha}$$

On the other hand, the energy density associated with the electrical displacement due to E_{loc} is

$$E_2 = \int E_{loc}. dP$$

$$= \int\left(E + \frac{P}{3\varepsilon_0}\right). dP$$

$$= \frac{P^2}{6\varepsilon_0} + \int E.dP \qquad (1.4.9)$$

since E_1 is set against E_2, the net energy density of a polarized dielectric is

$$E_2 - E_1 = \frac{P^2}{2N\alpha}\left(\frac{N\alpha}{3\varepsilon_0} - 1\right) + \int E.dP \qquad (1.4.10)$$

This shows that even when $E = 0$, E2>E1, provided that

$$N\alpha \geq 3\varepsilon_0 \qquad (1.4.11)$$

The above condition in a general case is written in the form

$$\sum_j N_j \alpha_j \geq 3\varepsilon_0 \qquad (1.4.12)$$

where Nj stands for the density of the j th type of particles (ions/electrons) in the crystal and α_j denotes the polarizability of a single particle of this type.

The sign of equality in (1.4.12) describes the condition of polarization catastrophe (1.4.3) with

$$\sum_j N_j \alpha_j \equiv N_i A_i + N_e \alpha_e \qquad (1.4.14)$$

From relation (1.4.10) it follows that the energy of the crystal becomes smaller in the presence of induced dipoles. The minimum value of $\sum_j N_j \alpha_j$ for which the ferroelectricity would occur is $3\varepsilon_0$. In any real ferroelectric crystal the situation that exactly corresponds to the polarization catastrophe is not found. However, a small deviation in the value of $\sum_j N_j \alpha_j$ from $3\varepsilon_0$ changes the value of ε (1.4.2) by a large amount.

If we express $\sum_j N_j \alpha_j = 3\varepsilon_0 - 3\beta$

with $\beta \ll 1$ and using (1.4.2), we get

$$\varepsilon \propto \frac{1}{\beta} \qquad (1.4.15)$$

If we assume that β is a linear function of temperature near the Curie point and given by

$$\beta = \frac{T - T_c}{\eta} \qquad (1.4.16)$$

η being a constant, then

$$\varepsilon \propto \frac{1}{T - T_c} \qquad\qquad (1.4.17)$$

The temperature dependence of ε as a given by this relation is in excellent agreement with the observed behaviour in several perovskite crystals.

Ferroelectricity in perovskite crystal is understood in view of the following remarks made in respect of barium titanate:

1. **The titanium ion motion**. The barium ions situated at the cube corners leave a big void at the centre position. Since titanium ion is smaller than barium ion, it is unable to fill the void and is free to rattle around in the void. Because the ionic polarizability is a measure of the ease of displacement, its value increased.

2. **The non-cubic symmetry around oxygen ions**. Unlike the barium and titanium ions, the oxygen ions are in the non-cubic environment. An oxygen ion has only two nearest neighbours in the form of titanium ions. Because of this reason, E_{loc} is greater than the value given by Lorentz expression.

A larger value of α predicted under point 1 leads to a smaller value of deformation energy E_1 or the work required to create induced dipoles. Similarly, a large value of E_{loc} as expected under point 2 implies that the dipolar attraction will be larger. Thus, larger values of both α and E_{loc} are favourable to the onset of ferroelectricity.

Soft mode approach

As mentioned earlier, a ferroelectric state can be regarded as a **frozen in** TO phonon. According to Lyddane-Sachs-Teller relation (popularly known as LST relation)

$$\frac{\omega_{TO}^2}{\omega_{LO}^2} = \frac{\varepsilon_\infty}{\varepsilon_s}$$

where ε_s is the static dielectric constant , ε_∞ is the dielectric constant at optical frequencies, ω_{TO} and ω_{LO} are the transverse and longitudinal optical mode frequencies.

Above expression shows that as ε_s increases, ω_{TO} decreases; thus, in the case of an infinitely large ε_s, which happens at the Curie point (T_c), ω_{TO} may even be zero. In practice , ε_s remains finite on approaching T_c. The TO modes in question are called soft modes. Such TO modes have surprisingly low frequencies. For example, $BaTiO_3$ has a soft mode of frequency 12 cm^{-1} at 297 K which is low for a TO mode.

We are not concerned here with LO phonons whose frequency is higher for the same value of the wave vector. At the transition point T_c when ω_{TO} approaches the zero value, the crystal

becomes unstable and anharmonic elastic forces come into play. In the presence of anharmonic forces, ω_{TO} may show a temperature dependence of the form

$$\omega_{TO}^2 \propto (T - Tc) \qquad\qquad (1.4.18)$$

On assuming that ω_{TO} are temperature dependent, the LST relation in view of (1.4.18) gives

$$\frac{1}{\varepsilon_s} \propto (T - Tc) \qquad\qquad (1.4.19)$$

Experimental results on several perovskite ferroelectrics strongly support that a large static dielectric constant (ε_s) is associated with a low TO phonon (the soft mode). In view of (1.4.18) and (1.4.19) the temperature dependence of the energy of a low frequency TO phonon can be directly compared with that of the inverse dielectric constant, as shown in Fig. 1.4.6 for a KTaO3 crystal. To have a clear idea, a schematic representation of the temperature dependence of $\varepsilon_s^{-1}, \omega_{TO}^2$ and the saturation polarization Ps is shown in Fig. 1.4.7
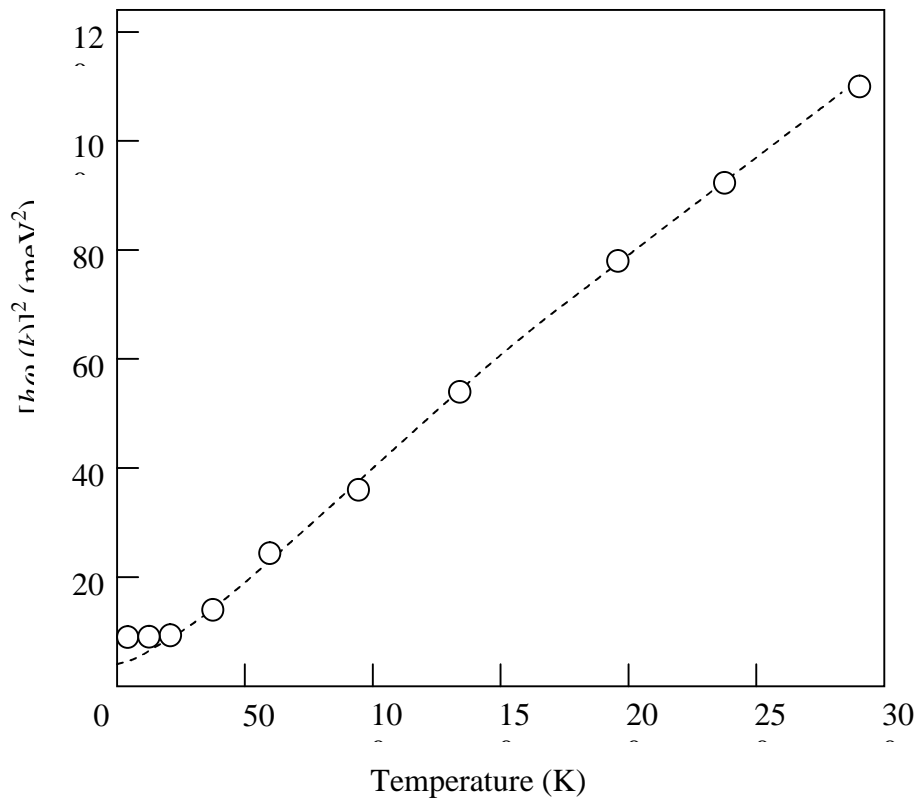

Fig. 1.4.6 Temperature dependence of TO mode at K = 0 in KTaO$_3$. The square of the phonon energy (points) is compared with the reciprocal of the dielectric constant (dashed line)
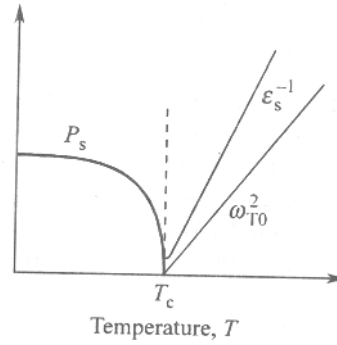
Fig. 1.4.7.

1.4.4. Thermodynamic theory of the ferroelectric transition

It is of interest to investigate the behaviour of a ferroelectric in the vicinity of its transition temperature T_c on the basis of thermodynamic arguments. A thermodynamic theory has the advantage of being independents of any particular atomic model and thus leads to quite general conclusions. Although such a theory does not provide the physical mechanism responsible for the ferroelectric properties of a given material, it does point to certain features one should look for in atomic models.

Consider a crystal which is ferroelectric for temperature $T < Tc$. Let x denote the relative displacement of the centres of the positive and negative ions in the crystal during a particular mode of vibration. If F_0 be the free energy of the unpolarized crystal, the free energy of the polarized crystal F is a function of the even powers of x. That is,

$$F-F_o = \phi_2 \, x^2 + \phi_4 \, x^4 + \phi_6 \, x^6 + \ldots \qquad (1.4.20)$$

The constants ϕ are functions of all other displacements and given by their thermal average values. They are thus functions of temperature. Since the electric polarization P is proportional to the displacement x, we have

$$F - F_o = \frac{1}{2} \lambda_2 P^2 + \frac{1}{4} \lambda_4 P^4 + \frac{1}{6} \lambda_6 P^6 + \ldots \qquad (1.4.21)$$

The constants λ are the functions of temperature. The numerical factors are introduced to facilitate calculations.

Consider first the paraelectric phase of the crystal, i.e., for $T>Tc$. If a small electric field E is applied in the absence of any external pressure, the following thermodynamic relation holds good :

$$dF = - SdT + E \, dP \qquad (1.4.22)$$

where S represents the entropy of the crystal.

For smaller E, P will also be smaller, and hence we retain only the first term in (1.4.21) neglecting all; and hence other terms in the first approximation. Then, using (1.4.22) we have

$$E = \left(\frac{\partial F}{\partial P}\right)_T = \lambda_2 P \qquad (1.4.23)$$

The electric susceptibility χ_P in the paraelectric phase is given by

$$\frac{1}{\chi_P} = \frac{\varepsilon_0}{P}\left(\frac{dE}{dP}\right) = \varepsilon_0 \lambda_2 \qquad \text{[from (1.4.23)]} \qquad (1.4.24)$$

using the Curie-Weiss law (1.4.1), we have

$$\varepsilon_0 \lambda_2 = \frac{T - Tc}{C}$$

or $$\lambda_2 = C_1(T\text{-}T_c) \qquad (1.4.25)$$

where C1 is another constant.

Relation (1.4.25) shows that λ_2 increases linearly with increase in temperature. As a result of this temperature dependence, λ_2 varies from positive values to negative values as the temperature is lowered from above T_c to below T_c.

In the state of thermal equilibrium, the free energy is minimum which requires that

$$\left(\frac{\partial F}{\partial P}\right)_T = 0$$

Applying this condition to (1.4.21) in the absence of the applied electric fields, we have

$$\lambda_2 P + \lambda_4 P^3 + \lambda_6 P^5 + \ldots\ldots = 0 \qquad (1.4.26)$$

The spontaneous polarization is bound to satisfy (1.4.26) and

$$P_s(\lambda_2 + \lambda_4 Ps^2 + \lambda_6 Ps^4 + \ldots) = 0 \qquad (1.4.27)$$

We find that $P_s = 0$ is always a root of (1.4.27). For this solution the free energy has a minimum provided λ_2 is positive $\left(\frac{\partial^2 F}{\partial P^2} = \lambda_2\right)$. However, if λ_2, λ_4 and λ_6 are all positive and higher order terms are neglected, the condition (1.4.27) is satisfied only for $P_s = 0$. Thus, $P_s = 0$ corresponds to the only minimum of the free energy and the paraelectric phase exists for the positive sign of λ_2, λ_4 and λ_6.

When the temperature is lowered through the transition point, λ_2 goes from positive do negative values while passing through $\lambda_2 = 0$ at the transition point. There are two interesting situations that are identified in terms of the signs of λ_2, λ_4 and λ_6. These characterize two cases of particular interest namely **second-order** and **first-order transitions**.

Second-order Transitions: If the coefficients $\lambda_4, \lambda_6, \ldots$ are all positive and the value of λ_2 varies from positive to negative as the temperature is lowered, the free energy changes as shown in Fig. 1.4.8 (a). Neglecting the terms beyond the second term in (1.4.27) are negligible, we get

$$P_s^2 = -\frac{\lambda_2}{\lambda_4} = \frac{C_1(T_c - T)}{\lambda_4} \qquad (1.4.28)$$

Hence Ps is a continuous function of temperature and falls continuously to zero at T = Tc as shown in Fig. 1.4. 8 (b).

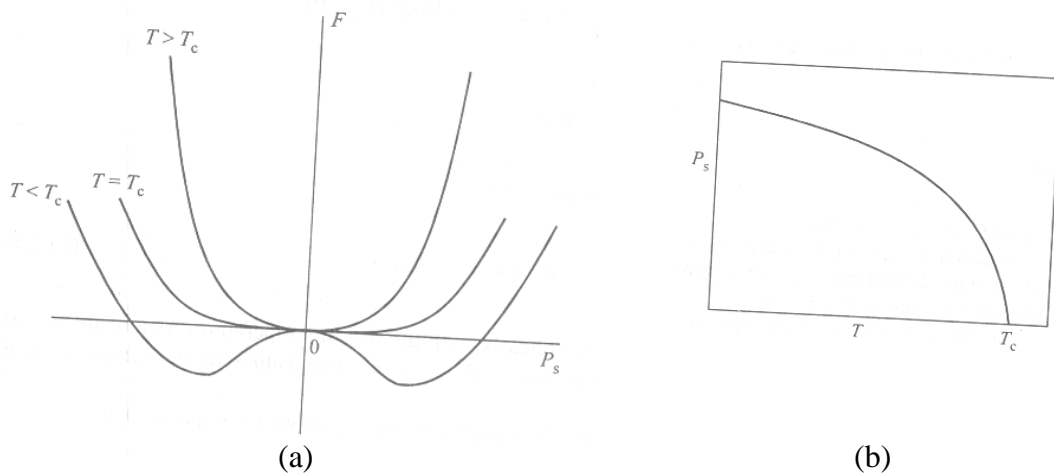(a)   (b)

Fig. 1.4.8 Second order transition (a) Free energy as a function of polarization as the temperature is varied. (b) Temperature dependence of the spontaneous polarization below the transition temperature T_c.

It is useful to examine the spontaneously polarized state in terms of the frequency of normal modes. From the forms of the free energy (1.4.20) and (1.4.21), it follows that

$$\phi_2 \text{ or } \lambda_2 = \omega_i^2(k)$$

and hence in view of (1.4.25),

$$\omega_i^2(k) \propto (T - T_c) \qquad (1.4.29)$$

where $\omega_i(k)$ is the frequency of the normal mode i (a TO mode). The transition takes place when $\omega_i(k) \to 0$. This decrease in the mode frequency is called ***softening***. This indicates that the harmonic restoring forces are becoming very weak, permitting a large displacement which is limited solely by anharmonic forces. When $\omega i^2(k)$ or λ_2 is small and positive then the crystal lattice becomes soft and close to instability. Below T_c, λ_2 is negative and hence also $\omega_i^2(k)$; which implies that the unpolarized lattice is unstable and the crystal is in the spontaneously polarized ferroelectric state.

       The heat capacity is given by

$$C_v = C_1^2 T / \lambda_4 \hspace{2cm} (1.4.30)$$

The heat capacity falls discontinuously to zero at T =Tc (see Fig. 1.4. 9). But there is no latent heat at the transition. Such a transition is called a second-order transition.
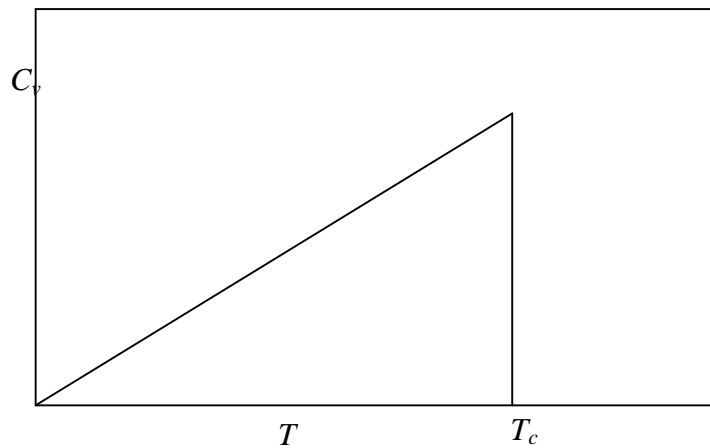

Fig. 1.4.9 Temperature dependence of specific heat showing anomaly at a second-order phase transition

       The transitions in Rochelle salt, KH_3PO_4 and $LiTaO_3$ are some examples of the second-order transition. The transition to the superconducting state is the most popular example of this type of transition.

First-order Transitions

We have seen that when λ_2 is negative and λ_4 is positive, the transition is of the second-order type. We now consider a situation where λ_4 is negative and λ_6 is positive. Positive values of λ_6 are considered to restrain the free energy from going to minus infinity. As per expression (1.4.25), λ_2 varies from positive to negative as the crystal is cooled through the Curie point. The corresponding free energy curves are shown in Fig. 1.4.10.

The thermal equilibrium condition, $\dfrac{\partial F}{\partial P} = 0$, in the absence of the applied electric field gives

$$\lambda_2 P_s + \lambda_4 P_s{}^3 + \lambda_6 P_s{}^5 = 0 \qquad\qquad (1.4.31)$$

which implies that either $P_s = 0$, or

$$\lambda_2 + \lambda_4 P_s{}^2 + \lambda_6 P_s{}^4 = 0 \qquad\qquad (1.4.32)$$

At $T = T_c$, the free energy in the paraelectric state is equal to that in the ferroelectric state, i.e.,

$$F_0(T_c) = F(T_c) \qquad\qquad (1.4.33)$$

Using (1.4.34) in (1.4.21), we have

$$0 = \frac{1}{2}\lambda_2 P_s{}^2 (T_c) + \frac{1}{4}\lambda_4 Ps^4 (T_c) + \frac{1}{6}\lambda_6 Ps^6 (T_c) + \qquad\qquad (1.4.34) \; ..$$

Then using (1.4.32), we get

$$\lambda_2 + \lambda_4 P_s{}^2 (T_c) + \lambda_6 P_s{}^4 (T_c) = 0 \qquad\qquad (1.4.35)$$

Substituting the value of $\lambda 2$ from (1.4.35) in (1.4.34) and solving for $P_s{}^2(T_c)$. We get

$$P_s{}^2(T_c) = -\frac{3}{4}\left(\frac{\lambda_4}{\lambda 6}\right) = \frac{3}{4}\frac{|\lambda_4|}{\lambda_6} \qquad\qquad (1.4.36)$$

And with

$$\lambda_2 = \frac{3}{16}\left(\frac{\lambda_4^2}{\lambda_6}\right) \qquad\qquad (1.4.37)$$

$$P_s{}^4(T_c) = \frac{3\lambda_2}{\lambda_6} \qquad\qquad (1.4.38)$$

At the transition point there are two minima of free energy with equal value; one at $P_s(T_c) = 0$ in the paraelectric phase and the other for the value of $P_s(T_c)$ given by (1.4.36) in the ferroelectric phase. Thus there is a jump [see Fig. (1.4.12)] in the value of P_s at T_c, meaning thereby that the spontaneous polarization (the order parameter) drops discontinuously to zero at $T = T_c$ when a ferroelectric crystal is heated slowly. Such transitions are called the first-

order transitions. The other important property of these transitions is that there is a latent heat at the transition. A well known example of this type of transition is the upper transition in a BaTiO$_3$ crystal.

T

Fig. 1.4.10. a) Free energy as a function of polarisation as the temperature is varied near a first order phase transition. (b) Fall of the spontaneous polarisation below the transition point T_c in a first order phase transition.

1.4.5 Ferroelectric Domains

When a ferroelectric is cooled from the paraelectric phase through the Curie temperature, the polarized phase may be nucleated at several points in the crystal. These nuclei generally differ in the direction of polarization since there may be several equivalent crystallographic directions in which the spontaneous polarization can occur. In the case of BaTiO$_3$, the spontaneous polarization may occur along any one of the three edges, giving six possible directions for the spontaneous polarization. Thus, as the nuclei grow through the crystal in the ferroelectric crystal in the ferroelectric phase, they form several regions or domains differing in their direction of polarization. The vector sum of these polarizations may not be always big enough to show up macroscopically.

Polarization is accompanied by some distortion of the unit cell and the domain walls are consequently in a state of strain; but the dimensional changes are relatively small. Though the domain walls act as interruptions in the regularity of the crystal, they are not regarded as grain boundaries between different crystals. A domain wall is instead, treated as a sub-grain within a single crystal. As soon as a single nucleus of the polarized phase is

formed, the polarized phase begins to grow much faster in the direction of polarization than in the transverse directions. Because of this reason the growing domains are usually wedge-shaped. This was revealed by optical birefringence studies on $BaTiO_3$.

The ferroelectric domains are regarded as the electrical analogues of the ferromagnetic domains despite the fact that there are some interesting differences in their origin and growth. When the electric field is applied on a ferroelectric crystal, the number and size of domains that are polarized in the field increase. As a result of this effect, upon the reversal of the field direction a hysteresis in the P versus E curve is observed.

1.4.6 Antiferroelectricity

Similar to ferroelectrics there is another group of solids, which has induced, ordered electric dipoles below a characteristic temperature but do not show spontaneous bulk polarization. In these crystals the neighbouring atomic lines are associated with antiparallel polarization because of which the bulk polarization of the crystal vanishes. Crystals exhibiting this property are called **antiferroelectric** crystals and the property is known as **antiferroelectricity**. The structural requirement for the ferroelectrics and antiferroelectric phases being common, a number of well-known antiferroelectric crystals are found to be isomorphous with some ferroelectrics. For example, ammonium dihydrogen phosphate (ADP) is isomorphous with potassium dihydrogen phosphate (KDP).

Perovskite type crystals are known to be susceptible to several types of deformation with almost equal energy difference between them. In many of them the coupling through the oxygen octahedral causes adjacent lines of basic cells to be polarized in opposite directions. Below a certain temperature the resultant deformation is such that the total energy in the antiparallel arrangement of adjacent lines of dipoles is lower, when compared separately to that in state of fully parallel arrangement of dipoles and to that in the state with no induced dipoles. Lead Zirconate ($PbZrO_3$) is a notable example of these perovskites. It shows to

antiferroelectric phases, one each ferroelectric and paraelectric phases over different ranges of temperature.

1.4.7   Summary of lesson

The origin of ferroelectric property and classification of various ferroelectric materials have been discussed in depth. The theory relating to first order and second order transition of $BaTiO_3$ has also been presented systematically. The phenomenon of antiferroelectricity has also been explained briefly.

1.4.8 Key-Terminology

Piezoelecticity-pyroelectricity-ferroelectricity-antiferroelectricity-polarization catastrophe-ferroelectric first-order and second order transitions.

1.4.9   Self-assessment questions

1. Explain piezoelectric, pyroelectric and ferroelectric crystals.

2. Discuss about the representative crystal types of ferroelectrics.

3. Explain the ferroelectric properties of Rochelle salt.

4. Explain the ferroelectric properties of $BaTiO_3$.

5. Discuss the ferroelectric transitions in perovskites based on polarization catastrophe.

6. Discuss the ferroelectric transitions in perovskites based on soft mode approach.

7. Explain the thermodynamic theory of ferroelectric transition for both second-order and first-order transitions.

1.4.10   Reference Books

1. Solid State Physics- A.J.Dekker (Macmillan India Limited).

2. Elements of Solid state Physics- J.P.Srivastava (Prentice-Hall of India, New Delhi).

UNIT-I
LESSON –5
PIEZOELECTRICITY

Objective

To discuss the concepts of piezoelectricity and electrostriction in piezoelectric crystals and also the applications of piezoelectric crystals.

Structure of the lesson

      1.5.1.. Introduction

      1.5.2 Electrostriction

      1.5.3 Applications of piezoelectric crystals

1.5.1 Introduction

Piezoelectricity is the ability of certain dielectric crystals to produce a voltage when subjected to mechanical stress. The word is derived from the Greek *piezein*, which means to squeeze or press. The effect is reversible; piezoelectric crystals, subject to an externally applied voltage, can change shape by a small amount. The effect is of the order of nanometres, but nevertheless finds useful applications such as the production and detection of sound, generation of high voltages, electronic frequency generation, and ultra fine focusing of optical assemblies.

History

Pyroelectricity, the ability of certain mineral crystals to generate electrical charge when heated, was known of as early as the 18th century, and was named by David Brewster in 1824. In 1880, Pierre Curie and Jacques Curie brothers predicted and demonstrated piezoelectricity using tinfoil, glue, wire, magnets, and a jeweler's saw. They showed that crystals of tourmaline, quartz, topaz, cane sugar, and Rochelle salt generate electrical polarization from mechanical stress. Quartz and Rochelle salt exhibited the most piezoelectricity. Twenty natural crystal classes exhibit direct piezoelectricity.

Converse piezoelectricity was mathematically deduced from fundamental thermodynamic principles by Lippmann in 1881. The Curies immediately confirmed the existence of the "converse effect," and went on to obtain quantitative proof of the complete reversibility of electro-elasto-mechanical deformations in piezoelectric crystals.

Piezoelectric materials

In addition to the materials listed above, many other materials exhibit the piezoelectric effect, including quartz analogue crystals like berlinite ($AlPO_4$) and gallium orthophosphate ($GaPO_4$), ceramics with perovskite or tungsten-bronze structures ($BaTiO_3$, $KNbO_3$, $LiNbO_3$, $LiTaO_3$, $BiFeO_3$, $NaxWO_3$, $Ba_2NaNb_5O_5$, $Pb_2KNb_5O_{15}$). Polymer materials like rubber, wool, hair, wood fiber, and silk exhibit piezoelectricity to some extent. The polymer polyvinylidene fluoride, ($-CH_2-CF_2-$)n, exhibits piezoelectricity several times larger than quartz. Bone exhibits some piezoelectric properties: it has been hypothesized that this is part of the mechanism of bone remodelling in response to stress.

Mechanism of piezoelectricity

In a piezoelectric crystal, the positive and negative electrical charges are separated, but symmetrically distributed, so that the crystal overall is electrically neutral. When a stress is applied, this symmetry is disturbed, and the charge asymmetry generates a voltage. A 1 cm cube of quartz with 500 lbf (2 kN) of correctly applied force upon it, can produce 12,500 V of electricity.

Piezoelectric materials also show the opposite effect, called **converse piezoelectricity**, where application of an electrical field creates mechanical stress (distortion) in the crystal. Because the charges inside the crystal are separated, the applied voltage affects different points within the crystal differently, resulting in the distortion. The bending forces generated by converse piezoelectricity are extremely high, of the order of tens of mega newtons, and usually cannot be constrained. The only reason the force is usually not noticed is because it causes a displacement of the order of a few nanometres.

Requirements for a crystal to show piezoelectric behaviour were discussed in the previous Lesson. We showed earlier that all ferroelectrics are piezoelectrics and that its converse is not true. For example, quartz is piezoelectric but it does not possess the ferroelectric property.

The foremost condition for a crystal to piezoelectric is the absence of the centre of symmetry. Figure 1.5.1(a) shows the array of a simple two-dimensional ionic crystal with no centre of symmetry. It is evident that a compressive force **F** [Fig. 1.5.1(b)] decreases the

electric dipole moment (hence the polarization) and a tensile force **F** [Fig. 1.5.1(c)] increases the same. This is essentially the piezoelectric effect. We must appreciate that the displayed crystal [Fig. 11.14(a)] could well be a ferroelectric crystal.
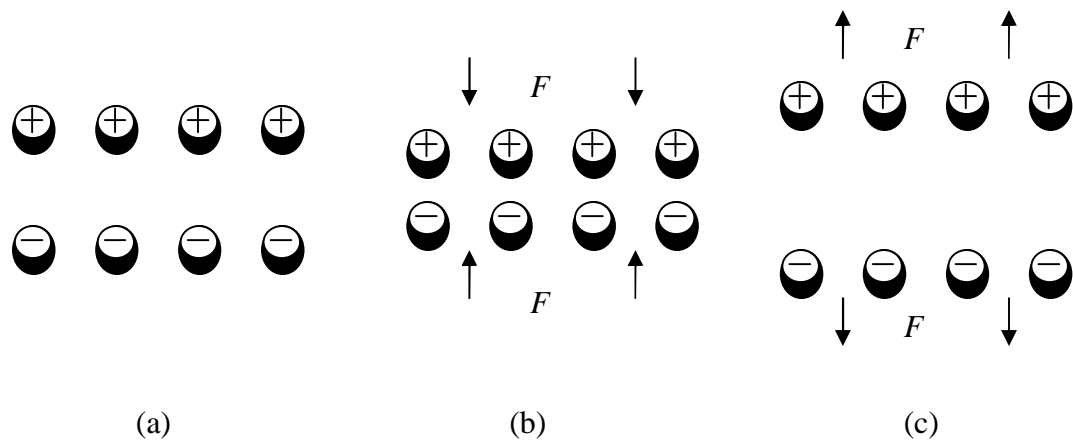

(a)   (b)   (c)

Fig. 1.5.1(a) A two-dimensional ionic crystal with no centre of symmetry. (b) Compression under the action of force *F* decreases the polarization. (c) Extension of structure under the action of force *F* increases the polarization

Next we take up another example to show how the symmetry of a non-centrosymmetric crystal controls firstly the magnitude and direction of polarization when the crystal is stressed and secondly the crystal dimensions when the crystal is polarized.

Consider a molecule of hypothetical ionic solid which at equilibrium has three electric dipoles of equal magnitude distributed over 360^0 at an interval of 120^0. The molecules belong to the point group 3m and its net dipole moment is zero. But if the molecule together with the crystal is stressed or compressed along a direction parallel or antiparallel to one of the three directions of the dipole moment, a net dipole moment would appear [see Fig. 1.5.2(b) and (c)]. Similarly, a molecule may be distorted by an electric field applied along one of the three arrows shown in the Fig. 1.5.2(a). The electric field produces an elongation or contraction of the crystal along the field direction and a length change of opposite sign in the lateral direction. An applied field that is perpendicular to one of the three dipole directions in Fig. 1.5.2(a) finds itself perpendicular to a mirror plane of symmetry and, therefore, is rendered ineffective in changing the crystal dimensions.

Because of lack of centre of symmetry and complex structure of piezoelectrics, their electrical behaviour under strain or strain behaviour under an electric field is not isotropic in nature. Nevertheless, a simple picture of the phenomena can be presented in a schematic one-dimensional notation by the following equations:

$$P = \sigma\, d + \varepsilon_0\, E\, \chi:; \qquad e = \sigma\, s + Ed \qquad\qquad (1.5.1)$$

where P is the polarization, σ the stress, d the piezoelectric strain constant, ε_0 the permittivity of free space, E the electrical field, χ the dielectric susceptibility, e the strain and s the elastic compliance constant.

In real crystals, however, the tensile, compressional or shear strains produced by an electrical field may develop in different directions and depend on the crystal orientation and the field direction in view of this fact the piezoelectric strain constants, that form a third rank tensor, are defined as

$$d_{ik} = \left(\frac{\partial e_k}{\partial E_j} \right)_\sigma$$

where $i \equiv x, y, z$ and $k \equiv xx, yy, zz,\ xy, yz, zx$

(a)   (b)   (c)
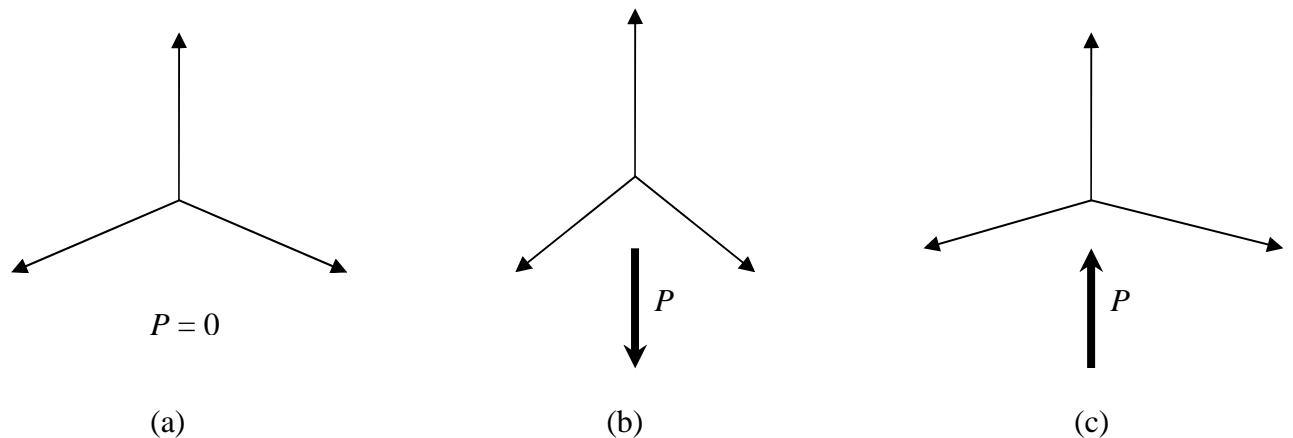
Fig. 1.5.2 Response of a piezoelectric molecule to strain: (a) Directions of polarization (in accordance with symmetry) in a molecule within an undistorted crystal in the state of equilibrium.
The net polarization of the molecules is zero. (b) A vertical tension or a horizontal compression causing a net polarization. (c) A vertical compression or a horizontal tension causing a net polarization

Depending on the application and the desired behaviour, a crystal is cut so as to have the parallel faces of the crystal in a specific orientation. ***An X-cut is defined as a section cut from the crystal such that the x-axis of the crystal is perpendicular to parallel crystal faces***. In order to obtain certain desirable properties the crystals are sometimes given oblique cut that is cut at angles is different from 90 degrees with the principal axes.

1.5.2 Electrostriction

It is appropriate to discuss a more universal phenomenon of deformation in crystals that is caused by an applied electrical field. It refers to the deformation in ionic crystals and the effect is commonly known ***electrostriction***.

Electrostriction is a property of all electrical non-conductors, or dielectrics that produces a relatively slight change of shape, or mechanical deformation, under the application of an electric field. Reversal of the electric field does not reverse the direction of the deformation.

In the first approximation the deformation of piezoelectric crystal is proportional to applied electrical field and the stress induced polarization varies linearly with the strain produced. But in ionic crystals, which do not have to be necessarily piezoelectrics, the strain is much smaller and proportional to the square of electrical field. We can understand the origin of electrostriction by appreciating that dipoles created by the applied electrical field would interact with each other. The inline dipoles attract each other with a repulsive poles acting perpendicular to the direction of the polarization.

Let p denote the moment of a dipole and r the separation between two inline dipoles. The value of the electric field caused by a dipole at its in-line neighbour may be written as

$$E = \frac{1}{4\pi\varepsilon_0} \frac{2p}{r^3} \qquad\qquad (1.5.2)$$

The energy of a dipole in the field U(r) and the corresponding attractive force F are related as

$$F = -\frac{dU(r)}{dr}$$

and $U r) = - p.E$

These relations yield

$$F = -\frac{1}{4\pi\varepsilon_0} \frac{6p^2}{r^4} \qquad\qquad (1.5.3)$$

Similarly, we can find that the repulsive force is given by

$$F = \frac{1}{4\pi\varepsilon_0}\frac{3p^2}{r^4} \qquad (1.5.4)$$

Since p = αE, the attractive force can be expressed as

$$F = -\frac{1}{4\pi\varepsilon_0}\left(\frac{6\alpha^2}{r^4}\right)E^2 \qquad (1.5.5)$$

To a first approximation the strain or deformation u may be assumed to follow the Hooke's law and then

$$u = -\frac{F}{k}$$

where k is the usual force constant in the direction of the in-line dipoles.

Using the expression (1.5.5) in the above relation, we get

$$U = \frac{1}{4\pi\varepsilon_0}\left(\frac{6\alpha^2}{kr^4}\right)E^2 \qquad (1.5.6)$$

Thus, there will occur a compression in the field direction and an extension perpendicular to the field direction. The above treatment holds for permanent dipoles as well on account of the effective dipole moment being proportional to the electric field.

1.5.3 Applications of piezoelectric crystals

It may be recalled all ferroelectrics are piezoelectrics, though the conversion is not true. As a result, ferroelectric materials have been frequently used in many applications that are based on the principle of piezoelectricity. But, because of importance of properties such

as mechanical and thermal strength the use of certain piezoelectric crystals becomes inevitable.

Piezoelectric crystals are used in numerous ways:

High-voltage sources

Direct piezoelectricity of some substances like quartz, as mentioned above, can generate thousands of volts (known as high-voltage differentials).

- Probably the best-known application is the electric cigarette lighter: pressing the button squeezes an piezoelectric crystal, and the high voltage thus produced ignites the gas as the current jumps over a small spark gap. The portable electrical sparkers used to light gas grills or stoves work the same way.

- A similar idea being researched by the **Defense Advanced Research Projects Agency** (DARPA) in the USA in a project called *Energy Harvesting*, which includes an attempt to power battlefield equipment by piezoelectric generators embedded in soldiers' boots.

- A piezoelectric transformer is a type of AC voltage multiplier. Unlike a conventional transformer, which uses magnetic coupling between input and output, the piezoelectric transformer uses acoustic coupling. An input voltage is applied across a short length of a bar of piezoceramic material such as PZT, creating an alternating stress in the bar by the inverse piezoelectric effect and causing the whole bar to vibrate. The vibration frequency is chosen to be the resonant frequency of the block, typically in the 100 kilohertz to 1 megahertz range. A higher output voltage is then generated across another section of the bar by the piezoelectric effect. Step-up ratios of more than 1000:1 have been demonstrated. An extra feature of this transformer is that, by operating it above its resonant frequency, it can be made to appear as an inductive load, which is useful in circuits that require a controlled soft start.

Sensors

- To detect sound, e.g. piezoelectric microphones (sound waves bend the piezoelectric material, creating a changing voltage) and piezoelectric pickups for electrically amplified guitars.
- Piezoelectric oscillators are used to convert mechanical pulses into electrical ones and vice versa. The crystal in these devices works as a transducer. The acoustic pulses are used in underwater search (sonars) and other applications. The acoustic pulses are generated by the piezoelectric transducers excited by electrical fields in almost all search cases. The generation of ultrasonic waves is invariably accomplished by exploiting the above principle.

- Piezoelectric microbalances are used as very sensitive chemical and biological sensors.
- The piezoelectric effect in synthetic poly vinyliden fluoride (PVF_2) is about five times stronger than that in quartz. Being flexible and easy to handle like ultrasonic transducers, the PVF_2 films are frequently used in applications such as monitoring blood pressure and respiration.

- Piezoelectric elements are used in electronic drum pads to detect the impact of the drummer's sticks.

Actuators

As very high voltages correspond to only tiny changes in the width of the crystal, this width can be changed with better-than-micrometer precision, making piezo crystals the most important tool for positioning objects with extreme accuracy.

- Loudspeaker: Voltages are converted to mechanical movement of a piezoelectric polymer film.

- Piezoelectric elements can be used in laser mirror alignment, where their ability to move a large mass (the mirror mount) over microscopic distances is exploited to electronically align some laser mirrors. By precisely controlling the distance between mirrors, the laser electronics can accurately maintain optical conditions inside the laser cavity to optimize the beam output.

- A related application is the acousto-optic modulator, a device that vibrates a mirror to give the light reflected off it a Doppler shift. This is useful for fine-tuning a laser's frequency.

- Atomic force microscopes and scanning tunneling microscopes employ converse piezoelectricity to keep the sensing needle close to the probe.

Frequency standards

- Quartz clocks employ a tuning fork made from quartz that uses a combination of both direct and converse piezoelectricity to generate a regularly timed series of electrical pulses that is used to mark time. The quartz crystal (like any elastic material) has a precisely defined natural frequency (caused by its shape and size) at which it prefers to oscillate, and this is used to stabilize the frequency of a periodic voltage applied to the crystal.

- The same principle is critical in all radio transmitters and receivers, and in computers where it creates a clock pulse. Both of these usually use a frequency multiplier to reach the megahertz and gigahertz ranges.

- Crystals shaped to have a prescribed mechanical resonance frequency are used as narrow band electrical filters. Only those electrical signals whose frequency is coincidence with the mechanical vibrational frequency pass through the crystal and all other are rejected.

- The piezoelectric materials are used as delay lines. When an electrical signal is converted into an acoustic one to one and of a quartz rod. The signal passes along rod as an acoustic wave, travelling at velocity of sound. At the other end acoustic may converted into an electrical signal. The initial signal is thus delayed. Such an arrangement is often used in communication devices.

Piezoelectric motors

- Types of piezoelectric motor include the well-known travelling-wave motor used for auto-focus in reflex cameras, inchworm motors for linear motion, and rectangular four-quadrant motors with high power density (2.5 watt/cm³) and speed ranging from 10 nm/s to 800 mm/s. All these motors work on the same principle. Driven by dual orthogonal vibration modes with a phase shift of 90°, the contact point between two surfaces vibrates in an elliptical path, producing a frictional force between the surfaces. Usually, one surface is fixed causing the other to move. In most piezoelectric motors the piezoelectric crystal is excited by a sine wave signal at the resonant frequency of the motor. Using the resonance effect, a much lower voltage can be used to produce a high vibration amplitude.

1.5.4 SUMMARY OF LESSON

- Piezoelectricity is the ability of certain dielectric crystals to produce a voltage when subjected to mechanical stress.

- Pierre Curie and Jacques Curie brothers predicted and demonstrated piezoelectricity in 1880. They showed that crystals of tourmaline, quartz, topaz, cane sugar, and Rochelle salt generate electrical polarization from mechanical stress.

- Piezoelectric materials also show the opposite effect, called converse piezoelectricity, where application of an electrical field creates mechanical stress (distortion) in the crystal.

- The foremost condition for a crystal to piezoelectric is the absence of the centre of symmetry.

- Depending on the application and the desired behaviour, a crystal is cut so as to have the parallel faces of the crystal in a specific orientation. *An X-cut is defined as a section cut from the crystal such that the x-axis of the crystal is perpendicular to parallel crystal faces*.

- Electrostriction is a property of all dielectrics that produces a relatively slight change of shape, or mechanical deformation, under the application of an electric field.

- Reversal of the electric field does not reverse the direction of the deformation.

- The compression will occur in the field direction and an extension perpendicular to the field direction.

- Piezoelectric crystals are used in high-voltage sources, sensors, actuators, frequency standards, piezoelectric motors etc.,

1.5.5 KEY TERMINOLOGY

Piezoelectricity-converse piezoelectricity-electrostriction-applications of piezoelectric crystal.

1.5.6 SELF-ASSESSMENT QUESTIONS

    (i)   What is piezoelectricity? Explain the mechanism involved in the occurrence of piezoelectricity.

    (ii)   Express piezoelectric strain constants in form of tensor and explain the terms involved.

    (iii)   What is electrostriction? Obtain an expression for the relation between strain and electric field produced in piezoelectric effect.

    (iv)   Discuss various applications of piezoelectric crystals.

1.5.7 Reference Books

1. Solid State Physics- A.J.Dekker (Macmillan India Limited).
2. Elements of Solid state Physics- J.P.Srivastava (Prentice-Hall of India, New Delhi).

Unit – II

Lesson - 1

IMPERFECTIONS IN CRYSTALS- I
POINT DEFECTS

Objectives

To give the classification of defects, to discuss in detail point defects and to estimate the concentration of point defects in metallic and ionic crystals.

Structure of the lesson

2.1.1 Introduction

2.1.2 Point Defects

   a) Vacancies

   b) Interstitial atoms

   c) Colour centres

   d) Substitutional impurity atoms

   e) Excitons

2.1.3 Lattice defects and configurational entropy

2.1.4. Estimation of concentration of vacancies

   a) In metallic crystals

   b. In ionic crystals

2.1.1 Introduction

Any deviation in a crystal from perfect periodic structure is called an imperfection or a defect. Examples of such defect are vacant lattice sites, interstitial atoms, pairs of vacancies impurities, colour centres etc. A point defect is localized near an atom in a structure in contrast to the line or plane imperfections. Plane imperfections on the other hand may occur in the initial stages of the formation of a new crystal structure. Real crystals are imperfect in one way or the other and the physical properties of the solids are infact controlled by these imperfections. For example the colour of the crystal arises from imperfections. Similarly the luminescence, conductivity of the crystal is always dependent on the impurity. The mechanical and plastic properties are usually controlled by imperfections. This lesson deals with point defects and its related aspects.

2.1.2 Point Defects

Vacant lattice sites, interstitial atoms, pairs of vacancies impurities, colour centres etc. are some of the examples of point defects.

f) Vacancies

A normal lattice site from where an atom is missing is known as Schottky defect or a vacancy(Fig 2.1.1).
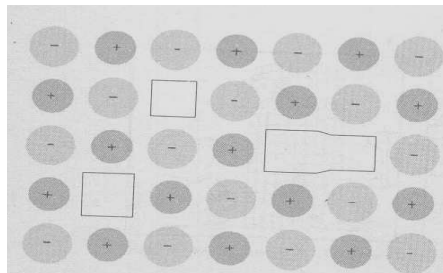
Fig : 2.1.1 A plane of a pure alkali halide crystal, showing a vacant negative positive ion site, a vacant negative ion site, and a coupled pair of vacant sites of opposite sign.

b) Interstitial atom

An atom located at a position different from the normal lattice is known as an interstitial or Frenkel defect(Fig 2.1.2)
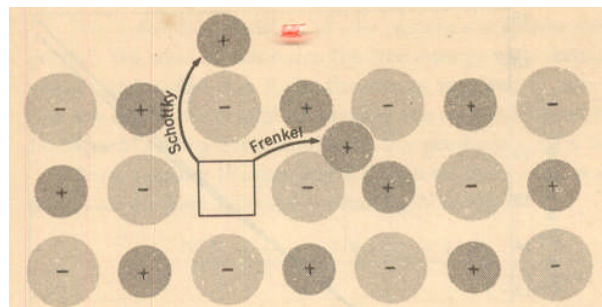
Fig. 2.1.2 Schottky and Frenkel defects in an ionic crystal. The arrows indicate the displacement of the ions. In a Schottky defect the ion is moved to the surface of the crystal; in a Frenkel defect

C. Colour Centres

When a crystal (especially the alkali halides like KCl, NaCl etc.) is exposed to ionizing radiations like rays or γ – rays or by introducing certain chemical impurities or by heating the

crystal in excess metallic vapour, the crystal gets coloured. The colour center absorbs visible light unlike a vacancy. Generally the most popular colour centres are F-centres when an electron is trapped at the negative ion vacancy this type of colour centres are formed

e^-

Fig 2.1.3 An F-center is a negative ion vacancy with one excess electron bound at the vacancy. The distribution of the excess electron is largely on the positive metal ions adjacent to the vacant lattice site.

D. Substitutional impurity atom

The presence of a foreign atom in the lattice it may be present at any interstitial position or any substitution position that is in place of any regular lattice site. In the latter case it is assumed to have the same valence shell configuration as that of the atom which is replaced. Sometimes these impurity atoms are essential for the use of the crystals in practical applications. For example Al_2O_3 mixed with Cr_2O_3 (Ruby) is used for the production of laser beam. Similarly, when a crystal like lithium fluoride mixed with manganese is used in radiation dosimetry. The following is the figure of substitution of NiO in MgO single crystal.
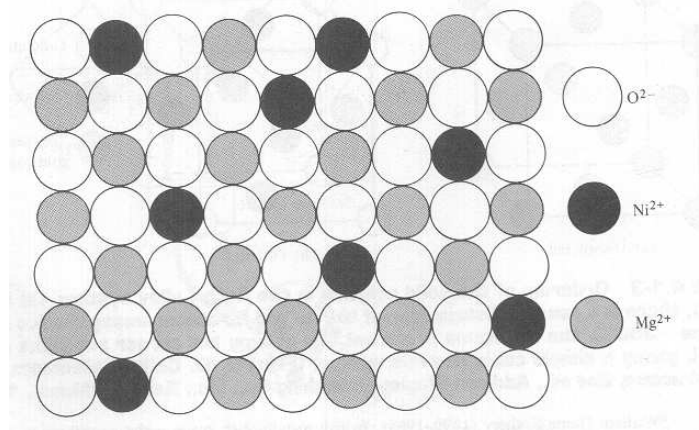
Fig. 2.1.4. MgO single crystal doped with a small concentration of NiO

E.   Excitons :

When a photon of energy greater than the energy of energy gap of the crystal are absorbed the electron will jump from valence band to conduction band. In this case the holes and electrons are free to move independently through the crystal. However if the photon energy is less than the energy gap the electron and hole will have the Coulomb interaction and are bound together as shown in the Fig. 2.1.5.   A bound electron –hole pair connected in this way is known an exciton. It moves through the crystal transporting excitation energy, but not charge. It is a neutral mobile entity.
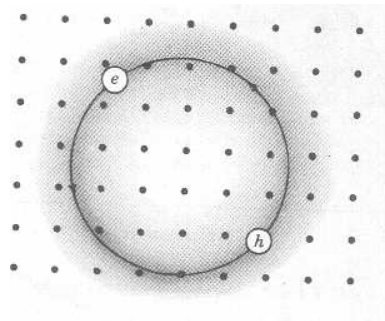
Fig.2.1.5 :An illustration of exciton, a bound electron- hole pair

2.1.3 Lattice defects and configurational entropy

According to thermodynamics, the equilibrium of a solid at temperature 'T' is determined by the minimum value of free energy $F = E-TS$

We shall see below that this condition necessarily leads to the existence on a certain amount of disorder in the lattice at all temperatures above $T > 0 K$

The simplest examples of lattice disorder are vacant lattice sites and interstitial atoms. The latter are atoms occupying positions in the lattice which in the perfect lattice would be unoccupied. Thermal and configurational entropy's are denoted as S_{th} and S_{cf}. According to Boltzmann relation the thermal entropy can be defined as

$$S_{th} = K \log W_{th} \qquad \text{……… (2.1.1)}$$

W_{th} stands for the number of different ways in which the energy of vibrations may be distributed over the 3N harmonic oscillators.

$$S_{th} = 3 NK [1+\log(KT/h\nu)] \qquad \text{……… (2.1.2)}$$

The configurational entropy of a crystal has nothing to do with the distribution energy . It is determined solely by the number of different ways (W_{cf}) in which the atoms may be arranged over the available no of lattice sites. For example a lattice containing 'Na' atoms of type 'A' and 'N_b' atoms of type 'B' and assume that lattice sites are equivalent in the sense that a given lattice site may be occupied by A (or) B.

$$W_{cf} = \frac{(N_a + N_b)!}{N_a! N_b!} \qquad \text{……… (2.1.3)}$$

The Configurational energy is given by

$$S_{cf} = K \log W_{cf}$$

$$= K \log \frac{(Na + N_b)!}{Na! N_b!} \qquad \text{……… (2.1.4)}$$

For a perfect crystal containing identical atoms and in the absence of any lattice defects.
$W_{cf} = 1$ and $S_{cf} = 0$ because there is only one possibility of arrangement of atoms.

The total entropy occurring in the usual thermodynamic formulas is equal to the sum of the thermal and configurational entropies

$$S = S_{th} + S_{cf} \qquad \text{……… (2.1.5)}$$

The reason for the existence of lattice defects at any temperature $T > 0$.

2.1.4. Estimation of concentration of vacancies

a. In metallic crystals

Suppose in a perfect crystal we produce a certain number of vacant lattice sites by transferring the atoms from the interior of the crystal to the surface. This will require a certain amount of energy. i.e. E increases. Consequently F increases and this by itself is thus unfavourable in the thermodynamic sense. On the other hand the creation of vacancies increases the disorder in the crystal and thus increases the configurational entropy from zero to certain value determined by the number of vacancies produced.

The configurational energy associated with the possible arrangements of N atoms and n vacancies over a total of (N+n) lattice sites is

$$S_{cf} = K \log \frac{(N+n)!}{N!n!}$$

It has been assumed for simplicity that the thermal energy is independent of n/N . The equilibrium corresponds to the minimum value of F at temperature T .

Consider a perfect lattice containing N similar atoms at a temperature T the free energy
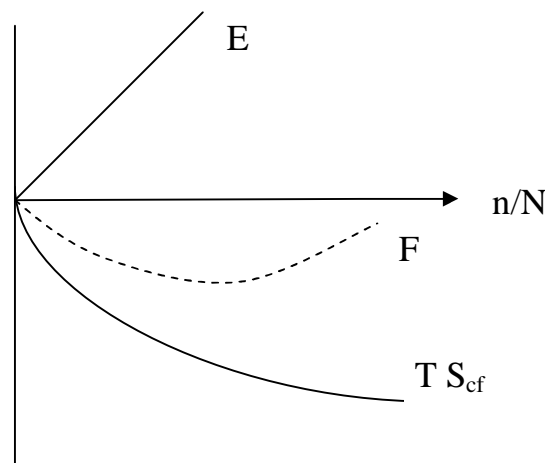
Fig : 2.1.6 Schematic representation of the energy and the configurational entropy term as lattice sites n/N.

of this crystal is denoted by $F_{perfect}(T)$. Suppose we create n vacant lattice sites. Let the energy required to create one vacancy be ϕ_v. We assume that ϕ_v is independent of n. We assume that no two vacancies are nearest neighbours of each other. The free energy of imperfect crystal is then increased by $n\,\phi_v$ relative to that of the perfect crystal. Configurational entropy is also associated with the imperfect crystal, furthermore we assume that thermal entropy increases per vacancy by an amount ΔS_{th}

The free energy of actual crystal is,

$$F_a = F_p + n\,\phi_v - T(S_a - S_p) - KT\,\log\left[\frac{(N+n)!}{N!\,n!}\right] \qquad \text{.....(2.1.6)}$$

Where 'S_a' is the thermal energy of actual crystal.

Under the equilibrium condition

$$\left(\frac{\partial F}{\partial n}\right)_T = 0 \qquad \text{.....(2.1.7)}$$

$$\left(\frac{\partial F}{\partial n}\right)_T = \phi_v - T\,\Delta S_{th} - KT\,\frac{\partial}{\partial T}\left[(N+n)\log(N+n) - N\log N - n\log n\right] = 0$$

$$\phi_v - T\,\Delta S_{th} - KT\,\frac{\partial}{\partial T}\left[1 + \log(N+n) - 1 - \log n\right] = 0$$

or $\qquad \phi_v - T\,\Delta S_{th} + KT\left[\log(\frac{n}{N+n})\right] = 0 \qquad \text{.....(2.1.8)}$

or $\left[\log(\frac{n}{N+n})\right] = -\phi_v/KT + \Delta S_{th}/K$

since $N \gg n$, $\quad\left[\log(\frac{n}{N})\right] = -\phi_v/KT + \Delta S_{th}/K$

$$\Rightarrow n/N = e^{-\phi_v/KT}\,e^{\Delta S_{th}/K} \qquad \text{......... (2.1.9)}$$

In general a change in the thermal entropy is negligible in this case, hence equation 2.1.5 becomes

$$n/N = e^{-\phi/KT} \text{ or } \boxed{n = N\,e^{-\phi_v/KT}} \qquad \text{......... (2.1.10)}$$

For metals ϕ_v is of the order of 1 electron volt.

b. In ionic crystsals

Crystal lattice in thermal equilibrium contains a certain number of lattice defects. Ionic crystal composition may be written as $A^+ B^-$. Positive ion vacancies are produced by a number of successive jumps of positive ions. The result would be equivalent to taking a positive ion some where from the interior of the crystal and placing it at the surface. Suppose that a number of positive ion vacancies would have been produced in this manner, while the negative ion lattice remains perfect. The surface of the crystal then contains an excess positive charge, the interior an excess of negative charge. Thus space charges would be set up. These space charges oppose the formation of more positive ion vacancies.

On the other hand the field setup by the space charges would be favour to the formation of negative ion vacancy. Hence in order to build up space charges and ionic crystal should contain equal number of negative and positive ion vacancies.

If ϕ^+ energy require producing a positive ion vacancy and ϕ^- is energy require producing a negative ion vacancy.

The total energy $\phi = \phi^+ + \phi^-$ .... (2.1.11)

The free energy of a perfect crystal is

$F_p = E_p - TS$ .... (2.1.12)

F_p is the sum of binding energy as well as vibrational energy. The entropy is thermal entropy only for a perfect crystal, the configurational entropy vanishes.

Let a crystal contains n^+ and n^- ion vacancies.

Then the configurational energy is

$$S_{cf} = K \log W_{cf} \quad = K \log \left[\frac{(N+n)!}{N!n!} \right]^2 \qquad ….. (2.1.13)$$

The free energy of actual crystal is,

$$F_a = F_p + n\phi - T(Sa-Sp) - 2KT \log \left[\frac{(N+n)!}{N!n!} \right]^2 \qquad …..(2.1.14)$$

Where 'Sa' is the thermal energy of actual crystal.

Δs_{th} is resulting from the production of +ve ion vacancy by

$n \Delta s_{th} = S_a - S_p$ …..(2.1.15)

Under the equilibrium condition

$$\left(\frac{\partial F}{\partial n}\right)_T = 0$$

$$\left(\frac{\partial F}{\partial n}\right)_T = \varphi - T\,\Delta\,S_{th} - 2KT\,\frac{\partial}{\partial T}\Big[(N+n)\log(N+n) - N\log N - n\log n\Big] = 0$$

$$\varphi - T\,\Delta\,S_{th} - 2KT\,\frac{\partial}{\partial T}\Big[1 + \log(N+n) - 1 - \log n\Big] = 0$$

or

$$\varphi - T\,\Delta\,S_{th} = 2KT\left[\log(\frac{n}{N+n})\right] \qquad \dots.(2.1.16)$$

The experimental term containing the change in thermal entropy per vacancy $\Delta S_{th}/2$ may be calculated on the basis of Einstein model.

Let 'ν' is the frequency of the ion neighbouring a vacancy in actual cystal ($\nu' < \nu$)

Then the actual crystal contains a 6zn no of linear harmonic oscillators of frequency ν' and (6n- 6zn) no of linear harmonic oscillators of frequency ν where z is the number of the nearest of neighbours surrounding a vacancy then the thermal entropy of perfect and actual crystal are

$$S_p = K \log \omega_p = 6NK \log\left(\frac{KT}{h\nu'}\right) + 6Nk \qquad \dots.(2.1.17)$$

$$S_a = 6\,Zn\,K \log\left(\frac{KT}{h\nu'}\right) + (6\,N - 6\,Zn)\,K\left[\log\left(\frac{KT}{h\nu}\right)\right] + 1 \qquad \dots.(2.1.18)$$

From the equations 2.1.7 and 2.1.8

$$S_a = S_p + 6\,Zn\,K \log\left(\frac{\nu}{\nu'}\right) \qquad \dots.(2.1.19)$$

or $\qquad \Delta\,S_{th} = 6\,ZnK \log\left(\frac{\nu}{\nu'}\right) \qquad \dots.(2.1.20)$

Hence $\quad n = N\,e^{-\varphi/2KT}\,e^{3NZ\,\log\left(\frac{\nu}{\nu'}\right)}$

$$n/N = C\,e^{-\varphi/2KT} \qquad \dots.(2.1.21)$$

where $C = \left(\frac{\nu}{\nu'}\right)^{3NZ}$

Interstitial ions are combination with vacancies also occur for example a positive ion may jump into an interstitial positions, leaving a vacancy behind. If the vacancy and interfacial ion are far enough, a part to prevent an immediate recombination known as Frenkel defects. In this case it is

not necessary to have equal number of positive and negative Frankel defects, because their formation does not require the setting up of a space charges over macroscopic distances. Their calculation of their density as a function of energy required to produce a Frankel defect is especially the same as that given above   Schotty defects. i.e. one finds an expression for the free energy of a crystal containing n defects and minimizes F.

We are neglecting thermal entropy changes in this case.

$$n = (N N_i)^{1/2} e^{-\varphi / 2KT} \qquad\qquad .....(2.1.22)$$

Where N is number of ions under consideration. N_i is the number of possible interstitial positions in the crystal. φ is the energy required to produce a Frenkel defect.

2.1.5   Summary of the lesson

Brief classification of various defect in crystals has been presented. The connection between the configurational entropy and the defect in crystals has also been discussed. Equation for the concentration of vacancies both in metallic and ionic crystals has been derived.

2.1.6 Key Terminology

Point defects – Vacancies – Interstitial atoms – Colour centres – Excitons Configurational entropy .

2.1.7   Self – Assessment questions

1. Give an account of the classification of various point defects in crystals.
2. Discuss the connection between the configurational entropy and lattice defects.
3. Derive the expressions for the concentration of vacancies in metallic and ionic crystals.

2.1.8   Reference Books :

1. Elements of Solid State Physics – J.P.Srivastava (PHI, New Delhi, 2003)
2. Introduction to Solid state Physics – C.Kittel (Wiley Eastern, New Delhi, 2003)
3. Solid state Physical Electronics   - Aldert van der Ziet (Prentice –Hall of India, New Delhi, 1971)
4. Solid State Physics – A. J.Dekker (Macmillan , Madras, 1986)
5. Indroduction to Solids   - Leonid V.Azaroff (Tata McGraw-Hill Publishing Co., Bombay , 1978)

Unit - II

Lesson - 2

IMPERFECTIONS IN CRYSTALS – II
LINE AND PLANAR DEFECTS

Objectives

To discuss in detail the Line defects like Edge and screw dislocations and the two dimensional defects such as planar defects an to explain the role of dislocations in the crystal growth.

Structure of the lesson

2.2.1. Introduction

2.2.2. Line Defects

      a. Edge dislocation

      b. Screw dislocation

      c. Plane Defects (Grain boundaries)

2.2.3. Stress fields of dislocations

2.2.4. Dislocations and crystal growth

2.2.1. Introduction

Line defect is another type of defect comes under one dimensional defect. The example of this defect is dislocation. In this a part of lattice undergoes a shearing strain equal to one lattice vector called a Burger's vector. There are two types of dislocations known as edge dislocation and screw dislocation and any general dislocation is a combination of both. In this chapter the formation and structure of these defects have been discussed. Description of the two dimensional or the planar defects like grain boundaries has also been presented in this chapter.

2.2.2. Line Defects

a. Edge dislocation

It occurs when the periodicity of the atomic lattice array is interrupted along certain directions in a crystal. Such dislocations occur along the rows of a crystal structure and so are called line defects. An edge dislocation is formed by missing of row of atoms or when a row of atoms is displaced (see the figures below).
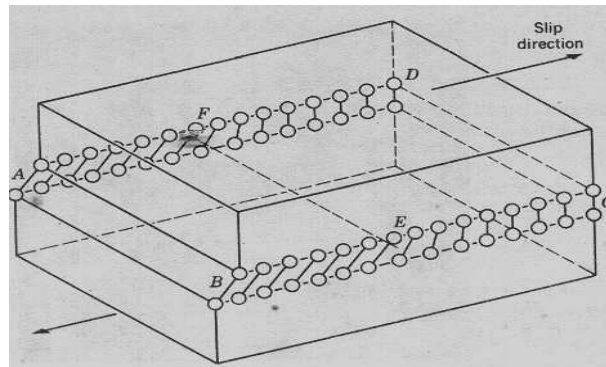
Fig 2.2.1. An edge dislocation EF in the glide plane ABCD. The figure shows the slipped region ABEF in which the atoms have been displaced by more than half a lattice constant and the unslipped region FECD with displacement less than half a lattice constant.
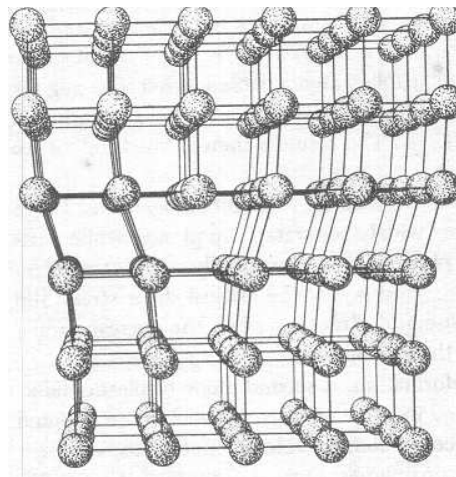

Fig 2.2.2. Structure of an angle dislocation. The deformation may be thought of as caused by inserting an extra plane of atoms on the upper half of the y axis. Atoms in the upper half-crystal are compressed by the insertion; those in the lower half are extended.
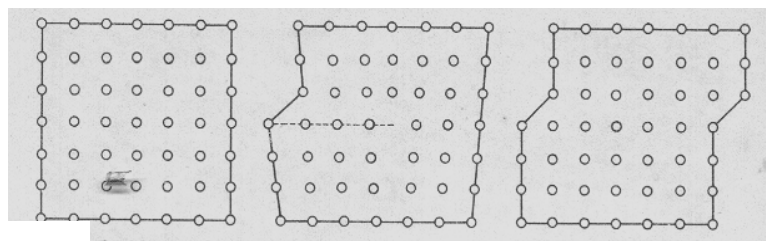

Fig 2.2.3. Motion of a dislocation under a shear tending to move the upper surface of the specimen to the right.

The vector representing the lattice displacement is called Burger's vector denoted by '**b**'. In the edge dislocation the Burger's vector is perpendicular to the dislocation line.

b.   Screw dislocation

The formation of a screw dislocation can be understood as follows: cut a perfect crystal partway through, then force the material on one side of the cut to move up with respect to the material. On other side by one unit of atomic spacing and finally glue the material on the two sides in this condition. The dislocation marks the boundary between the displaced and un-displaced parts of the crystal. The Burger's vector is again used to describe the displacement. It is a type of dislocation in which the dislocation line(Burger's Vector) is parallel to the slip direction.
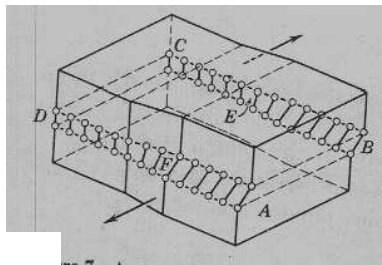
Fig 2.2.4. A screw dislocation. A part ABEF of the slip plane has slipped in the direction parallel to the dislocation line EF.
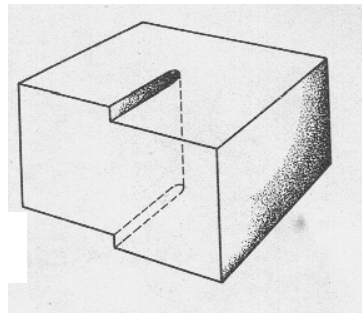
Fig. 2.2.5. Another view of a screw dislocation. The broken vertical line which marks the dislocation is surrounded by strained material.

c. Plane Defects (Grain boundaries)

These defects have an extension in an area and are confined to a small region. It is a boundary between two adjacent perfect regions in the same crystal which are slightly tilted with respect to each other or it may also be understood as a junction of two single crystals along a common

planar surface. These imperfections are common in poly crystalline materials which contain a large number of crystals. The two common examples of grain boundaries are tilt and twist grain boundaries. The first one is a result of a linear a sequence of edge dislocations where as the second one is result of a sequence of screw dislocations. The general grain boundaries (low angle grain boundaries) are the mixture of these two.
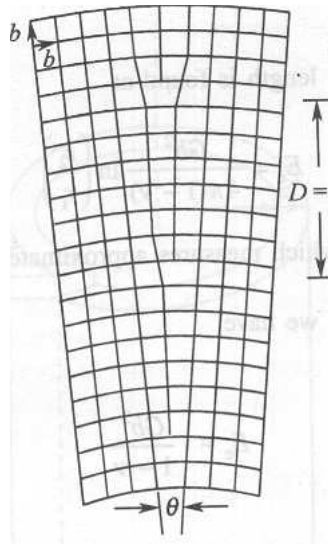

Fig 2.2.6. A view of typical low angle grain boundary

2.2.3. STRESS FIELDS OF DISLOCATIONS

The properties of the dislocations are in general determined by the stress fields they produce inside the material. The calculations of these fields is usually carried out with the assumption that the medium is isotropic and characterized by shear modulus G and poisons ratio ν

Consider a cylindrical crystal that has been sheared in the axial direction (Z axis). The shearing is as shown in Fig. 2.2.7. Suppose we produce a cut in the plane Y=0 which extended between the axis and the outer surface. Let the material above the cut slip to the left by an amount 'b' leading to the configuration as shown by the dotted line. We thus have produced a positive edge dislocation along the Z axis a burgers vector along the X axis.
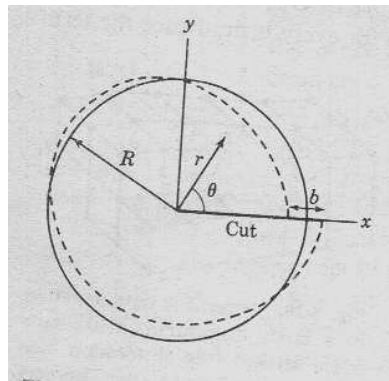
Fig 2.2.7. An edge dislocation along the z-axis in a cylindrical piece of material.

The plane Y=0 is the slip plane. In terms of the coordinates r and θ the stress filed of the dislocation line may be shown to be given by the following tensile and shear stresses

$$\sigma_{rr} = \sigma_{\theta\theta} = \frac{Gb}{2\pi r(1-v)} \sin\theta \qquad\qquad .... (2.2.1)$$

$$\tau_{r\theta} = \tau_{\theta r} = \frac{Gb}{2\pi r(1-v)} \cos\theta \qquad\qquad .... (2.2.2)$$

Where

σ_{rr} = radial compression or tension

$\sigma_{\theta\theta}$ = Compression or tension acting in a plane perpendicular to r

$\tau_{r\theta}$ = Shear stress acting in radial direction

On the basis of these results the energy formation of dislocation, of unit length can be shown to be equal to

$$\frac{1}{2}\int_{r_o}^{R} \frac{Gb^2}{2r\pi(1-v)}dr = \frac{Gb^2}{4\pi(1-v)} \log(R/r_0) \qquad\qquad .... (2.2.3)$$

Where R is the radius of the piece of material.

For a screw dislocation along the Z axis in a cylindrical piece of material, the stress field is completely given by a shear stress:

$$\tau_{z\theta} = \tau_{\theta z} = Gb/2\pi r \qquad\qquad .... (2.2.4)$$

2.2.4. Dislocations and crystal growth

Consider the growth of a crystal by hanging a small piece of crystal in a vopour of same kind of atoms. In some cases, it was observed that the dislocations are a controlling factor in crystal growth. When crystals are grown in conditions of low super saturation, of the order of 1 percent, it has been observed that the growth rate is enormously faster than that calculated for an ideal crystal. The actual growth rate is explained by Frank. It terms of the effect of dislocations on growth.

The theory of growth of ideal crystals predicts that in crystal growth from vapour a super saturation (pressure / equilibrium vapor pressure) of the order of 10 is required to nucleate new crystals, of the order of 5 to form liquid drops, and of 1.5 to form a two dimensional mono layer of molecules on the face of a perfect crystal.   However there is a large disagreement between the growth rate and experimental growth rate. This is because of the presence of screw dislocations during the growth of the crystals. The crystal will grow in spiral fashion at the edge of the discontinuity as shown in Fig. 2.2.8. The calculated growth rates of this mechanism are in good agreements with observations. We expect that nearly all crystals in nature grown at low super saturation will contain dislocations, as otherwise they could not have grown.
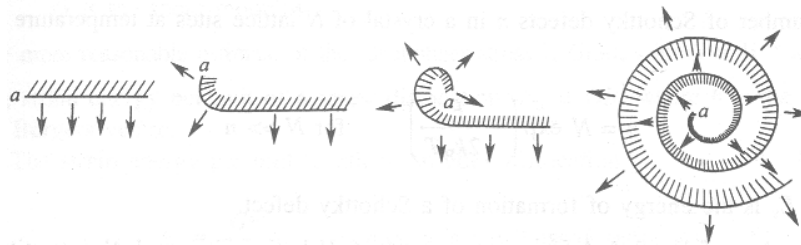
Fig 2.2.8. The intersection of a screw dislocation with a free surface to produce a spiral step.

Spiral growth patterns have been observed on a large number of crystals. A beautiful example of the growth pattern from a single screw dislocation is given in Fig 2.2.8.

If the growth rate is independent of direction of the edge in the plane of the surface, the growth pattern is an Archimedes spiral,

r = a θ,

where a is a constant . The limiting minimum radius of curvature near the dislocation is determined by the super saturation if the radius of curvature is too small, atoms on the curved edge evaporate until the equilibrium curvature is attained.

Away from the origin each part of the step acquires new atoms at a constant rate, so that dr/dt = Constant.

2.2.5. Stacking faults.

Consider a crystal. Let the nth layer of it is a closest packing is an A layer and the $(n + 1)^{th}$ layer is supposed to be a B layer (See the Fig. 2.2.x)   but because of a "mistake" in the stacking sequence it is a C layer instead. It is said that a stacking fault has been introduced between the nth and $(n + 1)^{th}$ layer in that case. For example, consider the stacking sequences

$$\ldots ABABABCBCBC\ldots \quad \ldots ABCABCBCABCA \qquad \ldots (21)$$
$$\ldots hhhhhchhhhh\ldots \qquad \ldots cccccchhccccccccc\ldots$$

In the first case, a stacking fault has occurred on one side of the c layer. (The choice of the side is based on which sequence is deemed to be the correct one.) In the second case, the stacking fault clearly lies between the two h layers.

  The stacking fault can be produced by at least two distinct mechanisms. When a closest packing of atoms forms in a crystal during its growth, it is possible for a new layer to start incorrectly;
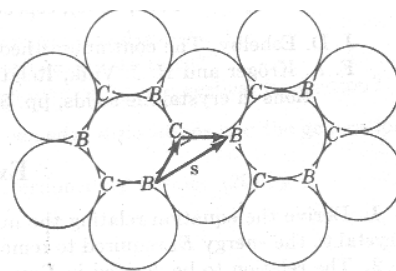
Fig. 2.2.9. Formation of stacking faults

That is, a C layer can start to grow instead of the B layer required by the preceding stacking sequence. If the crystal grows sufficiently rapidly, this so-called growth fault is incorporated in the final crystal. Similarly, it is possible to displace the atoms in, say, a B layer to the sites of a C

layer during plastic deformation of the crystal. (This actually takes place by the relative motion of the two parts of the crystal.) The energy of a stacking fault, therefore, can be calculated by taking into account the interactions between next-nearest neighbors only. (The contribution due to next-next-nearest neighbors is small so that it can be neglected.) The measured values of this energy are 19 ergs/cm^2 in copper and between 100 to 200 ergs/cm^2 in aluminum.

It is also possible to describe the production of deformation faults in terms of dislocations. Consider the hexagonal closest-packed layer, say the A layer shown in Fig. 2.2.9. Suppose that the next layer above is a B layer. It can be displaced along the Burgers vector **S** to produce a unit f dislocation. Actually, it is much easier to displace the layer to the , neighboring C sites. Remember, the nearest-neighbor forces acting on : each atom are not affected by this change.) When such a partial dislocation is formed in a closest packing, a stacking fault is produced. It is evident that the atoms probably move in a zigzag path so that it is not surprising that stacking faults have been found to exist in plastically deformed face-centered cubic metals.

2.2.5   Summary of lesson

The formation of screw and edge dislocations has been discussed. The role played by dislocations in the crystal growth has also been described. The geometrical structure of the grain boundaries in the crystals has also been presented. The brief summary of the general defects in the crystals is given below

Type of imperfection		Description of imperfection
Point defects	Interstitial	Extra atom in an interstitial site
	Schottky defects	Atom missing from correct site
	Frenkel defect	Atom displaced to interstitial site creating nearby
Line defects	Edge dislocation	Row of atoms marking edge of a crystallographic plane extending only part way in crystal
	Screw dislocation	Row of atoms about which a normal crystallographic plane appears to spiral
Plane defects	Lineage boundary	Boundary between two adjacent perfect regions in the same crystal that are slightly tilted with respect to each other
	Grain boundary	Boundary between two crystals in a polycrystallinc solid
	Stacking fault	Boundary between two parts of a closest packing having alternate stacking sequences.

2.2.6   Key Terminology

Line defects - Edge dislocation – Screw dislocation –Grain boundaries – Stress fields

2.2.7   Self – assessment questions

1. Discuss briefly the formation of edge and screw dislocations
2. Write a note on planar defects.
3. Derive the expression for ht stress filed of dislocations.
4. Discuss the role dislocations in the crystal growth

2.2.8   Reference Books :

1. Elements of Solid State Physics – J.P.Srivastava (PHI, New Delhi, 2003)

2. Introduction to Solid state Physics – C.Kittel (Wiley Eastern, New Delhi, 2003)

3. Solid state Physical Electronics   - Aldert van der Ziet (Prentice –Hall of India, New Delhi, 1971)

4. Solid State Physics – A. J.Dekker (Macmillan , Madras, 1986)

5. Introduction to Solids   - Leonid V.Azaroff (Tata McGraw-Hill Publishing Co., Bombay , 1978)

U n i t - 2

Lesson – 3

MAGNETIC PROPERTIES- DIA MAGNETISM

Objective of the lesson

This chapter is aimed to make the student familiar with certain fundamentals related to magnetic properties of the materials. Further it is also planned to discuss the general quantum theory of magnetic susceptibility and also of diamagnetism in particular.

Structure of the lesson

2.3.1. Introduction

2.3.2 Measurement of susceptibility

2.3.3. Atomic magnetic moment

2.3.4. Quantum theory of magnetic susceptibility

2.3.5. Diamagnetism

2.3.1 Introduction

The permanent atomic magnetism (paramagnetism) cannot be accounted for without restricting the circulating electrons to the discrete stationary orbits as required in the Bohr's quantum theoretical model of the Hydrogen atom. In the classical picture, there can be no magnetic moment associated with the current of circulating electrons because electrons in accelerated motion would radiate and finally fall on the nucleus, causing the atomic structure to collapse. Hence   the magnetism is essentially a quantum effect. The two fundamental forms of magnetism, Diamagnetism and paramagnetism have their origin in induced and permanent magnetic moments respectively. Diamagnetism, where the applied magnetic field is pushed out of the system, can be appreciated similarly by realizing that the discrete quantum states occupied by electrons are stable to a certain extent only against external perturbations, like a magnetic field in the present case. Paramagnetism can be accounted for with restricting the circulating electrons to the discrete stationary orbits as mentioned in Bohr's quantum mechanical atomic model of hydrogen atom.

We define below the certain fundamental physical quantities that concern the magnetic properties of materials.   In vacuum, the intensity of the applied magnetic field H and the magnetic induction B are related by the equation.

$$B = \mu_0 H \qquad \text{.......... (2.3.1)}$$

Where μ_0 is the permeability of free space ($\mu_0 = 4\pi \times 10^{-7}$ V S/A m.)

The magnetic state of a system is specified by its magnetization M, defined as the magnetic moment per unit volume. M is related to B and H by

$$B = \mu_0 (H + M) \qquad \text{.......... (2.3.2)}$$

For convenience in discussions it is a practice to introduce an external induction such that

$$B_0 = \mu_0 H$$

Mostly, there is a linear relationship between B_0 and M given by $\mu_0 M = \chi B_0$

Giving $\qquad \chi = \dfrac{\mu_0 M}{B_0} \qquad \text{.......... (2.3.3)}$

Where χ is called the magnetic susceptibility.

Substances with a negative magnetic susceptibility are called diamagnetic substances with a positive susceptibility are called paramagnetic.

2.3.2 Measurement of susceptibility

The magnetic contribution to the energy density of a magnetized specimen is $\dfrac{1}{2}\chi H^2$, provided χ is independent of H. The force on a unit volume is the gradient of the energy density. The x- component of the force on a small specimen of volume V is

$$F_x = \frac{1}{2}\chi V \frac{d}{dx} H^2 = \chi V H \left(\frac{dH}{dx} \right) \qquad \text{.......... (2.3.4)}$$

provided the field H and the derivative dH / dx do not vary appreciably over the volume (this why the specimen must be small). Given below is the method known as Gouy's method to measure the magnetic susceptibility of a paramagnetic substance.
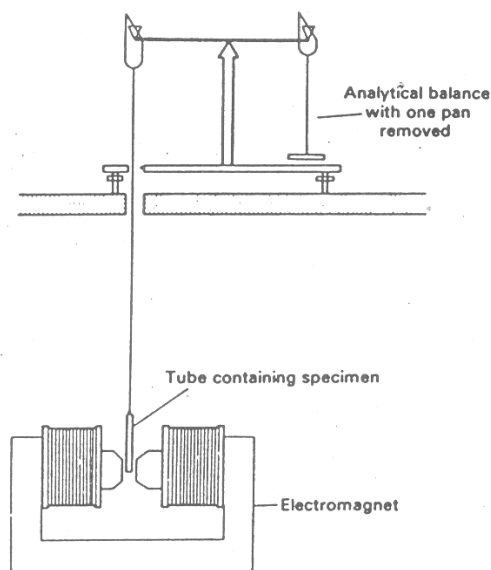
Fig 2.3.1 . Measurement of magnetic susceptibility by Gouy's method

In this method (Fig. 2.3.1.) a long cylindrical sample is suspended halfway into a strong field H: one end of the sample is in the maximum field and the other end is in a region where the field is negligible. The total force under these conditions on a specimen of cross – sectional area A is

$$F_x = \frac{1}{2}\chi A \int dx \frac{d}{dx} H^2 = \frac{1}{2}\chi A H^2 = \Delta mg \qquad \ldots\ldots (2.3.5)$$

$$\Rightarrow \quad \chi = 2\Delta mg / AH^2 \, emu \qquad \ldots\ldots (2.3.6)$$

where Δmg is the weight loss of the sample in the presence of magnetic field H. By measuring Δmg and H, the applied field one can calculate the susceptibility χ.

2.3.3. Atomic magnetic moment

Suppose an electron is orbiting with an angular frequency ω in an atom of radius r then according to amperes law the moment μ_l of the current loop is given by, area of the loop x current . This can be shown as

μ_l = - (e/2m) (**r** x **p**)

     = - (e/2m) x orbital angular momentum

here e is the charge of the electron, m is the mass of the electron and p is the linear momentum. When the atom is subjected to an external magnetic field, the orbital motion or the orbital frequency of the electron and as a result its magnetic moment will be affected as shown in the Fig.2.3.2. If an electron from an atom which satisfies the Bohr's quantization condition possesses angular momentum L then its magnetic moment is defined as

$$\mu_l = -\left(\frac{e\hbar}{2m}\right)l = \mu_B l \qquad \ldots\ldots\ldots (2.3.7)$$
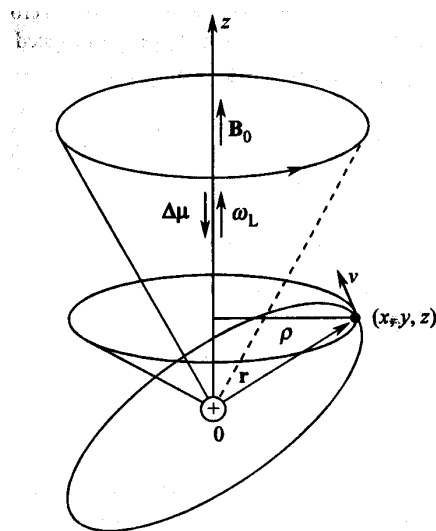
Fig. 2.3.2. Effect of the magnetic field (B_o) on the magnetic moment of the electron.

where μ_B is the Bohr Magneton = $\mu_B = \left(\frac{e\hbar}{2m}\right)$ = 9.2742 x 10^{-24} J/Tm……. (2.3.8)

Similarly the magnetic moment due to the spin motion of the electron is represented by

μ_s and it is expressed as

$$\mu_s = -g_o \mu_B s \qquad \ldots\ldots\ldots (2.3.9)$$

where g_o is called the electron g- factor whose value is given by 2.0023 for a free electron and s is the spin quantum number which is equal to $\pm 1/2$.

For the calculation of magnetic moment of an atom or an ion which contains more than one electron, , we combine the vectorially, the individual orbital and spin angular momenta either by L-S coupling or by j-j coupling. By taking

$\hbar\,L = \hbar\sum_{i}\ell_i$ and $\hbar\,S = \hbar\sum_{i}s_i$, one can have the total angular momentum, as

$$\hbar\,J = \hbar\,L + \hbar\,S \qquad\qquad\text{.......... (2.3.10)}$$

where J is the total quantum number. Then the total magnetic moment μ_J is related to J   as

$$\mu_J = \mu_B\,(L + g_o S) = g\,\mu_B\,J$$

$$\text{with}\qquad\qquad (L + g_o S) = gJ \qquad\qquad\text{.......... (2.3.11)}$$

where g is called Landes splitting factor for L-S (or Russel – Sanders) coupling the value of g is given by

$$g = 1 + \frac{J^{*2} + S^{*2} - L^{*2}}{2J^{*2}} \qquad\qquad\text{.......... (2.3.12)}$$

with $J^* = \sqrt{j(j+1)}$, $L^* = \sqrt{\ell(\ell+1)}$ and $S^* = \sqrt{s(s+1)}$

If we take the value of g_o as 2.0000 instead of 2.0023 the magnetic moment μ may be expressed as

$$\mu = -\mu_B\,(L + 2S) \qquad\qquad\text{.......... (2.3.13)}$$

2.3.4. Quantum theory of magnetic susceptibility

Magnetization or the intensity of magnetization of a quantum mechanical system having N magnetic ions per unit volume at T=0 is defined as

$$M = -N\frac{\partial E_0(H)}{\partial H} \qquad\qquad\text{..........(2.3.14)}$$

Where $E_0(H)$ is the ionic ground state energy in the presence of the field H.

In the state of thermal equilibrium at T, the thermal average of each excited state of energy $E_n(H)$ gives the measure of magnetization, i.e.

$$M(T) = \frac{\sum_n M_n \exp\left[\dfrac{E_n}{KT}\right]}{\sum_n \exp\left[-\dfrac{E_n}{KT}\right]} \qquad\qquad\text{..........(2.3.15)}$$

where $\qquad\qquad M_n = -N\frac{\partial E_n(H)}{\partial H}$

Thermodynamically the intensity of magnetization is defined as

$$M = -N\frac{\partial F}{\partial H} \qquad\qquad\text{..........(2.3.16)}$$

Where F is the magnetic Helmholtz free energy.

The general definition of susceptibility gives

$$\chi = \mu_0 \frac{\partial M}{\partial H} = -\mu_0 N \frac{\partial^2 F}{\partial H^2} \qquad ....(2.3.17)$$

But, in most of the cases, M is found to be very accurately linear in H for attainable field strengths. In such a case, the definition of χ reduces to

$$\chi = \frac{\mu_0 M}{H} \qquad ....(2.3.18)$$

A quantum mechanical approach of the magnetic susceptibility is discussed below.

The part of the Hamiltonian operator of the energy of an atomic dipole in a magnetic field H owing to its orbital magnetic moment μ_L is

$$\Delta H_L = - \mu_L . H = \mu_B L . H \qquad ....(2.3.19a)$$

$$\Delta H_S = - \mu_S . H = \mu_B S . H \qquad ....(2.3.19b)$$

where, $S_z = \sum_i s_z^i$ with $s_z^i = \frac{1}{2}\sigma_i$ (σ_i is a Pauli spin matrix)

It is assumed here that the magnetic field is applied along the z- direction. In the presence of a magnetic filed, the linear momentum of an electron is given by

$$P_{field} = p + eA(r) \qquad ....(2.3.20)$$

where P is the liner momentum of the electron in the absence of the field and A denotes the vector potential related to H as,   H = curl A with div A=0.

For a homogeneous field, a possible choice of a vector potential is

$$A = -\frac{1}{2} rXH \qquad ....(2.3.21)$$

A a result, we can write the kinetic energy part of the Hamiltonian as

$$H_{kin} = \frac{1}{2m} \sum_i \left(p_i - \frac{e}{2} r_i \ x \ H \right)^2$$

$$= T_0 + \mu_B \, L \cdot H + \frac{e^2}{8m} H^2 \sum_i (x_i^2 + y_i^2) \qquad \dots\dots\dots(2.3.22)$$

where T_0 is the kinetic energy in the absence of the field and $\hbar \, L = \sum_i \mathbf{r_i} \times \mathbf{p_i}$

Combining the spin term (2.3.19b) with (2.3.22) , we get the total interaction Hamiltonian as

$$\Delta H = \mu_B (L + g_o S) \cdot H + \frac{e^2}{8m} H^2 \sum_i (x_i^2 + y_i^2) \qquad \dots\dots\dots(2.3.23)$$

Changes in energy affected by (2.3.23) even with the strongest magnetic fields that can be produced in a laboratory are very small on the scale of atomic excitation energies. Hence it may be justified to follow the ordinary perturbation approach for calculating the changes in electron energies induced by a magnetic field.

The dependence of susceptibility on the second derivative of energy (2.3.18) indicated that it would be sufficient to confine the perturbation calculations to second order terms. If energy E_n changes be ΔE_n on applying the field, this change according to the standard result of the second order perturbation theory is expressed as

$$\Delta E_n = \langle \phi_n \, |\Delta H| \phi_n \rangle + \sum_{n' \neq n} \frac{|\langle \phi_n \, |\Delta H| \phi_{n'} \rangle |^2}{E_n - E_{n'}} \dots\dots\dots(2.3.24)$$

where ϕ_n denotes the eigen function of the nth energy state. On Substituting ΔH from (2.3.23) and retaining terms up to those in quadratic in H, we obtain

$$\Delta E_n = \mu_B H \cdot \langle \phi_n \, |L + g_0 S| \phi_n \rangle + \sum_{n' \neq n} \frac{|\langle \phi_n \, |\mu_B H.(L + g_0 S)| \phi_{n'} \rangle |^2}{E_n - E_{n'}}$$

$$+ \frac{e^2}{8m} H^2 \langle \phi_n | \sum_i (x_i^2 + y_i^2) | \phi_n \rangle \qquad \dots\dots\dots(2.3.25)$$

This relation serves as the basis for the description of magnetic susceptibility of individual atoms, ions or molecules. It can also applied to ionic and molecular solids by computing the susceptibility ion by ion, provided the concerned solid may be regarded as a collection of only slightly deformed ions.

2.3.5. Diamagnetism

Consider the case of a solid composed of ions whose all electronic shells are filled. An ion has zero spin and orbital angular momentum in its ground state represented by the wave function ϕ_0, i.e.

$$J|\phi_0\rangle = L|\phi_0\rangle = S|\phi_0\rangle = 0 \qquad \ldots\ldots\ldots(2.3.26)$$

In relation (2.3.25), only the last term contributes to the field-induced shift in the ground state energy

$$\Delta E_0 = \frac{e^2}{8m} H^2 \left\langle \phi_0 \left| \sum_i (x_i^2 + y_i^2) \right| \phi_0 \right\rangle$$

$$= \frac{e^2}{12m} H^2 \left\langle \phi_0 \left| \sum_i r_i^2 \right| \phi_0 \right\rangle \qquad \ldots\ldots\ldots(2.3.27)$$

In the state of thermal equilibrium ions are generally in their ground state, excepting the situation at high temperatures. Therefore, the susceptibility of a solid with N atoms or ions per unit volume at room temperature is given as

$$= -\mu_0 N \frac{\partial^2 \Delta E_0}{\partial H^2}$$

$$= -\frac{\mu_0 N e^2}{6m} \left\langle \phi_0 \left| \sum_i r_i^2 \right| \phi_0 \right\rangle \qquad \ldots\ldots\ldots(2.3.28)$$

If there are Z electrons in an ion, the mean square radius of the ion may be defined by

$$\langle r^2 \rangle = \frac{\left\langle \phi_0 \left| \sum_i r_i^2 \right| \phi_0 \right\rangle}{Z} \qquad \ldots\ldots\ldots(2.3.29)$$

This leads to

$$\chi = -\frac{\mu_0 N Z e^2}{6m} \langle r^2 \rangle \qquad \ldots\ldots\ldots(2.3.30)$$

which is same as obtained on the basis of purely classical considerations.

2.3.6 Summary of the lesson

Certain fundamental quantities related to magnetic properties of the materials has been discussed. A brief description of the experiment to measure the magnetic susceptibility has been given. The general quantum theory of magnetic susceptibility has been discussed in depth. The expression for diamagnetic susceptibility on the basis of quantum theory has also been derived.

2.3.7   Key terminology

Magnetic moment – Magnetic susceptibility – Quantum theory – Diamagnetism

2.3.8 Self assessment questions

1. Define the magnetic susceptibility and describe an experiment to measure the magnetic susceptibility.
2. Give the quantum mechanical formulation of magnetic susceptibility
3. Derive the expression for diamagnetic susceptibility by the quantum mechanical approach.

2.3.9 Reference Books

1. Elements of Solid State Physics – J.P.Srivastava (PHI, New Delhi, 2003)
2. Introduction to Solid state Physics – C.Kittel (Wiley Eastern, New Delhi, 2003)
3. Solid State Physics – A. J.Dekker (Macmillan , Madras, 1986)

Unit-2

Lesson – 4 .

MAGNETIC PROPERTIES- PARA MAGNETISM

Objective of the lesson

- To discuss the quantum theory of paramagnetism and to derive Curie's law

Structure of the lesson

2.4.1. Introduction

2.4.2 Quantum theory of paramagnetism

2.4.3 Susceptibility and Curie's law

2.4.4. Application to magnetic ions in solids: Effect of the crystal Field

2.4.1 Introduction

According to classical theory the atomic magnets can have any orientation of electronic orbits with respect to the external magnetic field applied. The number of magnetic dipoles that posses potential energy U = - μ . H are proportional, to   exp(-U/KT). Then the dipole moment of the dipoles along the field directions present within the solid angle dΩ is equal to exp(-U/KT) μ cosθ dΩ . Then the average dipole moment is given by

$$\overline{\mu} = \frac{\int_{0}^{\pi} e^{-\mu H Cos\theta / KT} . \mu Cos\theta . d\Omega}{\int_{0}^{\pi} e^{-\mu H Cos\theta / KT} d\Omega} \qquad ……..(2.4.1)$$

$$=Coth\ a\text{-}\ 1/a\ =\ L(a) \qquad\qquad ……..(2.4.2)$$

is known as Langevin's function. Here a = μH/KT. Then the total magnetization,

M =Nμ L(μH/KT).

As long as μH/KT << 1, M = Nμ^{2}H /3KT or χ = Nμ^2 /3KT

$$\Rightarrow \qquad \chi = C\ /\ T \qquad\qquad ……..(2.4.3)$$

This is known as Curie's law. However according to the quantum theory the magnetic moment of a given atom or ion is not freely rotating but restricted to a finite set of orientation relative to

the applied field. In this chapter we derive the magnetic susceptibility of the paramagnetic materials based up on this concept.

2.4.2 Quantum theory of paramagnetism

Consider a medium containing N atoms per unit volume , the total quantum number each atom being J gives raise to the possible components of the magnetic moment ,

M_J g μ_B where $M_{J=}$ J, (J-1), ……. –(J-1) , -J

where M_J is the magnetic quantum number associated with J.

Then the number of dipoles whose P.E. is -M_J g μ_B H are proportional to

$$dN \ \propto \ e^{\ Mg\ \mu_B\ H\ /\ KT} \ \ \text{or} \ dN \ = \ ce^{\ gM\ \mu_B\ H\ /\ KT} \qquad ……..(2.4.4)$$

Since the magnetic moment associated with each dipole is Mg μ_B The total magnetic dipole moment is given by

$$= \sum_{-J}^{+J} ce^{Mg\mu_B H / KT} \, gM\mu_B \qquad ……..(2.4.5)$$

Average magnetic dipole moment

$$\overline{M} = \frac{Total \ magnetic dipole \ moment}{No. \ of \ dipoles}$$

$$\overline{M} = \frac{\sum_{-J}^{+J} e^{Mg\mu_B H / KT} \, gM\mu_B}{\sum_{-J}^{+J} e^{Mg\mu_B H / KT}} \qquad ……..(2.4.6)$$

As T and H are kept constant. Let us assume x = g μ_BH/KT, then

$$\overline{M} = g\mu_B \frac{\sum_{-J}^{+J} Me^{Mx}}{\sum_{-J}^{+J} e^{Mx}} \qquad …….. (2.4.7)$$

but $\quad \dfrac{\sum_{-J}^{+J} Me^{Mx}}{\sum_{-J}^{+J} e^{Mx}} = \dfrac{d}{dx}(\log \sum e^{Mx}) \qquad ……..(2.4.8)$

$$\sum e^{Mx} = e^{jx} + e^{(j-1)x} + ... + e^{-(j-1)x} + e^{-jx}$$

$$= e^{jx}\left[1 + e^{-x} + ... + e^{-2jx}\right]$$

$$= \frac{e^{jx}\left[1 - e^{-x}\right]\left[1 + e^{-x} + ... + e^{-2jx}\right]}{\left[1 - e^{-x}\right]}$$

$$= \frac{e^{jx}\left[1 + e^{-x} + ... + e^{-2jx} - e^{-x} - e^{-2x} ...... - e^{-2jx} - e^{-(2j+1)x}\right]}{\left[1 - e^{-x}\right]}$$

$$= \frac{e^{jx}\left[1 - e^{-(2j+1)x}\right]}{\left[1 - e^{-x}\right]} = \frac{e^{jx} - e^{-(j+1)}}{1 - e^{-x}}$$

$$= \frac{e^{-x/2}\left[e^{(j+1/2)x} - e^{(j+1/2)x}\right]}{e^{-x/2}\left[e^{x/2} - e^{-x/2}\right]}$$

$$\sum e^{Mx} = \frac{Sinh(j+1/2)x}{Sinh x/2} \qquad ....(2.4.9)$$

$$\frac{\sum Me^{Mx}}{\sum e^{Mx}} = \frac{d}{dx}\log\left[\frac{Sinh(j+1/2)x}{Sinh x/2}\right]$$

$$= \frac{Sinh x/2}{Sinh(j+1/2)x} \cdot \frac{d}{dx}\left[\frac{Sinh(j+1/2)x}{Sinh x/2}\right]$$

$$= \frac{Sinh x/2}{Sinh(j+1/2)x} \cdot \left[\frac{Sinh x/2(j+1/2)Cosh(j+1/2)x - \frac{1}{2}Sinh(j+1/2)x.Cosh x/2}{\left(Sin\frac{hx}{2}\right)^2}\right]$$

$$= \frac{\sum Me^{Mx}}{\sum e^{Mx}} = (j+\frac{1}{2})Coth(j+\frac{1}{2})x - \frac{1}{2}Cot\frac{hx}{2}$$

$$\overline{M} = g\mu_B\left[\left(j+\frac{1}{2}\right)Coth\left(j+\frac{1}{2}\right)x - \frac{1}{2}Cot\frac{hx}{2}\right]$$

$$\overline{M} = gj\mu_B\left[\left(\frac{2j+1}{2j}\right)Coth\left(j+\frac{1}{2}\right)x - \frac{1}{2j}Cot\frac{hx}{2}\right]$$

$$= gj\mu_B \left[\left(\frac{2j+1}{2j} \right) Coth \left(\frac{2j+1}{2j} \right) jx - \frac{1}{2j} Cot \left(\frac{hjx}{2j} \right) \right]$$

$$= g_j\mu_B \left[\left(\frac{2j+1}{2j} \right) Coth \left(\frac{2j+1}{2j} \right) a - \frac{1}{2j} Coth \left(\frac{a}{2j} \right) \right] \quad ....(2.4.10)$$

Multiply with 'N' on both sides (where $a = jx$)

$$\overline{M}N = Ng_j\mu_B \left[\left(\frac{2j+1}{2j} \right) Coth \left(\frac{2j+1}{2j} \right) a - \frac{1}{2j} Coth \left(\frac{a}{2j} \right) \right]$$

$$\overline{M}_a = M_0 \left[\left(\frac{2j+1}{2j} \right) Coth \left(\frac{2j+1}{2j} \right) a - \frac{1}{2j} Coth \left(\frac{a}{2j} \right) \right]$$

Where $M_0 = NJg\mu_B$ is called saturated magnetic dipole moment. Then

$$\frac{\overline{M}_a}{M_0} = \left(\frac{2j+1}{2j} \right) Coth \left(\frac{2j+1}{2j} \right) a - \frac{1}{2j} Coth \left(\frac{a}{2j} \right)$$

$$\frac{\overline{M}_a}{M_0} = B(a) \quad\quad\quad ....(2.4.11)$$

where

$$B(a) = \frac{2j+1}{2j} Coth \left(\frac{2j+1}{2j} \right) a - \frac{1}{2j} Coth \left(\frac{a}{2j} \right) \quad ....(2.4.12)$$

is called Brillioun's function.

Case - I :- If $j = \infty$ then

$$B(a) = Coth a - \frac{1}{2j} . \frac{2j}{a}$$

$$= Cot \, ha - 1/a = L(a) \quad ....(2.4.13)$$

Where L(a) is called Langevin's function. It has been found that equation is good agreement with experiment result in comparison to the results obtained from classical equation. Where 'N' is No. of atoms in magnet per unit volume.

Case - II :- For J=1/2 then B(a) = 2 Cot h 2a - Cot h a = Tan h a

$$\therefore \frac{\overline{M}_a}{M_0} = Tan\,h\,a$$

……..(2.4.14)

The variation of Brilliouin's function with H for different values of J is as shown in Fig 2.4.1 The lowest curve indicates Langevin's curve.
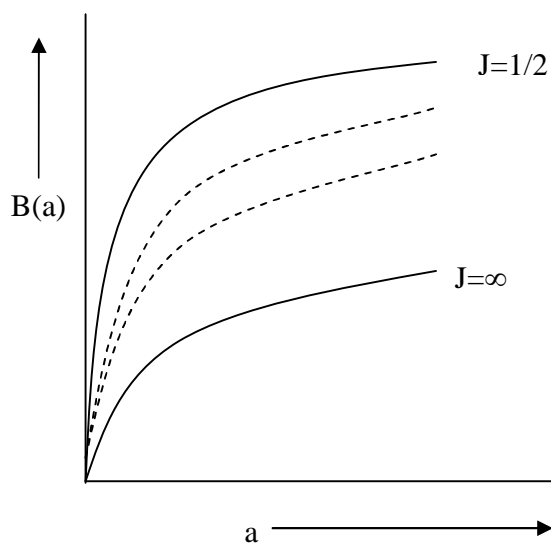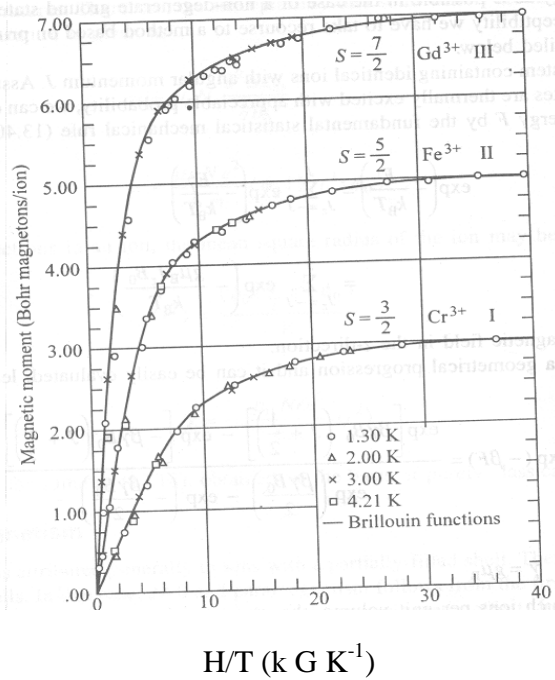

Fig.2.4.1

The experimental plot of magnetic moment verses H/T for certain materials is shown in Fig 2.4.2. As T →0 , the magnetic moment goes to its saturation value which means that the magnetic diploes will align completely with the field direction .

$$H/T \ (k \ G \ K^{-1})$$

Fig. 2.4.2. Magnetic moment verses H/T for certain materials I .Potassium chromium alum , II Ferric ammonium alum , III Gadolinium sulphate octahydrate

2.4.3 Susceptibility and Curie's law :

When   a $\ll$ 1 i.e . Jx $\ll$1 or Jgμ_BH/KT $\ll$ 1 means for low fields or higher temperatures

$$B(a) = \frac{\overline{M_a}}{M_0} = \left(\frac{j+1}{3j}\right)a = \left(\frac{j+1}{3j}\right)\frac{gj\mu_B H}{KT}$$

$$\text{Or} \quad \overline{M_a} = M_0 \left(\frac{j+1}{3j}\right)\frac{gj\mu_B H}{KT} = Ngj\mu_B \left(\frac{j+1}{3j}\right)\frac{gj\mu_B H}{KT}$$

$$= \frac{Ng^2\mu_B^2 j(j+1)}{3KT}H$$

or the susceptibility $\chi = \dfrac{\overline{M_a}}{H} = \dfrac{Ng^2\mu_B^2 j(j+1)}{3KT}$ ……..(2.4.15)

$\Rightarrow \chi = C/T$; where C $= \dfrac{Ng^2\mu_B^2 j(j+1)}{3K} = \dfrac{N\rho^2}{3K}$ ……..(2.4.16)

 is called as Curie constant .

$$\Rightarrow \chi \propto C/T \qquad\qquad ……..(2.4.17)$$

This is Curie's Law. i.e. If temperature decreases χ increases.

In the equation 2.4.11 $\qquad \rho = g \; \mu_B \sqrt{j(j+1)})$ $\qquad$ ……..(2.4.18)

is known as the effective magnetic moment .The order of magnitude of the paramagnetic susceptibility of a solid per cm^3 may be estimated from (2.4.15). With $N \approx 10^{22}$ and a dipole moment of one Bohr magneton , one obtains $\chi \approx 1/300T$. At room temperature $\chi \approx 10^{-5}$; at 1^0 K, $\chi \approx 10^{-3} - 10^{-2}$. These values are of importance in connection with the following question which may arise in the theory of the dielectric polarization of a solid it was necessary to introduce the internal electric field ,i.e., the actual field acting on a given atom was represented by sum of the applied field and the field due to polarization of the surroundings .On the other hand , in the derivation of magnetic susceptibility above , the field acting on a dipole in a paramagnetic solid was assumed to be equal to the field H. The justification for this is the following : the order of magnitude of the internal field is given by $H + \gamma M = H(1 + \gamma\chi)$, where $\gamma \approx 4$. Hence the fractional error made in neglecting the internal field correction is of the order of χ. As we have seen above , this small for paramagnetic materials .

The variation of effective magnetic moment for trivalent positive rare earth ions as a function of number of electrons evaluated using equation 2.4.18 is given in Fig 2.4.2
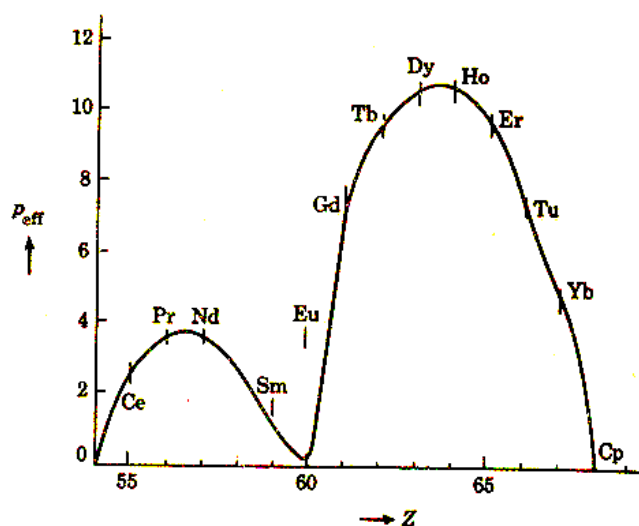
Fig 2.4.3 Variation of effective magnetic moment for trivalent positive rare earth ions as a function of number of electrons

2.4.4 Application to magnetic ions in solids: Effect of the crystal Field

Insulating **solids containing rare earth ions** obey the Curie law very well. The ρ-values (the effective Bohr Magneton numbers , equation 2.4.18) are derived from the coefficient of 1/T in using the measured values of χ . These are in exceedingly good agreement with those calculated with for all rare earth ions excepting samarium and europium. For both of these ions the J-multiple lying just above the ground state is very close in energy as a consequence of which a couple of assumptions made in the derivation of the Curie law remain no more valid :

1. 1. The second term is ignored in the derivation of the Curie law becomes important because the denominators ($E_n - E_{n^1}$) are now very small.

2. 2. There is an appreciable probability of thermally exciting some ions from the state(s) of lowest J to higher states, contrary to what is assumes for deriving the Curie law.

These observations explain the discrepancy noticed in respect of samarium and europium ions. Thus these observations lead to the conclusion that the rare earth ions can be treated as free ions even in solids. Effective magnetic moments for the trivalent lanthanide group ions are given in Table 2.4.1.

Table 2.4.1. Effective magnetic moments for the trivalent lanthanide group ions

Ion	Configuration	Basic level	$\rho = g\,\mu_B\sqrt{j(j+1)}$	ρ (exp)
Ce^{3+}	$4f^1\,5s^2p^6$	$^2F_{5/2}$	2.54	2.4
Pr^{3+}	$4f^2\,5s^2p^6$	$^3H_4$	3.58	3.5
Nd^{3+}	$4f^3\,5s^2p^6$	$^4I_{9/2}$	3.62	3.5
Pm^{3+}	$4f^4\,5s^2p^6$	$^5I_4$	2.68	-
Sm^{3+}	$4f^5\,5s^2p^6$	$^6H_{5/2}$	0.84	1.5
Eu^{3+}	$4f^6\,5s^2p^6$	$^7F_0$	0	3.4
Gd^{3+}	$4f^7\,5s^2p^6$	$^8S_{7/2}$	7.94	8.0
Tb3+	$4f^8\,5s^2p^6$	$^7F_6$	9.72	9.5
Dy^{3+}	$4f^9\,5s^2p^6$	$^6H_{15/2}$	10.63	10.6
Ho^{3+}	$4f^{10}\,5s^2p^6$	$^5I_8$	10.60	10.4
Er^{3+}	$4f^{11}\,5s^2p^6$	$^4I_{15/2}$	9.59	9.5
Tm^{3+}	$4f^{12}\,5s^2p^6$	$^3H_6$	7.57	7.3
Yb^{3+}	$4f^{13}\,5s^2p^6$	$^2F_{7/2}$	4.54	4.5

3d transition metal ions (the iron group). In the case of 3d transition metal ions, although the Curie law is obeyed, the experimental ρ-values are not accounted for by equation 2.4.13 . The agreement is close only if J is replaced by S in the relation, assuming that L is zero though S will be still given by the Hund's rules. This phenomenon is known as quenching of the orbital angular momentum and attributed to the crystal field effect. The crystal field effect is stronger in transition metal ions since their partially filled d-shell (3d in the iron group) happens to be the outermost shell. The electrons in the d-shell are thus directly exposed to the electric field created by ions surrounding the magnetic ion of concern. The coupling between L and S is largely broken so that the states are no longer specified by their J values. Further, the $(2L + 1)$ sublevels belonging to a certain L and degenerate in the free ion may be split by the crystal field. The splitting decreases the contribution of the orbital motion to the magnetic moment.

Table 2.4.2 . Effective magnetic moments for the iron group ions

Ion	Configuration	Basic level	$\rho = g\,\mu_B\sqrt{j(j+1)}$	$\rho = g\,\mu_B\sqrt{s(s+1)}$	ρ (exp)
Ti^{3+}, V^{4+}	$3d^1$	$^2D_{3/2}$	1.55	1.73	1.8
V^{3+}	$3d^2$	$^3F_2$	1.63	2.83	2.8
Cr^{3+}, V^{2+}	$3d^3$	$^4F_{3/2}$	0.77	3.87	3.8
Mn^{3+}, Cr^{2+}	$3d^4$	$^5D_0$	0	4.90	4.9
Fe^{3+}, Mn^{2+}	$3d^5$	$^6S_{5/2}$	5.92	5.92	5.9
Fe^{2+}	$3d^6$	$^5D_4$	6.70	4.90	5.4
Co^{2+}	$3d^7$	$^4F_{9/2}$	6.63	3.87	4.8
Ni^{2+}	$3d^8$	$^3F_4$	5.59	2.83	3.2
Cu^{2+}	$3d^9$	$^2D_{5/2}$	3.55	1.73	1.9

On the other hand, the crystal field effect for rare earth is almost negligible since their partially-filled shell (4f) lies deep inside the ion, sheltered by 5s and 5p shells. This explains why these ions behave as almost free ions even when they are embedded in crystals.

2.4.5   Summary

The difference between classical and quantum theory of paramagnetism have been discussed. Based upon the quantum theory the expression for magnetic susceptibility of paramagnet material has been derived. The paramagnetic properties of the materials containing rare earth ions and transition metal ions have also been discussed briefly.

2.4.6   Key terminology

Quantum Theory – Paramagnetism – Magnetic Susceptibility –Curie's Law– Crystal Field .

2.4.7   Self assessment Questions

1. Mention the differences between classical and quantum theory of paramagnetism
2. Discuss the quantum theory of paramagnetism. Derive Curie's law for paramagnetic material.
3. Discuss briefly the effect of crystal field on paramagnetic properties of solids.

2.4.8   Reference Books :

1. Elements of Solid State Physics – J.P.Srivastava (PHI, New Delhi, 2003)
2. Introduction to Solid state Physics – C.Kittel (Wiley Eastern, New Delhi, 2003)
3. Solid State Physics – A. J.Dekker (Macmillan , Madras, 1986)

Unit - II

Lesson 5

TYPES OF PARAMAGNETISM

Objective of the lesson

This chapter is aimed to discuss different contributions to the paramagnetism. It is also discussing with theory behind the method of cooling by adiabatic demagnetization.

Structure of the lesson

2.5.1 Introduction

2.5.2 van Vleck paramagnetism

2.5.3. Nuclear paramagnetism

2.5.4. Cooling by adiabatic demagnetization

2.5.1 Introduction

This chapter is aimed to discuss various types of paramagnetisms like vanVleck, Nuclear paramagnetism etc. More specifically the paramagnetic properties the material that contains the atoms of partially filled shells with J=0 have been discussed. The contribution to the paramagnetism from the nucleus magnetic moments has also been explained. Further the attainment of very low temperatures by the method of adiabatic demagnetization has also been described.

2.5.2 van Vleck paramagnetism

Consider the case of a partially-filled shell with J = 0, giving a non-degenerate ground state. It is the case of ions whose partially-filled shell is one electron short of being half filled. In a filled shell too, J = 0. But the present case is different in the sense that the second term in

2.3.25 does not vanish here, though it does so for ions having only completely occupies shell, simply because L and S are both independently zero for a completely filled shell. Hence the shift in the ground state energy induced by the magnetic filed in the present case is written as

$$\Delta E_0 = \frac{e^2}{8m}H^2\left\langle\phi_0\left|\sum_i x_i^2 + y_i^2\right|\phi_0\right\rangle - \sum\frac{\left|\left\langle\phi_0\left|\mu_B H(L + g_0 S)\right|\phi_n\right\rangle\right|^2}{E_n - E_0} \qquad\ldots\ldots\ldots(2.5.1)$$

If the system has N such ions per unit volume,

$$\chi = -\mu_0 N\frac{\partial^2 \Delta E_0}{\partial B_0^2} \qquad\ldots\ldots\ldots(2.5.2)$$

$$= -\mu_0 N\left[\frac{e^2}{4m}\left\langle\phi_0\left|\sum(x_i^2 + y_i^2)\right|\phi_0\right\rangle - 2\mu_B^2\sum_n\frac{\left|\left\langle\phi_0\left|(L_z + g_0 S_z)\right|\varphi_n\right\rangle\right|^2}{E_n - E_0}\right] \qquad\ldots\ldots\ldots(2.5.3)$$

In the above equation the first term with negative sign represents the diamagnetic susceptibility. The second term is an evidence for the paramagnetism it may be regarded as a correction to the diamagnetic contribution. The paramagnetic term is required to be examined in two extreme limits.

1. E_n-E_0 <<KT

In this limit , the excess population in the ground state over the excited state of energy E_n= $N(E_n$-E_0)/2KT

This gives raise to

$$M = \frac{NH\mu_B^2}{kT} \sum_n \left| \left\langle \phi_0 \right| (L_z + g_0 S_z) \left| \varphi_n \right\rangle \right|^2 \qquad ....(2.5.4)$$

and
$$\chi = \frac{N\mu_0 \mu_B^2}{kT} \sum_n \left| \left\langle \phi_0 \right| (L_z + g_0 S_z) \left| \varphi_n \right\rangle \right|^2 \qquad ....(2.5.5)$$

Here χ is independent of the separation of excited states from the ground state .

2. $E_n - E_0 >> KT$

In this case all the ions stay in the ground state. Then the magnetization

$$M = 2NH \, \mu_B^2 \sum_n \frac{\left| \left\langle \phi_0 \right| (L_z + g_0 S_z) \left| \varphi_n \right\rangle \right|^2}{E_n - E_0} \qquad ....(2.5.6)$$

and
$$\chi = 2N\mu_o \mu_B^2 \sum_n \frac{\left| \left\langle \phi_0 \right| (L_z + g_0 S_z) \left| \varphi_n \right\rangle \right|^2}{E_n - E_0} \qquad ....(2.5.7)$$

This expression indicates the paramagnetic susceptibility is independent of temperature and commonly known as van Vleck paramagnetism

## 2.5.3.Nuclear Paramagnetism

In   addition to the orbital motion and the spin of electrons, the nuclear spin also contributes to the magnetic moment of atoms. The nuclear magnetic moment is expressed in units of the nuclear Magneton in analogy with the Bohr defined by

$$\mu_n = \frac{e\hbar}{2M_P} = 5.051 x 10^{-27} J/T \qquad ....(2.5.8)$$

where M_P is the Proton mass.

Comparing with the 2.5.8 with 2.3.8 we see that the nuclear magneton is smaller than the Bohr magneton in the ratio of the Proton mass to the electron mass ($\approx 10^3$).

Therefore, the static nuclear paramagnetism is masked by the electron paramagnetism in paramagnetic substances. Solid hydrogen shows nuclear paramagnetism, though its electron configuration suggests diamagnetism only. The value of Proton magnetic moment is verified by these measurements. Heavy nuclei are found to possess even smaller magnetic moments. The method of nuclear magnetic resonance (NMR) is used to determine the nuclear magnetic moments. The nuclear magnetic moments, being very small compared to the electronic components, are almost ignored while discussing static magnetization. A comparative view of various forms of paramagnetism and diamagnetism are shown in Fig.2.5.1
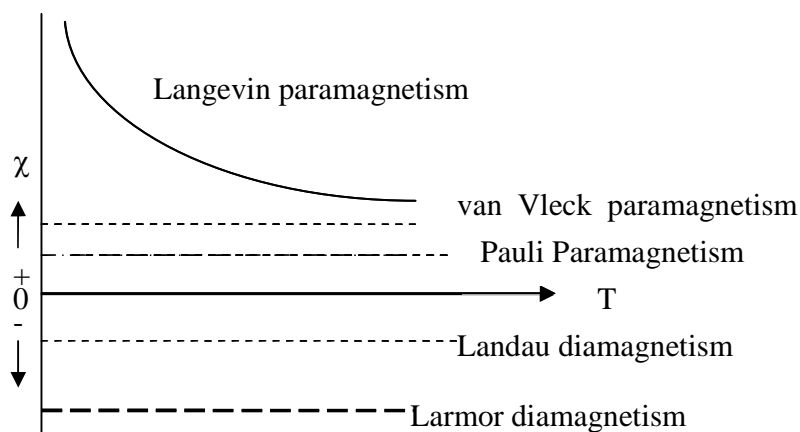
Fig. 2.5.1. A comparative view of various forms of para magnetism and diamagnetism, giving χ versus T plot.

2.5.4. Cooling by adiabatic demagnetization

For cooling below 1K, normally adiabatic demagnetization method is used. the selection of an appropriate system is not easy because at these low temperatures there is hardly any entropy left in any system. There may be only some solids suitable for the purpose. The

lattice entropy of a solid, at 1 K with $\theta_D = 100K$ it is merely $\sim 10^{-4}$ N K_B. (K_B- Boltzmann's constant) Hence this method is suitable only for paramagnetic solids which possess appreciable spin entropy. The underline principle is to apply magnetic field to reduce the entropy of paramagnetic salt immersed in liquid helium. The creation of a more ordered state of spins leads to the reduction of entropy. The liquid helium absorbs any head liberated in the process. The salt is then removed from the liquid helium bath and the magnetic field is switched on under adiabatic conditions implying that the entropy remains unchanged. The field is switched off slowly to ensure that the system passes through states always in thermal equilibrium. The temperature will have to fall if the entropy is to remain unchanged even after the magnetic field is completely withdrawn. In order to preserve the cooling thus produced, no heat should flow into the spin system. The most likely source of heat is the lattice entropy. Therefore, it is most important that the lattice entropy of the salt be smaller than its spin entropy to disallow heating. Salts containing rare earth elements because of their larger magnetic moments adequately satisfy the above condition and, therefore, used for adiabatic demagnetization.

Consider an entirely disordered spin system at high temperatures where the thermal disorder overpowers magnetic interactions that could produce any preferential spin orientations. A spin system of N ions, each of spin J, has (2J + 1) states in total over which the spins are distributed. If W represents the number of possible ways of distribution in a quantized spin system, the entropy S of the system is defined by

S = K ln W

Therefore, $W = (2J + 1)^N$

Showing that the entropy is temperature independent in the absence of a magnetic field.

For $J = \frac{1}{2}$, the entropy is equal to $NK \ln 2$. It shows that even for a two-level system, the spin entropy is far greater than the lattice entropy around 1 K ($\sim 10^{-4} Nk_B$). On the application of a magnetic filed H, the $(2J + 1)$ states are separated in energy is lowered when the lower levels gain in population. When the magnetic field is withdrawn adiabatically, the temperature falls so that the entropy may remain unchanged as required in an adiabatic change. A theoretical basis for this phenomenon is discussed below.

The entropy is defined in terms of the Helmholtz free energy F and the internal energy U as

$$S = \frac{U - F}{T} = K\beta(U - F) \qquad \ldots\ldots (2.5.9)$$

with $\beta = 1/KT$. Further, we learn from relation that for a system of non-interacting paramagnetic ions, βF depends on H only though the product βH. his requires F to be of the form

$$F = \frac{1}{\beta} f(\beta H) \qquad \ldots\ldots (2.5.10)$$

Where $f(\beta H)$ denotes a function of the product (βH)

Since U can be expressed as

$$U = \frac{\partial}{\partial \beta}(\beta F) \qquad \ldots\ldots (2.5.11)$$

The expression for entropy can now be written using 2.5.9 as

$$S = K\beta^2 \frac{\partial F}{\partial \beta}$$

or   using 2.5.10, $S = K\left[-f(\beta H) + \beta H f^1(\beta H)\right]$ ………. (2.5.12)

This relation indicates that S, also dependents on the product βH. Thus, if S is constant, βH also remains constant. $\Rightarrow$ H/T is also constant. Hence

$$\frac{(H)_{Initial}}{T_{Initial}} = \frac{(H)_{Final}}{T_{Final}}$$

$$T_{final} = \frac{(H)_{final}}{(H)_{Initial}} x T_{initial} \qquad ………. (2.5.13)$$

Instead of switching off the field, if we decrease it adiabatically to a certain value, according to 2.5.13, then, $T_{final} < T_{initial}$

The lowest possible temperature can be determined by the equation 2.5.12. In principle, we could even reach the absolute zero, if this relation is absolutely valid. Had it been true, the zero field entropy would not have been found to be temperature dependent as shown in Fig. 2.5.2.
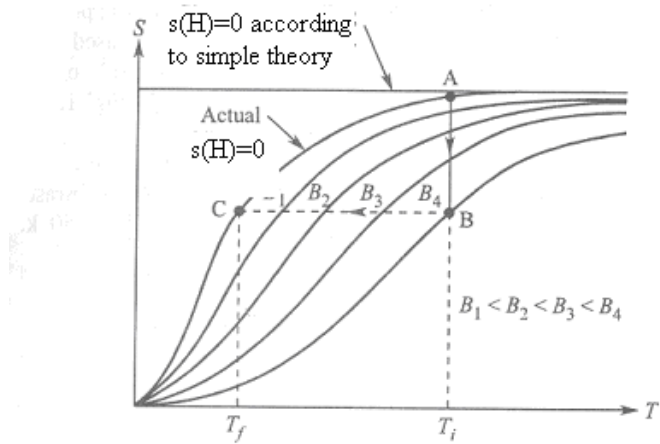
Fig. 2.5.2. Plot of entropy versus temperature cooling curves for interacting spins at various values of external induction Bo in an adiabatic demagnetization process.

The observed temperature dependence leads to the conclusion that the entropy will really drop to zero as the absolute zero is approached, a result that is consistent with the third law of thermodynamics.   Therefore, the condition must fail at small fields to account for the temperature dependence of the zero-field entropy.   In fact, even after the magnetic field is completely withdrawn there remains a magnetic field, though weak, mainly contributed by magnetic interactions between paramagnetic ions. This field in some cases may be as large as 100 gauss around 1 K.

When this aspect and other effects, such as strong crystal field splittings at low temperatures, are taken into consideration, the temperature dependence in question is properly explained using the resultant modified expression for entropy.

The process of cooling by adiabatic demagnetization is explained in Fig 2.5.2. with the help of S versus T curves for different magnetic fields. Initially, the paramagnetic salt rests immersed in liquid helium. The vertical line AB represents the first step of operation where the entropy is isothermally reduced from its initial value at A to a lower value at B by applying a magnetic field B_4 . Notice that the point A lies on the zero-field S versus T curve and the point B on a curve obtained in the presence of the field B4. There are other curves for fields lowers than $B_4 - B_3 > B_2 > B_1$. The S versus T behaviour in the absence of a magnetic field as predicted by simple theory and as observed as shown by two separate curves.

In the next step, the salt is removed from the liquid helium bath and the field reduced under adiabatic conditions (but slowly) through B_3, B_2, B_1 . . . . to zero value. The operation is represented by the horizontal line BC. The intersection of BC with

various S versus T curves gives the temperature $T_3 > T_2 > T_1$ corresponding to the fields B_3, B_2 & B_1 at three different stages during the process of adiabatic demagnetization. The lowest temperature approached is shown as T_f symbolized by the point C on the observed zero-field curve. As mentioned earlier, the lowest temperatures produced by adiabatic demagnetization are in the rage of 10^{-3}K.

2.5.5   Summary of the lesson

Different contributions to the paramagnetism like van Vlek paramagnetism, nuclear paramagnetism etc., have been discussed. The theory behind in cooling the material by adiabatic demagnetization has also been included.

2.5.6   Key terminology

van Vlek paramagnetism- Nuclear paramagnetism – Adiabatic demagnetization-

2.5.7   Self assessment questions

1. Discuss the concept of van Valek paramagnetism.

2. Explain the nuclear contribution to the paramagnetism.

3. Give the theory on cooling of the materials by adiabatic demagnetization

2.5.8   Reference Books

1. Elements of Solid State Physics – J.P.Srivastava (PHI, New Delhi, 2003)
2. Introduction to Solid state Physics – C.Kittel (Wiley Eastern, New Delhi, 2003)
3. Solid State Physics – A. J.Dekker (Macmillan , Madras, 1986).

UNIT -3

LESSON – 1

FERROMAGNETISM

Objective of the lesson

The objective of this lesson is to discuss the properties of ferromagnetic materials based on the quantum mechanical theory. It is also intended to interpret the phenomenon of ferromagnetism on the basis of the concept of domains.

Structure of the lesson

3.1.1. Introduction

3.1.2. Weiss theory of Ferromagnetism

3.1.3. Relationship between saturation magnetization and temperature

3.1.4. Ferromagnetic Domains

3.1.1. Introduction

Iron, cobalt, nickel and their alloys are well known Ferromagnetic materials since a long time. These materials exhibit hysteris loop. The susceptibility of these materials obeys Curie-Weiss law. i.e. $\chi = c/T-\theta$. Above the Curie temperature θ these materials act as paramagnets. Ferromagnetic specimens in general contain a number of small regions called domains which are spontaneously polarized. There exists a molecular filed within each domain and filed leads to produce parallel alignment of individual localized atomic moments. Based on these points, Weiss developed a formula for susceptibility of ferromagnetic materials.

3.1.2. Weiss theory of Ferromagnetism

In order to explain the relation between Para and Ferro magnets as well as to account for the special features of Ferromagnetics, Weiss gave his molecular theory.

Weiss theory is centered about the following two hypotheses.

1. A ferromagnetic specimen contains a number of small regions called "domain" which are spontaneously magnetized.

2. With in each domain, the spontaneous magnetization is due to the existence of internal molecular field, which tends to produce a parallel alignment of the atomic dipoles. The internal field is proportional to the intensity of magnetization

$$H_w \propto M_T$$

$$\text{or } H_w = N_W M_T \qquad\qquad \text{……….(3.1.1)}$$

M_T - Magnetization at the temperature T, N_w - Weiss constant. If H is external magnetic fields, the effective field acting on the ion (or) atom.

from the definition of the susceptibility, $\chi = M_T/H$

$$\text{or } M_T = \chi\, H = \frac{n\rho^2 \mu_B^2}{3KT} H \qquad\qquad \text{……….(3.1.2)}$$

The value of χ is substituted from the quantum theory of paramagnetism.

Taking $H_{eff} = H + N_W M_T$ in 3.1.2,.

$$M_T = \frac{n\rho^2 \mu_B^2}{3KT}(H + N_W M_T) \qquad\qquad \text{……….(3.1.3)}$$

$$= \frac{n\,\mu_J^2}{3KT}(H + N_W M_T), \qquad \text{where } \mu_J = \rho\mu_B$$

$$M_T\left(1 - \frac{n\mu^2 N_W}{3K_T}\right) = \frac{n\mu_J H}{3K_T}$$

Therefore volume susceptibility $\chi = M_T/H$

$$= \frac{n\mu_J^2}{3K(T - \dfrac{n\mu_J^2 N_W}{3K})} = \frac{C'}{T - \theta_W} \qquad\qquad \text{……….(3.1.4)}$$

is known as Curie - Weiss Law. In the equ. (3.1.4)

$$C' = \frac{n\mu_J^2}{3K} \qquad \text{and } \theta_W = \frac{n\mu_J^2 N_W}{3K} = C' N_w$$

are called as the Curie constant and Ferro magnetic Curie temperature respectively.

From the paramagnetic theory we have $M_T = M_0\, B(a)$, where $a = g J \mu_B H/KT$. In this case

$$a = g J \mu_B (H + Nw\, M_T)/KT. \qquad\qquad \text{……….(3.1.5)}$$

Since we are interested in spontaneous magnetization if we keep H=0 (the applied field) in 3.1.5. we get

$$M_T = KT\, a\, /\, gJ\, \mu_B N_W \qquad\qquad \text{……….(3.1.6)}$$

Since M_T should satisfy the equations $M_T = M_0$ B(a) and 3.1.6. Its value at a given temperature can be obtained from the point of intersection of the two corresponding M_T verses "a" curves as shown in the Fig. 3.1.1.
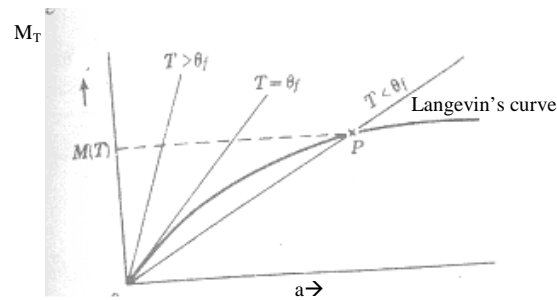
Fig. 3.1.1. Graphical method of finding spontaneous magnetization at a temperature T.

The straight line in Fig. 3.1.1 indicates that the slope is proportional to T. If T<θ , a non vanishing value for spontaneous magnetization exists. For T = θ the slope of the straight line represented by the equation. 3.1.6. is equal to tangent of the curve at the origin. If T > θ, the spontaneous magnetization vanishes. In the Table 3.1.1 the Curie temperature and saturation magnetization for some of the ferromagnetic substances are presented.

Table 3.1.1.

Substance	Saturation magnetization M_s in gauss		Ferromagnetic Curie
	Room Temperature	0 K	temp. in K
Fe	1707	1740	1043
Co	1400	1446	1400
Ni	485	510	631
Gd	-	2010	292
Dy	-	2920	85
Cu_2MnAl	500	(550)	710
MnAs	670	870	318
MnBi	620	680	630
Mn_4N	183	-	743
MnSb	710	-	587
MnB	152	163	578
CrTe	247	-	339
$CrBr_3$	-	-	37
CrO_2	515	-	392
$MnOFe_2O_3$	410	-	573
$FeOFe_2O_3$	480	-	858
$CoOFe_2O_3$	400	-	793
$NiOFe_2O_3$	270	-	858
$CuOFe_2O_3$	135	-	728
$MgOFe_2O_3$	110	-	713
UH_3	-	230	180
EuO	-	1920	69
$GdMn_2$	-	215	303
$Gd_3Fe_5O_{12}$	0	605	564
$Y_3Fe_5O_{12}$(YIG)	130	200	560

3.1.3. Relationship between saturation magnetization and temperature

At $M_T = M_s$, $H = N_W M_S$, then $\dfrac{M_T}{M_0} = B(a)$ gives

$$\frac{M_T}{M_0} = \frac{2j+1}{2j}\coth\left(\frac{(2j+1)}{2j}\frac{jg\mu_B N_W M_S}{KT}\right) - \frac{1}{2j}\coth\left(\frac{1}{2j}\frac{jg\mu_B N_W M_S}{KT}\right) \ldots\ldots\ldots(3.1.7)$$

But $\theta_W = \dfrac{n\mu_J^2 N_W}{3K} = \dfrac{(j+1)jNg^2\mu_B^2}{3K}N_W$

$$\Rightarrow \qquad \frac{g\mu_B N_W}{K} = \frac{3\theta_C}{j(j+1)Ng\mu_B} = \frac{3\theta_C}{(j+1)M_0}$$

Hence $\dfrac{M_S}{M_0} = \dfrac{2j+1}{2j}\coth\left(\dfrac{(2j+1)}{2j}\dfrac{j3\theta_C}{(j+1)T}\dfrac{M_S}{M_0}\right) - \dfrac{1}{2j}\coth\left(\dfrac{1}{2j}\dfrac{j3\theta_C}{(j+1)T}\dfrac{M_S}{M_0}\right)$

$$= \frac{2j+1}{2j}\coth\left(\frac{(2j+1)}{2}\frac{3\theta_C}{(j+1)T}\frac{M_S}{M_0}\right) - \frac{1}{2j}\coth\left(\frac{1}{2}\frac{3\theta_C}{(j+1)T}\frac{M_S}{M_0}\right) \qquad \ldots(3.1.8)$$

Now we shall verify this theoretical formula by practical considerations.

(i) If $j = 1/2$,

$$\frac{M_S}{M_0} = 2\coth\left(2\frac{\theta_C}{T}\frac{M_S}{M_0}\right) - \coth\left(\frac{\theta_C}{T}\frac{M_S}{M_0}\right) = \text{Tanh}\left(\frac{\theta_C}{T}\frac{M_S}{M_0}\right) \quad \ldots(3.1.9)$$

(ii) If $j = \infty$

$$\frac{M_S}{M_0} = 2\coth\left(2\frac{\theta_C}{T}\frac{M_S}{M_0}\right) - \left(\frac{1}{3}\frac{\theta_C}{T}\frac{M_0}{M_S}\right) \qquad\qquad \ldots(3.1.10)$$

since Coth x = $(1/x) + (x/3) - \ldots\ldots$ for j = ∞, Cothx $\approx (1/x)$ has been used   in (3.1.10). The variation of M_T/M_0 evaluated using equation 3.1.8 for three different values of j for Fe , Ni , Co , are given in Fig 3.1.2
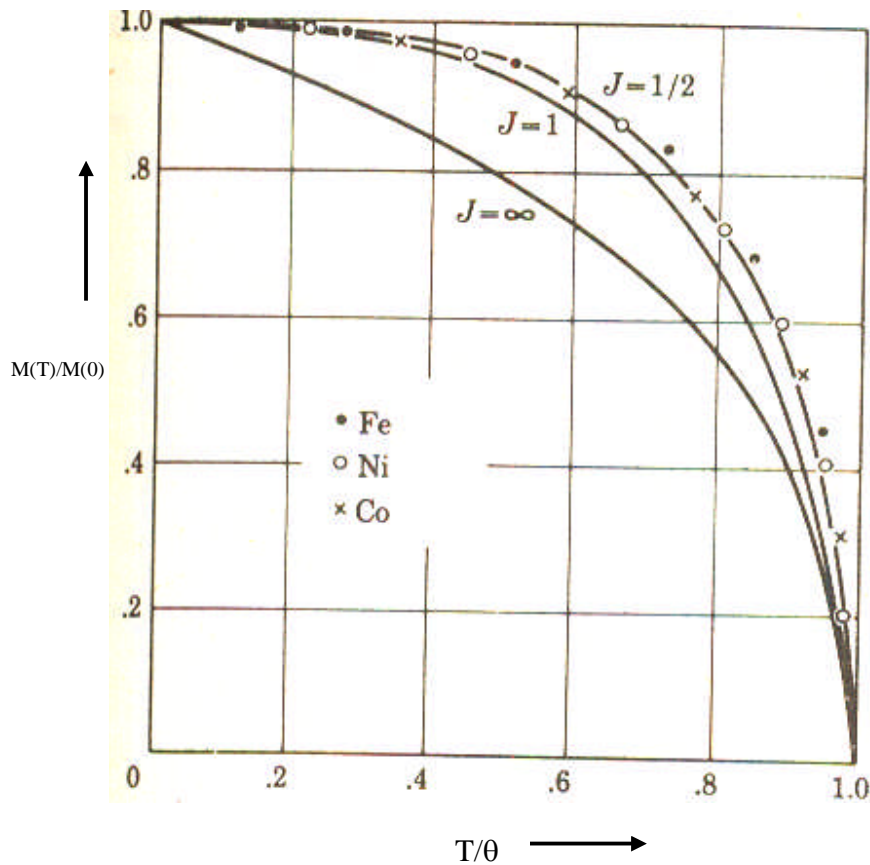
Fig 3.1.2 The variation of M_T/M_0 for three different values of j for Fe , Ni , Co .

As the experimental curves for these three metals are coinciding with theoretical curves for j=1/2 .The normal states of free atoms are Fe = $^5D_4$ (j=4) , Co = $^5F_{9/2}$ (j=9/2) ,Ni= $^3F_4$ (j=4) .For none of these metals J=1/2 .Hence there is a discrepancy between the theory and the experiment. This discrepancy can however be overcome if take L = 0. Then, J = L+S = 0+1/2 =1/2 . This indicates the magnetization associated with electron spins rather than orbital motion. This type of magnetization is known as the orbital quenching.

3.1.4. Ferromagnetic Domains

It is known that a piece ferromagnetic material may exist in the non magnetized state, whereas a weak magnetic field may produce saturation magnetization in the same specimen. To explain this Weiss introduced the domain hypothesis. Each domain is spontaneously magnetized. The overall magnetization is given by the sum of the domain vectors, which may vanish under certain circumstances.

Magnetization of a specimen may occur either by the growth of one domain at the expense of another, i.e. by the motion of domain walls (Fig. 19-6b), or by rotation of domains (Fig. 19-6c). A representative magnetization curve is given in Fig. 19-7, indicating the predominant processes in the different regions. We may note here that originally it was thought that the well-known Barkhausen jumps were due to the rotation of a complete domain and that the size of the Barkhausen discontinuities was a measure of the size of the domains.

However, it was later shown that the Barkhausen jumps are mainly associated with irregular fluctuations in the motion of the domain walls rather than with domain rotation..
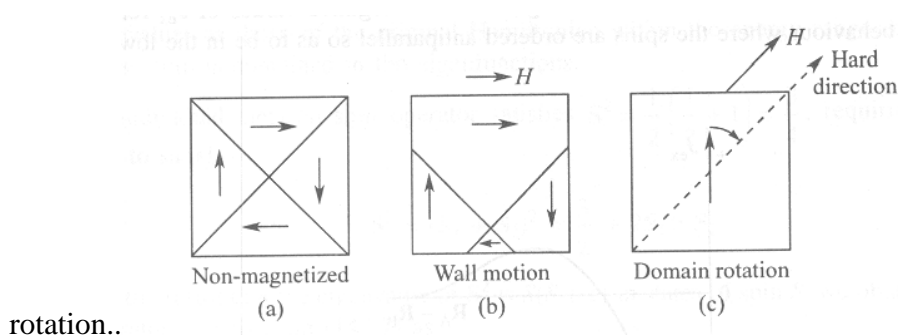
Fig.3.1.3. Domain structures.

These are different methods for observing the domains, the main method is known as Bitter powder pattern method. In this method, a few drops of colloidal suspension of ferromagnetic material, the particles of the suspension will settle upon the walls of domain of ferromagnetic materials. These boundaries are clearly seen with the help of powerful microscope.
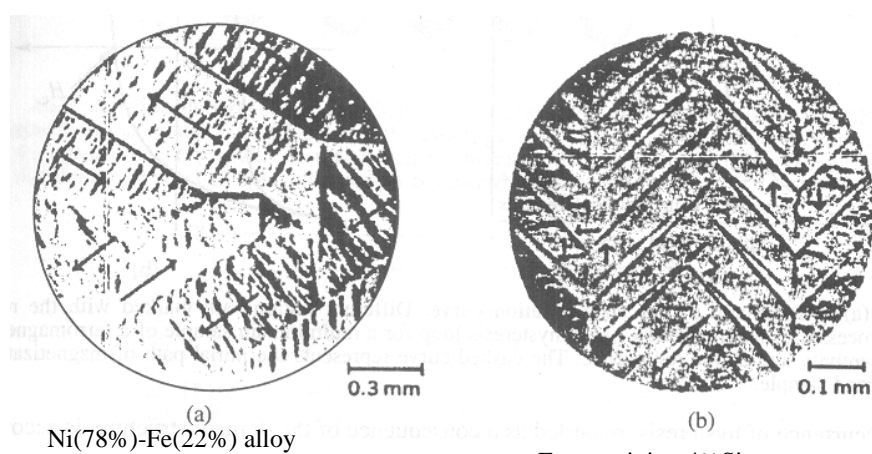

(a)
Ni(78%)-Fe(22%) alloy

(b)
Fe containing 4%Si

Fig 3.1.4.Domain structures observed under a microscope for some iron alloys

On the surface of the specimen; since there are strong local magnetic fields near the domain boundaries, the particles collect there and the domains can be observed under a microscope. Domain structures observed under a microscope for some iron alloys are shown in Fig3.1.4.

The ferromagnetic material exhibit hysterics if the external field is increased up to certain point A, linearity exists between the magnetization and the applied field (Fig.3.1.5.), if the field is decreased from the point A, then the curve traces its original path. Up to the point A, it is the reversible wall displacement that contributes to the magnetization. If the field is increased beyond A, the saturation magnetization is achieved and if the field is decreased from the point of saturation C, the curve no longer traces the original path and it cuts the Y-axis at a point indicating the retention of certain magnetization even for H = 0 and that point is known as retentively. If we want to demagnetize the material completely, the external field is to be applied in the reverse direction and field is known as coercive field H_c. If the field is reversed in this way a cycle will be completed as shown in the Fig.3.1.5. This curve is known as hysterisis loop. The area under the curve represents the loss of energy during magnetization.
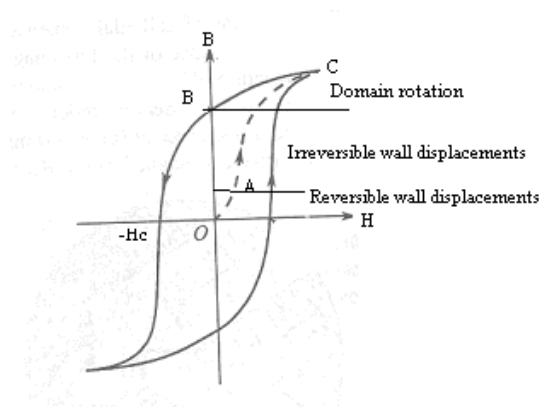

Fig. 3.1.5. Magnetization curve of a ferromagnetic substance

The physical origin of domains can be understood from the general thermodynamic principle that the free energy E -TS of a solid tends to reach a minimum value. As a result of the high degree of order in the magnetic system, the entropy term may be neglected. Thus, minimizing the energy E of the system should be sufficient to understand the existence of domains. To illustrate this point, consider the cross section of a ferromagnetic single crystal Fig.

3.1.6.. In Fig. 3.1.6.(a) we have a single domain, i.e., the specimen acquired saturation magnetization. Because of the free magnetic poles at the ends of the specimen, the expression for the energy will contain a term $(1/8\pi) \int H^2 \, dV$ associated with the field outside the crystal. In Fig. 3.1.6.(b) on the other hand, the field energy is strongly reduced because the spatial extension of the field is much smaller. There is a certain amount of energy involved in producing a domain wall. Hence, one ultimately arrives at an equilibrium situation with a number of domains such that the energy required to produce one more domain boundary is equal to the resulting reduction of the field energy.
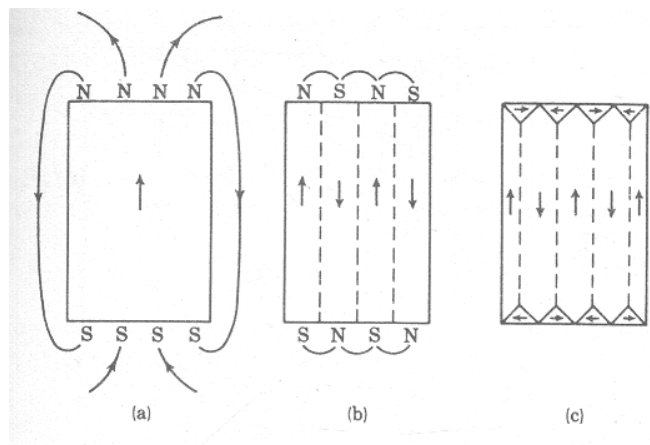
Figure 3.1.6. The origin of domains.

A domain structure such as in Fig. 3.1.6.(c) has zero magnetic field energy. This is achieved by introducing the triangular prism domains at top and bottom of the crystal; such domains are called closure domains. Note that the wall between a closure domain and a vertical domain in Fig. 3.1.6.(c), makes an angle of 45^0 with the magnetization directions in both types of domains. Hence the normal component of the magnetization in crossing such a wall is continuous, i.e., there are no free poles and there is no field energy. The energy required to produce a closure domain is essentially determined by the anisotropy of the crystal, i.e., by the fact that ferromagnetic materials have "easy" and "hard" directions of magnetization. For example, from the magnetization curves represented in Fig. 3.1.7 one sees that in iron, which is cubic, the easy directions of magnetization are the cube edges.
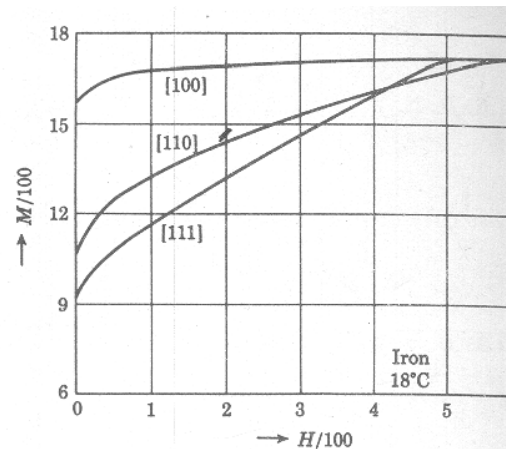
Fig .3.1.7. Magnetization curves for a single crystal of iron along different directions   of the crystal axis.

In nickel, which is also cubic, the easy directions of magnetization are the body diagonals. In cobalt the hexagonal axis of the T crystal is the only preferred direction; thus in a cobalt crystal with b prominent domains magnetized along the hexagonal axis, the closure domains are necessarily magnetized along a hard direction. In iron and nickel, on the other hand, it is possible to have both the closure domains and the dominant domains magnetized along easy directions. Summarizing the ideas discussed above we may say that domain structure has its origin in the principle of minimum energy.

3.1.5   Summary of the lesson

Wiess theory of ferromagnetism has been discussed briefly using quantum mechanical concepts and Curie- Weiss law for the susceptibility of the ferromagnetic materials has been derived. Comparison of the theoretical results with the experimental results has also been presented. Origin for the spontaneous magnetization has also been discussed using the concept of domains.

3.1.6 Key Terminology

Wiess theory – Spontaneous magnetization – Hysterisis loop - Domains

3.1.7 Self – assessment questions

1. Discuss the Wiess theory of ferromagnetism and arrive at an expression for the susceptibility of ferromagnetic materials.

2. Discuss the dependence of saturation magnetization on temperature..

3. Write a note on ferromagnetic domains.

3.1.8 Reference Books :

1. Elements of Solid State Physics – J.P.Srivastava (PHI, New Delhi, 2003)

2. Introduction to Solid state Physics – C.Kittel (Wiley Eastern, New Delhi, 2003)

3. Solid State Physics – A. J.Dekker (Macmillan , Madras, 1986)

Unit – 3

Lesson – 2

INTERPRETATION OF THE WEISS FIELD AND
THE THEORY OF MAGNONS

Objective of the lesson

To deal with the explanation of the Weiss field-Exchange Interaction
and to discuss spin wave or Magnon theory

Structure of the lesson

3.2.1. Introduction

3.2.2 The interpretation of the Weiss field-Exchange Interaction

3.2.3. Theory of Magnons

3.2.3a Dispersion relation for magnons

3.2.3b Quantization of spin waves

3.2.3c Bloch $T^{3/2}$ Law

3.2.1. Introduction

In 1928 Heisenberg showed that the large molecular field may be explained in terms of exchange interaction between the electrons. The principle of this explanation has been illustrated by considering the hydrogen molecule as an example . A part of this chapter deals with the theory of magnons which means quantized spin waves, these are analogous to lattice vibrations (or) phonons.

3.2.2 The interpretation of the Weiss field-Exchange interaction

In this section we shall discuss Heisenberg's interpretation of Weiss internal field.First of all, a rough estimate of the required molecular field H_m may be made as follows. The energy of a given atomic dipole in this field should be of the order $\mu_B H_m \approx K\theta$ .For a Curie temperature $\theta \approx 1000K$ this gives $H_m \approx 10^7$ gausses. From this one concludes immediately that the internal

field is not due to a simple dipole-dipole interaction between neighbors, because such fields would be of the order $\mu_B / a^3 \approx 10^3$ gausses.

Heisenberg showed that the large molecular field may be explained in terms of exchange interaction between the electrons. The principle of this explanation may be illustrated by considering the hydrogen molecule. Let the two nuclei of hydrogen molecule be denoted by a and b, the atomic wave functions by ψ_a and ψ_b and the electrons by 1 and 2. The interaction potential between the two atoms is then given by

$$V_{ab} = e^2 \left(\frac{1}{r_{ab}} + \frac{1}{r_{12}} - \frac{1}{r_{b1}} - \frac{1}{r_{a2}} \right) \qquad\qquad \ldots\ldots\ldots(3.2.1)$$

From the Heitler-London theory of chemical binding one knows that the energy of the system is in the form, $E = K \pm J_e$. where K is the Coulomb interaction energy and J_e is the exchange integral, given by

$$j_e = \int \psi_a^*(1)\psi_b^*(2) V_{ab} \psi_a(2)\psi_b(1) dv_1 dv_2 \qquad\qquad \ldots\ldots\ldots(3.2.2)$$

The plus sign in the expression for energy E refers to the nonmagnetic state of the molecule in which the two electronic spins are anti parallel. The minus sign corresponds to the case in which the two spins are parallel, i.e., to the magnetic state .It is evident from the equation $E = K \pm J_e$. that the magnetic state is stable only if J_e is positive, because then $(K - J_e) < (K + J_e)$. expression for energy E may be written in a more convenient form which contains the relative orientation of the two spins, viz.,

$$E = \text{const.} \ -2J_e \ S_1.S_2 \qquad\qquad \ldots\ldots\ldots(3.2.3)$$

In other words, the exchange energy appears in the total energy as if there is a direct coupling between the two spins. It must be emphasized, however, that the exchange interaction is fundamentally electrostatic and that the spin enters into the energy expression as a consequence of the Pauli Exclusion Principle.

We shall now assume that for two atoms i and j the effective coupling between the spins due to exchange interaction is equivalent with a term $-2J_e S_i.S_j$ in the energy expression; J_e is the exchange integral for the two atoms. In general, the exchange integral is negative, i.e., in general the non- ferromagnetic state is favored. However, J_e is likely to be positive when the distance r_{ab}

between the nuclei is fairly large compared with the orbital radii of the electrons involved. The behavior of J_e as function of r_{ab} is indicated in Fig. 3.2.1.
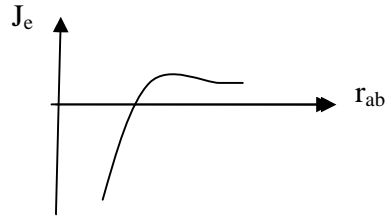
Fig. 3.2.1.Behavior of the exchange integral
J_e as function of inter atomic distance r_{ab}

According to Slater, the ratio r_{ab}/r_o where r_o is the orbital radius should be larger than 3 for J_e to be positive but not much larger. The ratios r_{ab}/r_o for some metals are given below.

	Fe	Co	N	Cr	Mn	Gd
r_{ab}/r_o	3.26	3.64	3.94	2.60	2.94	3.1

Note that Cr and Mn are not ferromagnetic. One might raise the question here whether an element with uncompensated spins, which itself is not ferromagnetic because the r_{ab}/r_o value is not favorable, may be combined with another non ferromagnetic element to form a compound for which the r_{ab}/r_o value is suitable for ferromagnetism. That this seems indeed possible, for example MnAs and MnSb are both ferromagnetic; the lattice constants of these compounds are, respectively, 2.85 and 2.89 A^o, as compared with 2.58 A^o for pure Mn. The ferromagnetism of the other alloys can be explained in a similar manner.

Because of the importance of the exchange integral, one would like to relate it to the Weiss constant N_w and to the ferromagnetic Curie temperature. An approximate relationship between J_e and N_w can be found as follows. We assume that the exchange integral is negligible except for nearest neighbors and that its value is J_e for all neighboring pairs. We may then write for the exchange energy of a given atom i with its neighbors as

$$V = -2J_e \sum_j S_i S_j, \qquad\qquad \ldots\ldots\ldots(3.2.4)$$

where the summation is taken over to the nearest neighbors of atom i. Replacing the instantaneous values of the neighboring spins by their time averages that there are z nearest neighbors to the atom i we get,

$$V = -2zJ_e \left(S_{xi} \langle S_{xj} \rangle + S_{yi} \langle S_{yi} \rangle + S_{zi} \langle S_{zj} \rangle \right) \qquad \ldots\ldots\ldots(3.2.5)$$

Assuming that the magnetization M is along the z-direction, we may take

$\langle S_{xj} \rangle = \langle S_{yj} \rangle = 0$ and $\langle S_{zj} \rangle = M / g\mu_B N$

According to (3.2.4) and (3.2.5.),

$$V = - 2z\, j_e\, S_{zi}\, M/g\, N\mu_B \qquad \ldots\ldots\ldots(3.2.6)$$

Now, this expression should be equal to the potential energy of spin i in the Weiss field N_w M, i.e.,

$$V = - g\, S_{zi}\, \mu_B\, N_w\, M \qquad \ldots\ldots\ldots(3.2.7)$$

From the equations (3.2.6) and (3.2.7) we obtain

$$N_w = 2\, z\, J_e\, /\, N\ g^2 \mu_B^2 \qquad \ldots\ldots\ldots(3.2.8)$$

From the expression for Curie temperature(§ 3.1.2), we obtain the relation between θ_f and J_e as

$$\theta_f = 2\, zJ_e\, S(S+1)/3\ K \qquad \ldots\ldots\ldots(3.2.9)$$

Thus for a simple cubic lattice with z = 6 and with S = ½ , one finds

$$J_e/K\theta\ = 1/3 \qquad \ldots\ldots\ldots(3.2.10)$$

more exact calculations by Opechowski and P. R. Weiss give, respectively 0.518 and 0.540 for the $J_e/K\theta_f$ for a simple cubic lattice.

3.2.3. Theory of Magnons

Magnon means quantized spin wave, these are analogous to lattice vibrations (or) Phonons.

Consider i^{th} and j^{th} atoms and S_i & S_j are their corresponding spins. Then the energy of the interaction between two spins is

u = -2$J_e S_i.S_j$,   where J_e is exchange energy

According to Heisenberg model, at T=0 K we can represent all the spins as parallel vectors. The spin $S = \dfrac{1}{2}$ and lie on a single line as shown in Fig.3.2.2
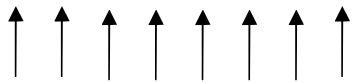
Fig.3.2.2 The spins as parallel vectors.

Then the spins interaction energy (if there are 'n' such type of spins) is

$$U = -2J_e \sum_{p=1}^{N} S_p . S_{p+1} \qquad \text{.........(3.2.11)}$$

S_p stands for p^{th} spin and S_{p+1} stands $(p+1)^{th}$ spin

If the temperature of the system is increased, due to thermal agitation some of the spins may be reversed. Now let us consider the situation, if one of the spins is exited, means one of spins is in the reverse direction. The reversal of spin is shared by all the other spins also. All the spins but not limited to the neighbouring spin alone. The situation of the spins corresponding to this state can be pictured as in Fig 3.2.3. The spin vectors moves in the preferred directions as shown in the Fig 3.2.3(a) . The heads of spins form a wave as shown in the Fig 3.2.3(b).
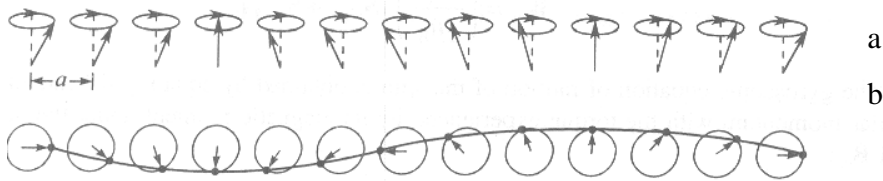
Fig 3.2.3 Formation of a spin wave

This wave is knows as spin wave corresponding to each atom, there is a spin wave. The quantized spin wave is known as "Magnon".

3.2.3a Dispersion relation for magnons

The interaction energy between magnetic moment and applied magnetic field is represented by

$$U = -g\mu_B \sum_{p=1}^{N} \vec{\mu}_p . \vec{H}_p \quad = \qquad \text{.........(3.2.12)}$$

$\vec{\mu}_P = -g\mu_B \vec{S}_p$ is the magnetic moment and $\vec{H}_p$ is the magnetic field at the site p.

Now the interaction between spins is represented by

$$U = -2J_e \sum_{P=1}^{N} S_P S_{P+1} = 2J_e \sum_{P=1}^{N} \left[S_{P-1} S_P + S_P S_{P+1} \right] \qquad \ldots\ldots\ldots(3.2.13)$$

comparing the coefficients of S_P in equations (3.2.12)and (3.2.13) ,we get

$$\vec{H}_p = -\frac{2 j_e}{g\mu_B} \left(S_{p-1} + S_{p+1} \right) \qquad \ldots\ldots\ldots(3.2.14)$$

from the elementary mechanics we know that the rate of change of angular momentum i.e

., $\frac{d}{dt}\left(\hbar S_p\right)$ is equal to torque $\tau = \vec{\mu}_p \times \vec{H}_p$

i.e. $\qquad\qquad \frac{d}{dt}\left(\hbar S_p\right) = \vec{\mu}_p \times \vec{H}_p \qquad \ldots\ldots\ldots(3.2.15)$

$$\Rightarrow \frac{d}{dt}\left(S_p\right) = \frac{1}{\hbar}(\vec{\mu}_p \times \vec{H}_p) = \frac{1}{\hbar} \vec{\mu}_p \times \left[-\frac{2 j_e}{g\mu_B}\left(S_{p-1} + S_{p+1} \right) \right]$$

$$= -\frac{2 j_e}{g\mu_B} \frac{1}{\hbar} g\mu_B (\vec{S}_p \times (S_{p-1} + S_{p+1}))$$

$$= -\frac{2 j_e}{\hbar} (\vec{S}_p \times (S_{p-1} + S_{p+1})) \quad \ldots\ldots\ldots(3.2.16)$$

Resolving S_p in to three components, we have

$$\frac{dS_p^x}{dt} = \frac{2 j_e}{\hbar} \left[S_p^y \left(S_{p-1}^z + S_{p+1}^z \right) - S_p^z \left(S_{p-1}^y + S_{p+1}^y \right) \right] \qquad \ldots\ldots\ldots(3.2.17)$$

$$\frac{dS_p^y}{dt} = \frac{2 j_e}{\hbar} \left[S_p^z \left(S_{p-1}^x + S_{p+1}^x \right) - S_p^x \left(S_{p-1}^z + S_{p+1}^z \right) \right] \qquad \ldots\ldots\ldots(3.2.18)$$

$$\frac{dS_p^z}{dt} = \frac{2 j_e}{\hbar} \left[S_p^x \left(S_{p-1}^y + S_{p+1}^y \right) - S_p^y \left(S_{p-1}^x + S_{p+1}^x \right) \right] \qquad \ldots\ldots\ldots(3.2.19)$$

All these three equations are linear set of equations .If we assume that the amplitude of the excitation is very small , then $S_p^x , S_p^y \ll S$ and $S_p^z = S_{p-1}^z = S_{p+1}^z = S$,the equations 3.2.17,3.2.18 and 3.2.19 will be modified to

$$
\left.
\begin{aligned}
\frac{dS_p^x}{dt} &= \frac{2 j_e}{\hbar} S \left[2 S_p^y - S \left(S_{p-1}^y + S_{p+1}^y \right) \right] \\
\frac{dS_p^y}{dt} &= \frac{2 j_e}{\hbar} S \left[\left(S_{p-1}^x + S_{p+1}^x \right) - 2 S_p^x \right] \text{ and} \\
\frac{dS_p^z}{dt} &= 0
\end{aligned}
\right\}
\qquad \ldots\ldots\ldots(3.2.20)
$$

Equation 3.2.20 can be solved by assuming the solution as

$$
S_p^x = u e^{i(pka - \omega t)} \quad \text{and} \quad S_p^y = v e^{i(pka - \omega t)} \qquad \ldots\ldots\ldots(3.2.22)
$$

where u, v are amplitudes of spin waves, p is an integer, a is the lattice constant and k is the propagation constant.

Substituting eqn.3.2.22 in eqn.3.2.21, one gets,

$$
(-i\omega) u \; e^{i(pka - \omega t)} = \frac{2 j_e}{\hbar} S \left[2 v e^{i(pka - \omega t)} - v e^{i(ka(p-1) - \omega t)^i} - v e^{i(ka(p+1) - \omega t)} \right]
$$

$$
\Rightarrow (-i\omega) u = \frac{2 j_e}{\hbar} S \left[2v - v e^{-ika^i} - v e^{ika} \right] = \frac{4 j_e}{\hbar} S v \left[1 - \left(e \frac{-ika^i + e^{ika}}{2} \right) \right]
$$

$$
= \frac{4 j_e}{\hbar} S (1 - \cos ka) v \qquad \ldots\ldots\ldots(3.2.23)
$$

 similarly from y component we get

$$
(-i\omega) v = -\frac{4 j_e}{\hbar} S (1 - \cos ka) u \qquad \ldots\ldots\ldots(3.2.24)
$$

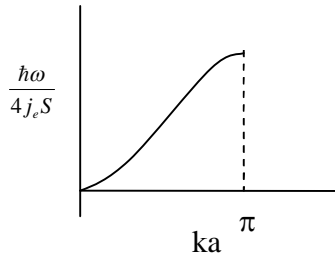For non-vanishing values of u and v, we must have

$$
\begin{vmatrix}
-i\omega & -\frac{4 J_e S}{\hbar} \left(1 - Coska \right) \\
\frac{4 J_e S}{\hbar} \left(1 - Coska \right) & i\omega
\end{vmatrix} = 0
$$

or $-\omega^2 + \left[\dfrac{4J_e S}{\hbar}\right]^2 (1 - Coska)^2 = 0$

$$\hbar\omega = 4 j_e S (1 - \cos ka) = 8 j_e S \left(\sin^2 \dfrac{ka}{2} \right) \quad \ldots\ldots\ldots(3.2.25)$$

for small values of ka , $\omega = \dfrac{2 j_e S a^2}{\hbar} k^2 \implies \hbar\omega \propto k^2$, $\ldots\ldots\ldots(3.2.26)$

this is known as the dispersion relation for magnons . A plot between $\dfrac{\hbar\omega}{4 j_e S}$ and ka is as shown in Fig 3.2.4.


Fig 3.2.4. Dispersion relation for Magnon in ferromagnetic material

3.2.3b Quantization of spin waves

  If we have got 'N' parallel spins in the system each of value S .Then the total spin quantum number of system if all the spins are parallel is N.S. If the some of the spins are anti-parallel(exited) the total spin decreases. Now let us find the relation between the amplitude of the spin wave and reduction of Z-component of total spin quantum number .

The z -component and the amplitude of the spin are related to each other as in the Fig 3.2.5,
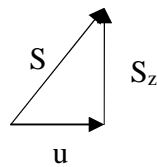
Fig 3.2.5

From the Fig. we have, $S_z = \left(S^2 - u^2\right)^{1/2} = S\left(1 - \dfrac{u^2}{S^2}\right)^{1/2} \approx S\left(1 - \dfrac{u^2}{2S^2}\right) = \left(S - \dfrac{u^2}{2S}\right)$

Or $\qquad\qquad$ S-$S_z \approx \dfrac{u^2}{2S}$ $\qquad\qquad\qquad\qquad$ ....(3.2.27)

The spin wave k exited the total spin N.S is reduced by n_k. Then the total excited spinsor magnons of wave vector k are given by

$$n_k \approx N \frac{u_k^{\,2}}{2S} \qquad \text{Or} \qquad u_k^2 \approx \frac{n_k\, 2S}{N} \qquad\qquad ....(3.2.28)$$

u_k is the amplitude of the k-spin wave and n_k the integer represents the number of magnons that are excited. The amplitude is quantized and hence the reduction in the spin (S-S_z) is quantized i.e., the spin wave is quantized.
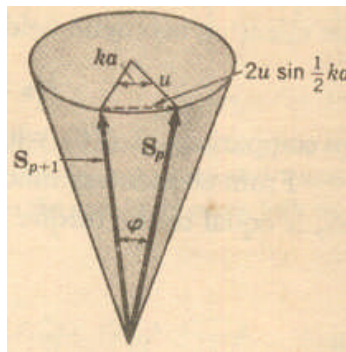
Fig 3.2.5

The exchange energy given by 3.2.11 depends on cosine of the angle between the spins p and p+1. The tips of the two spin vectors as shown in the Fig 3.2.5 are separated by a distance sin(ka/2) so that the angle between the two vectors is given by

$\sin \varphi / 2 = \dfrac{u}{S} \sin ka/2$; for (u/S) $\ll$ 1 ,$\cos \varphi = 1 - 2\left(\dfrac{u}{S}\right)^2 \sin^2 \dfrac{ka}{2}$ ....(3.2.29)

The exchange energy is now given by

U $\approx$ -2J$_e$NS^2 + 4Nu^{2}sin^2(ka/2) = -2J$_e$NS^2 + 4J$_e$Nu^2(1–coska)

The excitation energy of a spn wave of amplitude u_k and wave vector k is

$\in_k = 4J_eNu_\kappa{}^2(1-\cos ka)$, substituting the value of u_k from 3.2.28 we have ,

$\in_k = 4J_eS(1-\cos ka) \; n_{k =} \; n_k\hbar\omega_k$ from the equation 3.2.25

Hence the energy of the spin waves can also be taken as integral multiples of $\hbar\omega_k$.

i.e., $\in_k = n_k\hbar\omega_k$ ....(3.2.30)

3.2.3c   Bloch $T^{3/2}$ **Law**

We known the expression for the interaction energy as

$$U = -2j_e \sum_{p=1}^{n} S_p.S_{p+1}$$

$\Rightarrow$ Exchange energy, $U \propto S_p.S_{p+1}$.

The number of energy states whose wave vectors lies below 'k' then per unit volume is represented by

$$\left(\frac{1}{2\pi}\right)^3 \frac{4\pi k^3}{3}$$ ....(3.2.31)

Then the No. of mangnons in the range ω and $d\omega$ is

$$D(\omega)d\omega = \left(\tfrac{1}{2\pi}\right)^3 \tfrac{4}{3} 3\pi k^{\,2} \tfrac{dk}{d\omega}.d\omega$$ ....(3.2.32)

We know that,

$$\omega = \left(\frac{2j_eS_a^2}{\hbar}\right)k^2 \quad \Rightarrow \frac{d\omega}{dk} = \left(\frac{2j_eS_a^2}{\hbar}\right)2k$$ ....(3.2.33)

From this

$$D(\omega)d\omega = \frac{1}{4\pi^2}\left(\frac{\hbar\omega_k}{2j_eS_a^2}\right)^{1/2}\left(\frac{\hbar}{2j_eS_a^2}d\omega\right) \; \text{ or }$$

$$D(\omega) = \frac{1}{4\pi^2}\left(\frac{\hbar}{2j_eS_a^2}\right)^{3/2}\omega_k^{1/2} \; ....(3.2.34)$$

The total number of magnons excited

$$\sum_k n_k = \int D(\omega)\langle N(\omega)\rangle d\omega \; ....(3.2.35)$$

$$= \left(\frac{1}{4\pi^2}\right)\left[\frac{\hbar}{2J_e S_a^{\;2}}\right]^{3/2} \int_0^\infty \frac{\omega_k^{\;1/2}}{(e^{\beta\hbar\omega}-1)}.d\omega$$

$$= \left(\frac{1}{4\pi^2}\right)\left[\frac{1}{2J_e S_a^{\;2}}\right]^{3/2} \int_0^\infty \frac{(\hbar\omega_k)^{1/2}}{(e^{\beta\hbar\omega}-1)}.d\left(\frac{\hbar\omega_k}{KT}\right)$$

$$= \left(\frac{1}{4\pi^2}\right)\left[\frac{1}{2J_e S_a^{\;2}}\right]^{3/2} (KT)^{3/2}\int_0^\infty \frac{x^{1/2}}{(e^x-1)}.dx \qquad \text{where x} = \frac{\hbar\omega}{KT}$$

$$= \frac{0.0587(KT)^{3/2}}{\left(2J_e S_a^{\;2}\right)^{3/2}} \qquad ....(3.2.36)$$

The number of atoms per unit volume is given by $\quad N = \dfrac{Q}{a^3}$

Where Q= No. of atoms per unit volume

$\qquad\qquad$ = 1 for simple cubic

$\qquad\qquad$ =2 for b.c.c

$\qquad\qquad$ =4 for f.c.c

$\qquad a^3$ = volume   of the unit cell

$\sum \dfrac{n_k}{N_S} \qquad$ = the fractional charge of ground state magnetization   = $\qquad \sum \dfrac{n_K}{N_S} = \dfrac{\Delta M}{M_0}$

Where M_0 is magnetization at absolute zero.

$$\frac{\Delta M}{M_0} = \left\{\frac{0.0587}{N.S}\left(\frac{K}{2J_e S_a^{\;2}}\right)^{3/2}\right\}T^{3/2}$$

$$\frac{\Delta M}{M_0} \; \alpha \; T^{3/2} \qquad ....(3.2.37)$$

This result is due to Felix bloch, known as the Bloch $T^{3/2}$ Law and is found to hold good at low temperatures. At high temperatures, a high density of magnons is created and the assumes spin model breaks down, resulting in the invalidity of the law at such temperatures.

3.2.4   Summary of the lesson

Detailed explanation on the Weiss internal molecular field has been given. The spin wave theory quantization of spin waves and thermal excitation of magnons have been discussed in detail

3.2.5   Key words

Weiss field-Exchange Interaction-Magnons- spin waves -Bloch $T^{3/2}$ Law

3.2.6   Self – Assessment questions

1. Explain Weiss internal molecular field in detail.
2. What are magnons ?.Derive the dispersion relation for the magnons.
3. Derive the quantization condition of spin waves .
4. Derive Bloch $T^{3/2}$ Law for magnons

3.2.7   Reference Books :

1. Elements of Solid State Physics – J.P.Srivastava (PHI, New Delhi, 2003)
2. Introduction to Solid state Physics – C.Kittel (Wiley Eastern, New Delhi, 2003)
3. Solid State Physics – A. J.Dekker (Macmillan , Madras, 1986)

UNIT -3

LESSON – 3

ANTI- FERROMAGNETISM

Objective of the lesson

To discuss the Neel's theory of anti-ferromagnetism

Structure of the lesson

3.3.1 Introduction

3.3.2 Neel's theory

3.3.1 Introduction :

In the case of ferromagnetism, the internal field in ferromagnetic material arises due to exchange interaction that lines up neighbouring spin moments. For such cases, in ferromagnetism exchange integral is positive. However, in some compounds and transition metals, the exchange interaction is negative below a certain critical temperature that leads to anti parallel alignment of electron spin in the neighbouring atoms. This phenomenon is known as anti ferromagnetism and that critical temperature is known as Neel's temperature and above this temperature the materials behave like paramagnets.

3.3.2 Neel's theory

Anti ferromagnetism was first investigated by Neel's and Bitter in MnO. The most characteristic property of a polycrystalline antiferromagnetic is that its susceptibility shows a maximum as function of temperature; An example of this behaviour is given in Fig. 3.3.1a. where a graph is plotted between magnetic susceptibility 'χ' and temperatures 'T' for MnF_2. For the sake of comparison the variation of susceptibility with the temperature for paramagnetic and ferromagnetic materials are also presented in the same figure.This characteristic feature may be
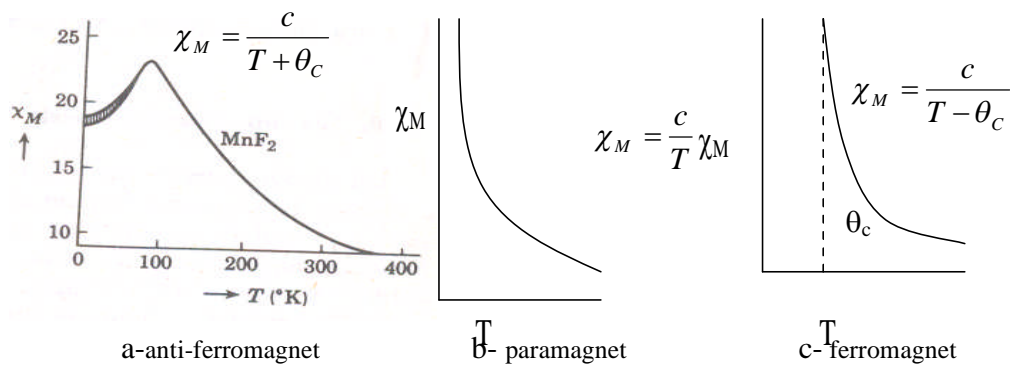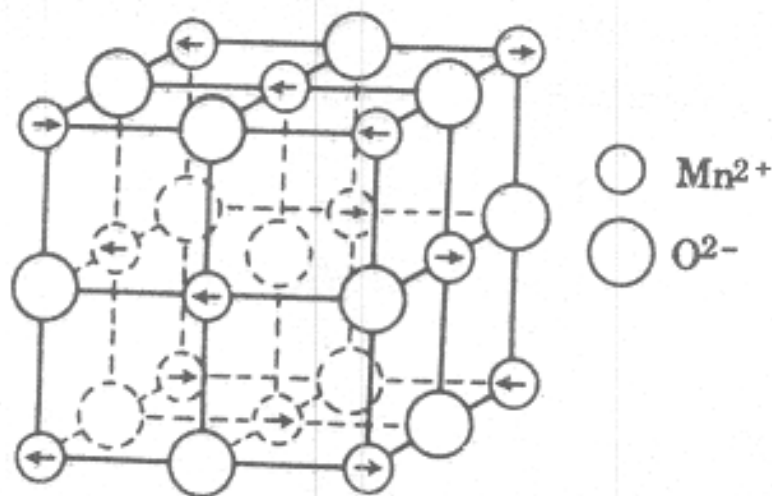
a-anti-ferromagnet   b- paramagnet   c-ferromagnet

Fig 3.3.1a Molar susceptibility 'χ' as a function of temperature 'T for MnF_2 an anti-ferromagnetic material. Figs b and c represent the same plots for paramagnetic and ferromagnetic materials

explained qualitatively on the basis of two sub-lattice model considering the unit cell of MnO. The alignment of the spins in the unit cell are as shown in the Fig. 3.3.2.

Fig. 3.3.2. Alignment of the spins in the unit cell of MnO

In the two sub lattice model we have two sub-lattices - one parallel and another is anti parallel. The interaction between parallel and anti-parallel spins gives anti- ferromagnetism.   The manganese ions are at the corners and the oxygen ions are at the centres with opposite spins

(Fig. 3.3.2) A similar saturation can be represented like MnF_2 & FeF_2 etc. In antiferro magnetism, we expect two types of interactions.

1. A - B interaction i.e. the interaction between the two anti parallel spins.

2. A - A & B - B interactions i.e. the interaction of parallel spins.

     The magnetic field at the sites A and B is given by

   $H_{ma} = H - \alpha M_a - \beta M_b$ ……….3.3.1

   $H_{mb} = H - \beta M_a - \alpha M_b$ ……….3.3.2

     Where H is the applied field and M_a and M_b represent the magnetization of the A & B lattices. α is Weiss constants corresponds to A - A & B - B interactions and β corresponds to A-B interaction

3.3.2a When T > T_N , when the temperature is above the Neel temperature, we are for away from saturation.

$$M_a = \frac{N\mu^2}{3KT} H$$

with $\mu^2 = \mu_B{}^2 g^2 J(J+1)$

where N is the number of A atoms per unit volume. If we assume that the dipoles on the B sites are identical with those of the A sites and that there are equal numbers of A and B sites, we may write similarly,

$$M_b = \frac{N\mu^2}{3KT} H_b$$

Substituting equations (3.3.2) in the equations for M_a and M_b gives the following equation for the total magnetization $\overline{M} = \overline{M}_a + \overline{M}_b$

$$= \frac{N\mu^2}{3KT})(2H - (\alpha + \beta)M$$ …………..3.3.3

This equation becomes a scalar equation if we assume that M and H are parallel. On this assumption we can solve for the susceptibility, leading to

$$\Rightarrow \chi = \frac{\overline{M}}{H} = \frac{2N\mu^2/3K}{T + \left(N\mu^2/3K\right)\left(\alpha + \beta\right)} = C/(T+\theta) \qquad \ldots\ldots\ldots\ldots 3.3.4$$

Where $C = 2N\mu^2/3K$ and $\theta = \left(N\mu^2/3K\right)\left(\alpha + \beta\right)$ $\qquad \ldots\ldots\ldots\ldots 3.3.5$

This may be compared with expression for the susceptibility of a magnetic material above the critical temperature. It is observed that the antiferromagnetic case contains $T + \theta$ rather than $T - \theta$; moreover the Curie constant C is twice the Curie constant C is twice the Curie constant of the individual A or B lattice. In order to illustrate the difference between the paramagnetic, the ferromagnetic, and the antiferromagnetic behavior in the high- temperature region, we have plotted in Fig. 19-13 I/l versus T. For the three cases one obtains
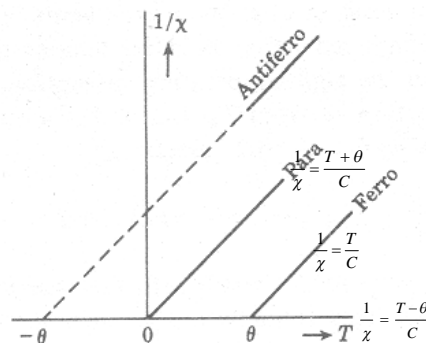
Fig.3.3.3 . The reciprocal Susceptibility versus temperature for a para-,Ferro-,Antiferro magnetic material above the critical temperature.

3.3.2b When $T = T_N$,

At the Neel temperature T_N itself, one is still sufficiently far away from saturation effects to employ the equations given above for M_a and M_b . Thus in the absence of an applied magnetic field we may write for $T = T_N$, we have,

$$M_a = -\left(\frac{N\mu^2}{3KT_N}\right)(\alpha M_a + \beta M_b)$$

or $\quad \left[\left(1 + \frac{N\mu^2}{3KT_N}\right)\alpha\right]M_a + \left(\frac{N\mu^2}{3kT_N}\right)\beta M_b = 0 \qquad \ldots\ldots\ldots\ldots 3.3.6$

and similarly, from M_b, we have ,

$$\left(\frac{N\mu^2}{3kT_N}\right)\beta M_a + \left[1 + \left(\frac{N\mu^2}{3kT_N}\right)\alpha\right]M_b = 0 \qquad \ldots\ldots\ldots\ldots 3.3.7$$

The   equations 3.3.6 and 3.3.7 have a non-vanishing solution for M_a and M_b only if the determinant of their coefficients vanishes.

i.e . $\quad \begin{vmatrix} \left(1 + \dfrac{N\mu^2}{3KT_N}\right)\alpha & \dfrac{N\mu^2}{3KT_N}\beta \\[4mm] \dfrac{N\mu^2}{3KT_N}\beta & \left(1 + \dfrac{N\mu^2}{3KT_N}\right)\alpha \end{vmatrix} = 0$

$\Rightarrow \quad T_N = \dfrac{N\mu^2}{3K}(\beta - \alpha) = C(\beta-\alpha)/2 \qquad \ldots\ldots\ldots\ldots 3.3.8$

(since $2N\mu^2/3k = C$)

The equation 3.3.8 indicates that the Neel temperature

 (i) increases as the antiferromagnetic AB interaction (β) becomes stronger,

(ii) decreases with increasing antiferromagnetic AA and BB interaction (α)

Relation between the Neel temperature and θ,

From the equation 3.3.4 we have

$$\theta = N\mu^2(\alpha + \beta)/3k = C(\alpha + \beta)/2 \qquad \text{.............3.3.9}$$

from equations 3.3.8 and 3.3.9, we get

$$\frac{T_N}{\theta} = (\beta - \alpha)/(\beta + \alpha) \qquad \text{.............3.3.10}$$

A comparasion of this result with the observed values of T_N and θ are given in Table 3.3.1 for some anti-ferromagnetic materials It is noted that experimentally $T_N < \theta$ in all cases, indicating that α must be positive; this in turn seems to indicate that in so far as the present model is applicable, there is indeed an antiferro- magnetic AA and BB interaction.

Table 3.3.1. Some Parameters of selected Antiferromagnetics.

Compound	Crystal Structure	Cation Lattice structure	T_N (°K)	θ (°K)	$\dfrac{\chi_\theta}{\chi_{T_N}}$
MnF_2	rutile	b.c.tetragonal	72	113	0.76
FeF_2	rutile	b.c.tetragonal	79	117	0.72
CoF_2	rutile	b.c.tetragonal	38	53	-
NiF_2	rutile	b.c.tetragonal	73	116	-
MnO_2	rutile	b.c.tetragonal	84	316	0.94
MnO	NaCl	f.c.c.	122	610	0.67
MnS	NaCl	f.c.c.	165	528	0.82
FeO	NaCl	f.c.c.	198	570	0.79+
CoO	NaCl	f.c.c.	292	280	-

3.3.2c : when $T < T_N$

Let us now consider the susceptibility of an anti-ferromagnetic material below the Neel temperature; for simplicity we shall assume only AB interaction, i.e., we shall assume $\alpha = 0$. First, as a result of crystalline anisotropy, there will be one or more natural spin directions along which the spins will tend to align themselves. There are therefore two cases of special interest;

  (a) An applied magnetic field perpendicular to the natural spin direction.

  (b) An applied field parallel to the natural spin direction.

Case (a) has been represented schematically in Fig. 3.3..3

(a)   (b)
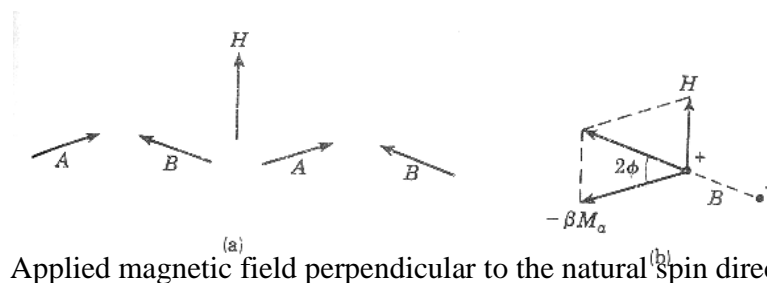
Fig. 3.3.4 Applied magnetic field perpendicular to the natural spin direction.

In the present case, the field tends to line up the dipoles along the field direction, but as a result of the tendency for the A and B dipoles to remain antiparallel, a compromise is obtained in which the dipoles make a certain angle ϕ with the original spin direction. To calculate the susceptibility $\chi_\perp$ for this case, consider one of the dipoles B as made up of two unit poles, as indicated in Fig. 3.3.4 b. The forces on the positive pole are H and $-\beta M_a$, as indicated; the forces on the negative pole are equal but of opposite sign. In equilibrium, the resultant forces should lie along the line joining the poles.

From the Fig. 3.3.4 b, we have $\beta M_a \text{Tan} 2\phi = H$,so that for small angles ϕ we must have $2\beta M_a \phi = H$

since $M_a = M_b$, the total magnetization along the external field direction is equal to

$M = (M_a + M_b) \phi = H/\beta$ Or $\chi_\perp = 1/\beta$ 3.3.11

$\Rightarrow$ $\chi_\perp$ is independent of temperature. It can readily be shown that $\chi_\perp$ is equal to the susceptibility at the Neel temperature when approached from the high-temperature .

 Case (b) applied field parallel to the natural spin direction.

 (b) The calculation of the susceptibility $\chi_\parallel$ corresponding to an applied field along the natural spin direction is much more complicated, since statistical methods involving Brilliouin functions must be employed. Detailed theoretical calculations show the variation of susceptibility $\chi_\parallel$ with temperature for different J values: the susceptibility rises smoothly from zero to $\chi (T_N)$ as the temperature increases.
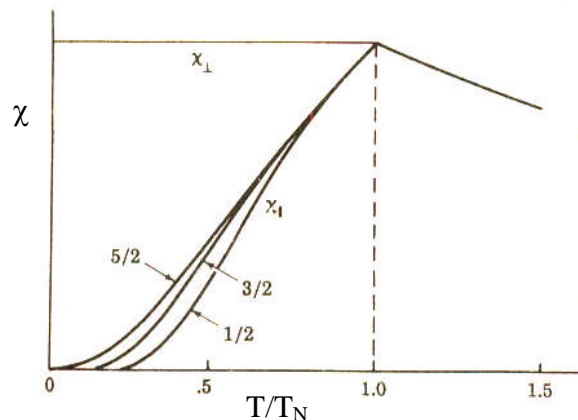
Fig.3.3.4 The variation of susceptibility $\chi_\parallel$ with temperature for different J values:

The susceptibility below the Neel temperature in polycrystalline materials is given by an average value lying between $\chi_\perp$ and $\chi_\parallel$; as a result, one obtains in such cases a susceptibility versus temperature curve of the type indicated in Fig. 3.3.1 a.

3.3.3 Summary of the lesson

The origin of the anti- ferromagnetism and the detailed theory Neel's theory

Anti ferromagnetism are discussed in detail. Various cases of anti- ferromagnetic susceptibility with the temperature have also been discussed at in depth

3.3.4   Key words

Anti- ferromagnetism - Neel's theory –Neel's temperature

3.3.5   Self – Assessment questions

1.   Discuss briefly Neel's theory of Anti- ferromagnetism

2.Derive the expressions for anti- ferromagnetic susceptibility at (a) $T>T_N$ (b) $T=T_N$

and (c) $T < T_N$

3. Obtain Relation between the Neel temperature and Curie temperature

3.3.6   Reference Books :

1. Elements of Solid State Physics – J.P.Srivastava (PHI, New Delhi, 2003)

2. Solid State Physics – A. J.Dekker (Macmillan , Madras, 1986)

Unit : 3

Lesson : 4

Ferrimagnetism

Objective of the lesson

- To discuss the origin of ferrimagnetism
- To explore the structure and characteristics of ferrimagnets
- To discuss the expression for the susceptibility based on Neel's theory
- To discuss briefly the methods to probe the structure of the magnetically ordered materials.
- To describe the characteristics of other novel magnetic materials

Structure of the lesson

3.4.1. Introduction

3.4.2. Structure of Ferrites

3.4.3. Characteristics of ferrites

3.4.4. Neel's theory of Ferrimagnetism

3.4.5. Determination of magnetically ordered structures

3.4.6. Novel magnetic materials

3.4.1. Introduction

The material most popularly called as load-stone with the chemical formula Fe_3O_4 (magnetite) is probably the oldest magnetic known to mankind. The general formula of this material is $Me^{2+}Fe_2^{3+}O_4$. where Me^{2+} stands for divalent ferrous ion or any other another divalent metal such as Mn, Co, Ni, Cu, Mg, Zn, or Cd, In mixed ferrites the Fe^{2+} ion is replaced by a mixture of ions like MnZn.. The d-c resistivity of ferrites is 10^4 to 10^{11} times is large as that of iron. Thus in transformer cores they can be used up to much higher frequencies than iron.

3.4.2.   Structure of Ferrites

The ferrites belong to the large class of compounds which have the spinel structure (after the mineral spinel, $MgAl_2O_4$). The unit cell contains 32 oxygen ions, 16 Fe^{3+} ions, and 8 divalent metal ions. The total of 24 metal ions, ranging in radius between 0.4 and 1 A^o, are distributed amongst eight tetrahedral interstices (surrounded by four O^{2-} ions) and sixteen octahedral interstices (surrounded by six O^{2-} ions).

The distribution of the metal ions is very important for an understanding of the magnetic properties of these Materials; the following distributions may occur,

3.4.2. a. The "normal" spinel structure :

In this case the structure of ferrite consists 8 divalent metal ions occupy tetrahedral positions; 16 trivalent iron ions occupy octahedral positions.

The notation for this structure: may be given as

$$Me^{2+}[Fe_2^{3+}]O_4$$

the brackets around the Fe^{3+} ions indicating that they occupy octahedral sites.

Examples for this structure are , $ZnFe_2O_4$, $CdFe_2O_4$

3.4.2. b. Inverse spinel structure of a ferrite,

In this case the divalent Me^{2+} ions occupy octahedral sites; the Fe^{3+} ions are distributed in equal numbers over the tetrahedral and octahedral sites, that means 8 in each site . The arrangement may thus be represented by

$$Fe^{3+}[Fe^{3+}Me^{2+}]O_4$$
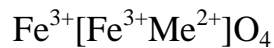
Examples for this structure are , $CoFe_2O_4$, $CuFe_2O_4$, $MgFe_2O_4$

3.4.2.c. In the intermediate structure we have arrangements of the type

$$Fe_x^{3+} Me_{1-x}^{2+} [Fe_{2-x}^{3+}Me_x^{2+}] O_4$$

3.4.3. Characteristics of ferrites

Some of the important characteristics of the ferrimagnetic materials are given below:

1. These materials have got very high resistivity of 10 to 10,000 Mega ohm – cm.
2. The microwave dielectric constant of thes materials is of the order of 10 to 12.
3. The dielectric loss of these materials is extremely low.
4. Magnetic permeability of the ferrites is very high.
5. Saturation magnetic moment is appreciably high but noticeably smaller than the ferromagnetic materials.
6. The Curie temperature of these materials is very high.
7. Eddy current losses of these materials are very low.

These are all the extra-ordinary properties of the ferromagnetic materials that make them suitable for industrial applications like microwave devices, isolators and gyrators etc.

3.4.4. Neel's theory of Ferrimagnetism

In order to explain the magnetic properties of ferrites, Neel in 1948 developed this theory. The importance of the distribution of the metallic ions over the tetrahedral and octahedral sites may be illustrated with reference to the saturation magnetization for simple and mixed ferrites. The ferrites are essentially ionic compounds; the saturation magnetization of these materials may therefore be calculated from the number of unpaired spins of the ions.

For example, in magnetite, i.e., $Fe^{3+} [Fe^{2+} Fe^{3+}]O_4$

the Fe^{2+} and Fe^{3+} ions have, six and five 3d electrons respectively.

The magnetic moment of Fe^{2+} ion$= 4 \mu_B$

The magnetic moment of Fe^{3+} ion$=5 \mu_B$

The net magnetic moment per molecule of Fe_3O_4 is therefore $=(4+5)-5 = 4 \mu_B$,

which is in close agreement with the experimental value.

According to this theory, there exists a "negative" interaction between the ions on the tetrahedral sites (A sites) and the octahedral sites (B sites) which tends to promote an antiparallel spin alignment of the A and B ions. Besides this negative AB interaction, we must also take into account an AA and BB interaction. Thus the ferromagnetic behavior can be explained in terms of three antiferromagnetic interactions. Neel coined the term "ferrimagnetism" for this type of behavior.

In order to give the essential features of Neel's theory, we shall consider the relatively simple case of a ferrite represented by the formula

$$Fe_x^{3+} Me_{1-x}^{2+} [Fe_{2-x}^{3+} Me_x^{2+}] O_4$$

where Me^{2+} is a diamagnetic ion. We shall assume that the AB interaction is a negative. The AA and BB interactions will be represented by a factor $-\alpha$ and $-\beta$ respectively, giving the sign and strength of these interactions relative to the AB interaction. Thus, when α turns out to be negative, it indicates that the AA interaction is antiferromagnetic.

Let M_a denotes the magnetization associated with the A sites (tetrahedral sites) similarly M_b denotes the magnetization associated and B sites (octahedral) per gram ion, then the total magnetization per mole is

$$M = xM_a + (2-x)M_b . \qquad \text{..........(3.4.1)}$$

Now, the molecular field H_a acting on an ion occupying an A site may be written as

$$H_a = H - \gamma\ [(2-x)M_b - \alpha x M_a\ ] \qquad \text{..........(3.4.2)}$$

where H is the applied field, $-\gamma(2-x)M_b$ is due to the negative AB interaction, and $\gamma\alpha x Ma$ is due to the AA interaction.

Similarly, the molecular field acting on a B atom is given by

$$H_b = H - \gamma[xM_a - \beta(2-x)M_b] \qquad \text{..........(3.4.3)}$$

We shall first consider the **paramagnetic region above the Curie point.**

Under these circumstances the partial magnetizations may be assumed to follow a Curie-Weiss law, i.e.,

$$M_a = C_m H_a/T \quad \text{and} \quad M_b = C_m H_b/T \quad\text{..........(3.4.4)}$$

where C_m is the Curie constant per mole; the $C_m\text{'s}$ are the same for the *A* and *B* lattices, because for the example chosen here, the Fe^{3+} ions are the only magnetic ions. substituting H_a and H_b, we get

$$\frac{H}{M} = \frac{1}{\chi_{mole}} = \frac{T}{C_m} + \frac{1}{\chi_o} - \frac{\sigma}{T-\theta} \qquad\text{..........(3.4.5)}$$

where $\quad \dfrac{1}{\chi_0} = (\gamma/4)\left[2x(2-x) - \alpha\ x^2 - \beta(2-x)^2\right] \qquad\text{..........(3.4.6)}$

$$\sigma = \frac{1}{16}\gamma^2 C_m x(2-x)\left[x(1+\alpha) - (2-x)(1+\beta)\right]^2 \qquad\text{..........(3.4.7)}$$

$$\text{and } \theta = \frac{1}{4}\gamma C_m x(2-x)(2+\alpha+\beta) \qquad\text{..........(3.4.8)}$$

When $\quad\dfrac{1}{\chi_{mole}}\quad$ is plotted against T as per the equation 3.4.5, we get a concave curvature toward the T-axis. This is well in agreement with experiment. From the shape of the experimental curves we can find χ_0, σ and θ; hence x, α, β, and γ can also be obtained, at least qualitatively. For several ferrites Neel found that both α and β are negative (i.e., the AA and BB interactions are also antiferromagnetic). Furthermore, $|\alpha|$ and $|\beta|$ are both <<1, indicating that the *AB* interaction predominates over AA and BB interactions in the region above Curie point.

The spontaneous magnetization in the region below the Neel point

We put H = 0 in (3.4.2) and (3.4.3). Since there are saturation effects, we cannot employ the Curie- Weiss law, and We therefore must replace equations (3.4.5) by the following general expressions

$$M_a = NgS\mu_B B_S(gS\mu_B H_a / kT) \qquad\text{..........(3.4.9)}$$

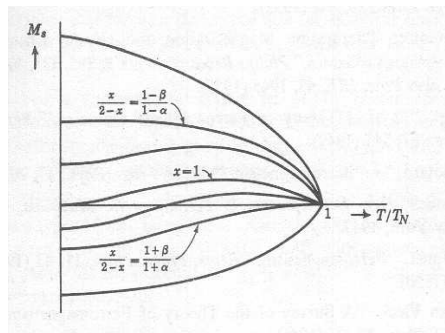$$M_b = NgS\mu_B B_S(gS\mu_B H_b / kT) \qquad\text{..........(3.4.10)}$$

here N represents Avogadro's number, since *Ma* and *Mb* refer to a mole.

From these expressions together with (3.4.2) and (3.4.3) *(With H= 0)*
one can obtain M_a and M_b, i.e., the total magnetization

$$M = (2 - x)M_b - xMa$$

as function of T. The solutions depend on the values of x as given in Fig. 3.4.1

Fig. 3.4.1. The calculated spontaneous magnetisation as a function of temperature for varying ratio of Ferric ions in A and B sites.

We may make here some further remarks on the curves given in Fig.3.4.1. From X-ray diffraction data it follows that in the mixed zinc ferrites the Zn^{2+} ions occupy tetrahedral *(A)* sites, as they do in the pure zinc ferrite (which has the normal spinel structure). The other divalent ions Mn^{2+}, Ni^{2+}, etc. occupy octahedral sites and the Fe^{3+} ions are distributed over the remaining tetrahedral and octahedral sites. Thus the mixed zinc ferrites satisfy the representation

$$Z_x^{2+} Fe_{1-x}^{3+} \left[Fe_{1+x}^{3+} Me_{1-x}^{2+} \right] O_4$$
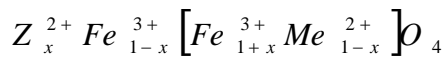
Thus apart from certain details , Neel's theory describes the experimental observations quite well.

3.4.5. Determination of magnetically ordered structures

The use of a slow neutron beam diffraction has certain distinct advantages, especially while dealing with the magnetically ordered materials when compared with the conventional X-ray diffraction method. The diffracted X-ray photons provide details about the spatial distribution of electronic charge, but carry no information about the atomic magnetic moment vectors in a magnetically ordered structure. On the other hand, a beam of slow neutrons serves as an excellent probe of local moments since the neutron itself has a magnetic moment which couples to the spin of elementary moments in a magnetic crystal. As a result of this coupling there appear peaks, in the diffraction pattern in addition to those belonging to the non-magnetic Bragg reflection of neutrons by the atomic nuclei.

The advantages of neutron beam are best appreciated in antiferromagnetic solids. As an example, consider the neutron diffraction pattern of MnO below and above the Neel temperature (120 K) in Fig. 3.4.2. Several lines in the pattern recorded at 80 K are not observed at 293 K, simply because the corresponding Bragg reflections originate from the magnetic ordering which exists no more above 120 K.
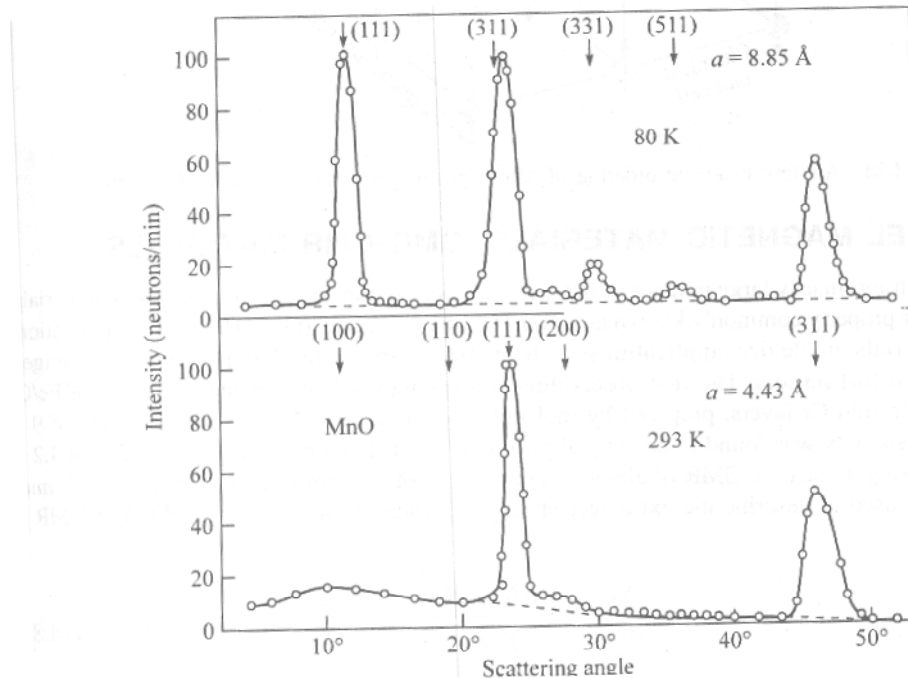
Fig. 3.4.2. Neutron diffraction patterns for an aniferromagnetic solid (MnO) below and above the Neel temperature (120 K).

Nuclear magnetic resonance offers another way to investigate the microscopic spin structure. For determining the size of a unit cell of a crystal having magnetic ordering it becomes imperative to take into consideration not only the equivalence of the sites but also the equivalence of the magnetic moment vectors located at those sites.

The size of a unit cell for an anti ferromagnetic crystal as obtained by the X-ray diffraction is just half the size given by the neutron diffraction. The unit cells determined by the two techniques are referred to as chemical unit cell and magnetic unit cell, respectively. This point is clarified in Fig. 3.4.3. with the help of the ordering of moments of Mn^{2+} ions in the unit cell of $RbMnF_3$ ($T_N = 54.5$ K).
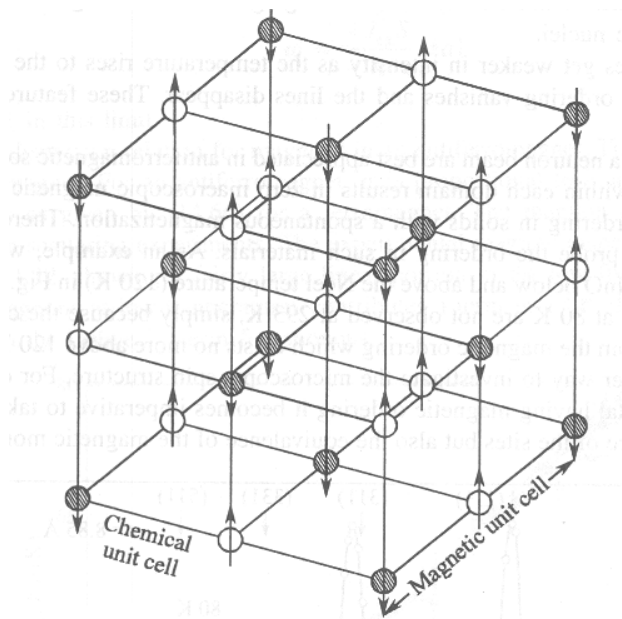
Fig. 3.4.3. Antiferromagnetic ordering of Mn^{2+} spin moments in a crystal of $RbMnF_3$.

## 3.4.6. Novel magnetic materials: GMR-CMR Materials

Recently, some magnetic materials are found to exhibit an extraordinarily large magnetoresistance known as Giant Magneto Resistance (GMR). This spectacular property of the materials makes them suitable for applications in device applications such as (i) magnetic recording (memory storage), (ii) actuators and (iii) sensors.

The first observation concerning GMR was made in respect of Fe/Cr multilayers with thin Cr layers, prepared by molecular beam epitaxy (MBE). For Cr layers of 9 A^o thickness the resistivity was found to drop by almost a factor of 2 in a magnetic field of 2T at 4.2 K (Fig. 3.4.2), giving a negative GMR of about 50 per cent.

Another term Colossal Magneto Resistance (CMR) is often used to describe the extremely strong influence of the magnetic field. The CMR is defined as

$$\frac{\Delta\rho}{\rho(B)} = \frac{\rho(B) - \rho(0)}{\rho(B)}$$

The GMR-CMR effect is observed generally at low temperatures in the presence of large
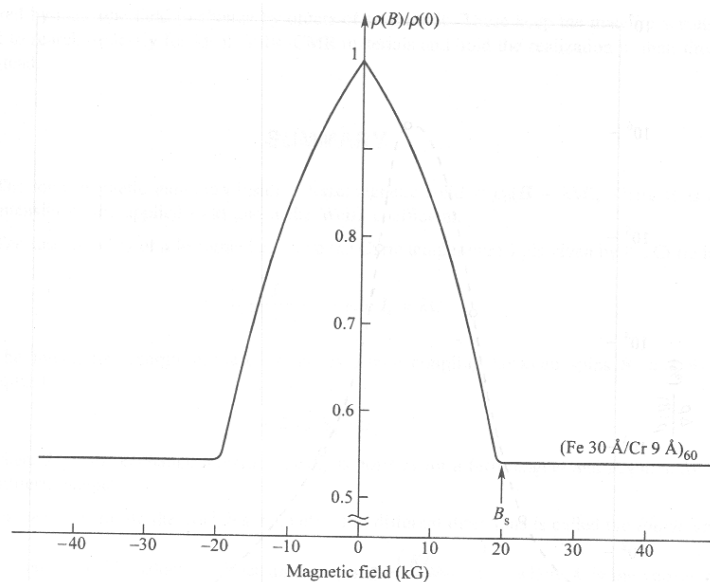
Fig.3.4.4 Variation of resistivity of multilayers [(001) Fe 30 A^o /(001) Cr 9 A^o] as a function of the magnetic field at 4.2 K.

magnetic fields (- a few tesla). But we require to exploit this property ideally near room temperature and at low fields for enhancing the technological viability of GMR-CMR materials. Hence, ever since the discovery of GMR and CMR a relentless activity has been on to develop such materials. Recently, a promising class of magnetic materials with composition $R_{1-x}A_xMnO_3$ (R = La, Nd, Gd, Y; A = Ca, Sr, Ba, Pb) has been identified. These manganites having perovskite structure have the unique distinction of being paramagnetic and

semiconducting at high temperatures. They make a transition to the ferromagnetic and metallic state at low temperatures. This is unusual of metal insulator systems because they are generally metallic at high temperatures. In the metallic state the resistivity is unexpectedly high.

In epitaxially grown thin films of La-Ca-Mn-O, MR is found to depend strongly on film thickness and temperature. The CMR reaches its maximum (in excess of 10^6 per cent) at 110 K with the magnetic field at 6 T (Fig. 3.4.5). The peak occurs just below the Curie temperature. For films thicker than -2000 A, the MR is reduced by few orders of magnitude. The presence of grain boundaries leading to lattice strain is detrimental to achieving large MR. The MR improves further on heat treatment.
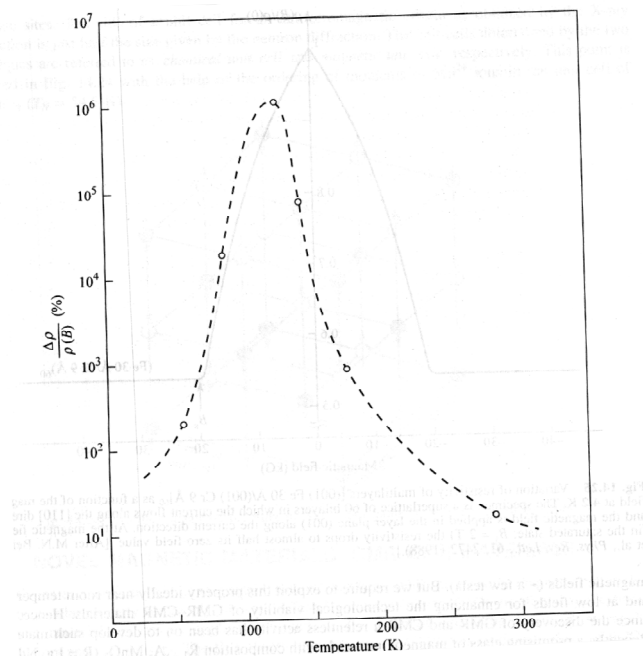
Fig.3.4.5. Variation of magnetoresistance of a thin film of La-Ca-Mn-O as a function of temperature.

Several theoretical approaches have been advanced to understand ferromagnetism and the GMR effect in manganites. The ferromagnetism is interpreted in terms of the coupling between charge carriers and the coupling between localized spin moments of Mn ions. There are two striking features of GMR-CMR effect in manganites. Firstly, the MR peak can be shifted to

occur at room temperature by adjusting the processing parameters. Secondly, the resistivity can be manipulated by magnetic field to change by orders of magnitude.

3.4.7 Summary of the lesson

Different possible structures for ferromagnetic materials have been described in detail. Neel's theory of ferromagnetic materials that gives the information about the variation of susceptibility with temperature has been discussed in depth. Different methods for determining the structure of the magnetically ordered materials have been described in brief. Information about other classes of novel magnetic materials that exhibit some extraordinary properties has also been given.

3.4.8 Key words

Ferrimagnetism – Ferrites – Spinel structure – GMR and CMR magnetic materials.

3.4.9 Self – Assessment questions

1. What is ferrimagnetism? . Discuss briefly different structures of ferrites.
2. Discuss Neels theory of ferrimagnetism.
3. Discuss briefly the structural determination of magnetically ordered materials.
4. Write a note on GMR andf CMR materials.

3.4.10 Reference Books :

1. Elements of Solid State Physics – J.P.Srivastava (PHI, New Delhi, 2003)
2. Theory of magnetism – D.C.Mattis (Springer, 1985)

SUPERCONDUCTIVITY AND PHYSICAL PROPERTIES OF SUPERCONDUCTORS

Objective of the lesson

To discuss the phenomenon of the superconductivity and some of their physical properties.

Structure of the lesson

4.1.1. Introduction

4.1.2   Magnetic properties of superconductors

4.1.3. Electrical properties of superconductors

4.1.4. Thermal entropy

4.1.5. Microwave and infrared properties

4.1.6. Isotope effect

4.1.7. The two fluid model

4.1.1. Introduction

Generally, the resistance of metals deceases when cooled below room temperature.   However, prior to 1911, it was not known what limiting value the resistance would approach, when the sample temperature is reduced to very close to 0 K.   William Kelvin believed that electrons flowing through a conductor would come to a complete halt as the temperature approaches absolute zero.   In 1911, Kamerlingh Onnes began to investigate the electrical properties of metals in extremely low temperatures.   Onnes measured the resistance of pure mercury as a function of temperature. Much to his surprise there was no levelling off of resistance.   Instead the resistance at 4.2 K suddenly vanished (Fig. 1.1) and the current continued to flow without the voltage drop.   According to Onnes, "Mercury has passed into a new state, which on account of

its extraordinary electrical properties may be called the superconductive state". Kamerlingh Onnes called this newly discovered state, **Superconductivity**.   For his discovery of superconductivity, he was awarded the Nobel Prize in 1913. The magnetic field associated with the super current was measured by File and Mills using nuclear magnetic resonance technique and concluded that the decay time of the super current is not less than 100, 000 years. But in some superconducting materials finite decay times are also observed.

The superconductivity appears only in some substances and the transition temperature T_c is different for different substances.

Critical Temperature

The critical temperature, T_c, is the temperature at which the transition from normal substance to superconducting vice versa occurs, in the absence of external magnetic field. The properties of substance are normal above critical temperature T_c, whereas below T_c substance exhibits superconducting properties (Fig.4.1.1)
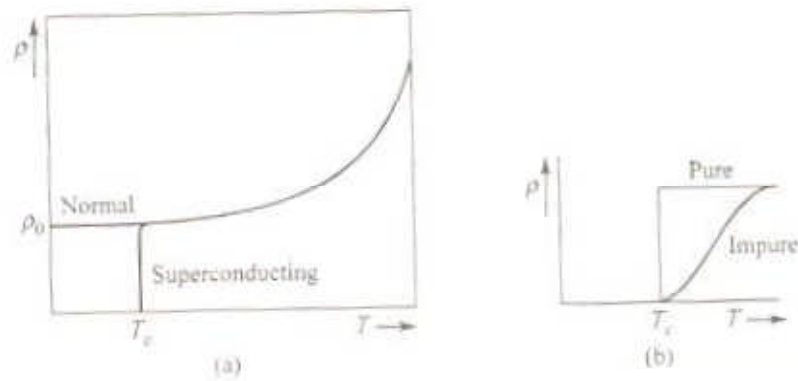

Fig.4.1.1.   a. DC resistivity ρ as a function of temperature of a super conductor

b.   The superconducting transition in impure and pure samples.

4.1.2 Magnetic properties of superconductors

a. The critical field

The superconductivity property of a substance can be destroyed by an application of magnetic field. The magnetic filed required to destroy the superconductivity is called the critical field, H_c, above which it becomes normal and recovers its normal resistivity even at $T < T_c$. For a given substance, the critical field decreases as the temperature is increased from $T < T_c$ to T_c, following the relation:

$$H_c (T) = H_c (0) [1 - (T/T_c)^2] \qquad\qquad ……….(4.1.1)$$

Remember, the critical field need not be external. The current flowing in a superconducting ring creates its own magnetic field, and if this current is large enough so that its own field attains the critical value, then the superconductivity gets destroyed. This is called Silsbee's rule.

b. Meissner Effect

The expulsion of magnetic flux completely from a superconductor is known as Meissner effect. In 1933, Meissner and Ochsenfeld observed that a superconductor expels magnetic flux completely (see Fig. 1.2). They also demonstrated that this effect is reversible, when the temperature is raised from below T_c, the flux suddenly penetrates the specimen after it reaches T_c, and the substance attains the normal state.
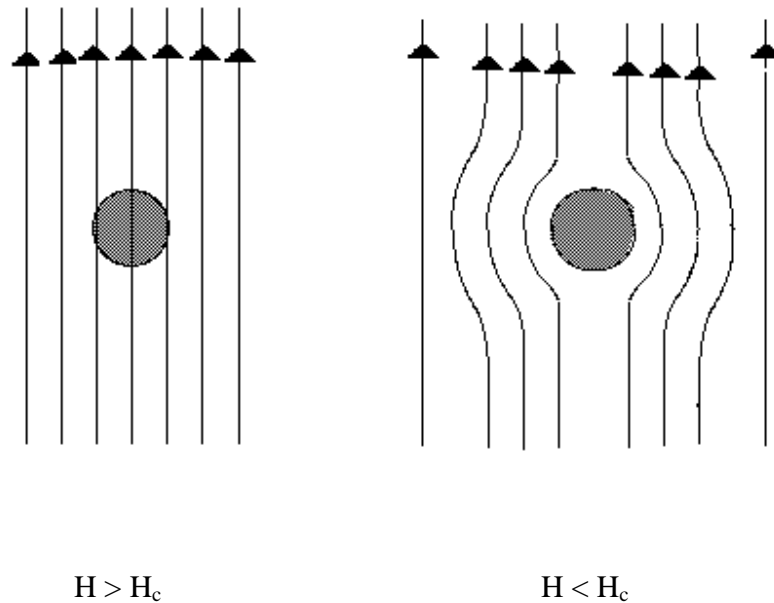
$$H > H_c \qquad\qquad\qquad H < H_c$$

Fig.4.1.2 The Meissner effect : The magnetic flux is expelled from superconductor.

The magnetic induction inside the substance is given by

$$\mathbf{B} = \mu_0 \, (\, H + M \,) = \mu_0 \, (\, 1 + \, \chi \,) \, H \qquad\qquad \ldots\ldots\ldots(4.1.2)$$

where H is the external intensity of the magnetic filed, M is the magnetization of the medium, and χ is its magnetic susceptibility. Since B = 0 in the superconducting state, it follows that M = - H,

It means that the magnetization is equal to and opposite to H. The magnetic susceptibility is then given by

$$\chi \ = \ M/H = \ - \, 1 \qquad\qquad\qquad \ldots\ldots\ldots(4.1.3)$$

i.e., the superconductor is a perfect diamagnet.

c. Type I and Type II superconductors

A material which exhibits complete Meissner effect is called Type I superconductor (Fig. 4.1.3). The values of H_c are always too low for type I superconductors. Other class of superconductors which can exist in a mixed state, with superconducting and normal regions (Fig.4.1.3) and are known as type II superconductors. These materials are alloys or transition metals with high values of the electrical resistivity in the normal state.

Type II superconductors have two critical fields, $H_{c1} < Hc < H_{c2}$. In the region between H_{c1} and H_{c2} the superconductor is said to be in the vortex state.   They are characterized by a lower critical filed H_{c1} at which magnetic flux begins to enter the superconductor
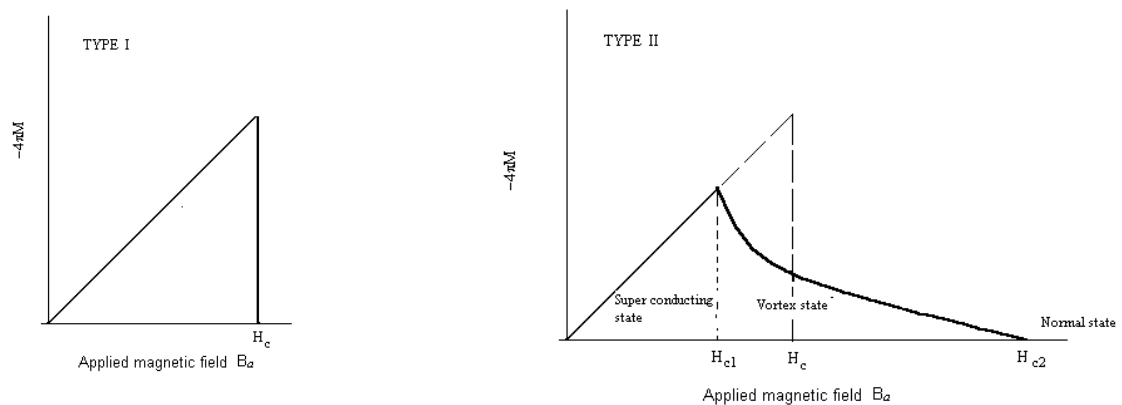
Fig.4.1.3 Type I and type II superconductors

and an upper critical field H_{c2} at which superconductivity disappears. A material can change from type I to type II on the substitution of some impurities.

4.1.3. Electrical properties of superconductors

A superconductor has no resistance. This would mean that there is no voltage drop along the superconducting material when current is passed through and no power is dissipated by the passage of the current. This is true for the direct currents of constant value.   If the current is changing an induced electric field is developed and as such some power is dissipated. Let us try to understand the reason for this.

Below transition temperature the conduction electrons get divided into two classes; some of the electrons behave as "superelectrons", which can pass through the superconductor without resistance, the remaining behave as conduction electrons in a normal metal.   In a superconductor the current can in general be carried by both the normal and superelectrons. However, below transition temperature the current is carried by superconducting electrons. This can be explained as follows: if the current is to remain constant, there must be no electric field in the superconductor, otherwise the superelectrons would be accelerated continuously in this field and the current would increase indefinitely. If there is no field there is nothing to drive the normal electrons and so there is no normal current. We conclude that a constant value of total current would mean that all the current is carried by the superelectrons. A superconductor is like two conductors in parallel, one having a normal resistance and the other zero resistance. We can say that the superconducting electrons short circuit the normal electrons.

But if an alternating field of sufficiently high frequency is applied, a superconductor responds in the same way as a normal metal.   This is due to the superconducting electrons are in a lower energy state than normal electrons and the applied frequency has enough energy to excite superconducting electrons into the higher states where they behave as normal electrons.   This happens for frequencies higher than about 10^{11} Hz.

4.1.4. Thermal entropy of superconductors

The entropy is a measure of disorder of a system. In all superconductors the entropy decreases on cooling below the critical temperatures. The decrease in entropy between normal state and superconducting state represents that the superconducting state is more ordered than the normal state (See Fig. 4.1.4).
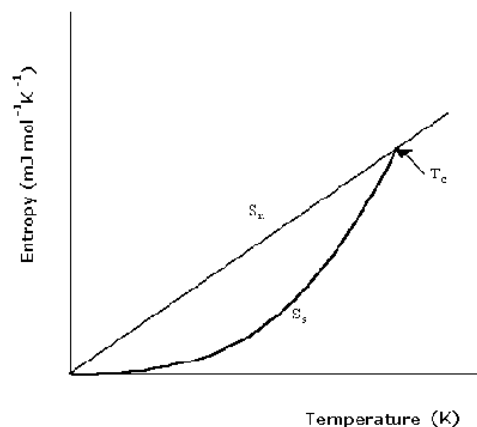

Fig.4.1.4. Variation of entropy of a super conducting and a normal conducting material with temperature

The peaking C_v just below indicates an appreciable increase in entropy as T increases toward T_c , and transition to the normal state becomes imminent. Thus the superconducting state has a greater degree of order than the normal state.

4.1.5. Microwave and infrared properties

The existence of an energy gap in superconductors means that photons of energy less than the gap energy are not absorbed. Nearly all the photons incident are reflected as for any metal because of the impedance mismatch at the boundary between vacuum and metal, but for a very thin (~ 20 A^0) film more photons are transmitted in the superconducting state than in the normal state. For photon energies less than the energy gap, the resistivity of a superconductor vanishes at absolute zero. At T $\ll$ Tc the resistance in the superconducting state has a sharp threshold at

the gap energy.   Photons of the lower energy see a resistance less surface.   Photons of higher energy see a resistance that approaches that of the normal state because such photons cause transitions to unoccupied normal energy levels above the gap.   As the temperature is increased not only does the gap decrease in energy, but the resistivity for photons below the gap energy no longer vanishes, except at zero frequency.   At zero frequency the superconducting electrons short-circuit any normal electrons that have been thermally excited above the gap.   At finite frequencies the inertia of the superconducting electrons prevents from completely screening the electric field, so that thermally excited normal electrons now can absorb energy.

4.1.6. Isotope effect

The variation of critical temperature of superconductors with the average isotopic mass is called isotopic effect.   The transition temperature changes smoothly when different isotopes of the same element are mixed. The empirical relation between the critical temperature and average atomic mass can be represented as

$$M^a T_c = \text{constant.} \qquad \text{……….(4.1.4)}$$

The original BCS model gave the result T_c is proportional to $M^{-1/2}$, so that a=1/2, but the inclusion of coulomb interactions between electrons changes the relation.

4.1.7.   The Two Fluid Model

According to the two fluid-model, introduced by Gorter and Casimir in 1934, the conduction electrons in a superconductor fall into two classes: superelectrons and normal electrons. The superelectrons experience no scattering, have zero scattering (perfect order), and long coherent length (about 10^4 A^0), but the normal electrons behave in the usual fashion as in normal conductors.   The number of superelectrons depend on the temperature. The concentration of superelectrons, given by Gorter and Casimir, is

$$n_s = n \left[1 - (T/T_c)^4 \right] \qquad \text{……….(4.1.5)}$$

At T = 0 K all the electrons in the superconductor are superelectrons, but as T increases the superelectrons decreases and all they become normal electrons at T = T$_c$.

4.1.8   Summary of the lesson

The phenomenon of superconductivity has been discussed in detail. Electrical and magnetic of super conductors have also been discussed.

4.1.9   Key Terminology

Superconductivity – Zero resistivity – Meissner effect– Type I and Type II superconductors.

4.1.10   Self – Assessment questions

1. Give a brief account on the experimental survey of superconductivity
2. Write a note on
    a). Meissner effect
    b) Type I and Type4 II superconductors
    c).Isotope effect
    d) Microwave and infrared properties of superconductors
    e) Energy gap of superconductors

4.1.11   Reference Books

1. Elementary Solid State Physics by M.A. Omar
2. Elements of Solid State Physics by J.P. Srivastava
3. Solid State Physics by Neil W. Ashcroft and N. David Mermin
4. Introduction to Solid State Physics by Charles Kittel

UNIT – IV

LESSON 4

BCS THEORY AND HIGH TC SUPERCONDUCTORS

Objective of the lesson

To discus the BCS theory of superconductivity and its predictions.

4.1 BCS THEORY OF SUPERCONDUCTIVITY

Three American physicists at the University of Illinois, John Bardeen, Leon Cooper, and Robert Schrieffer, in 1957, developed a model that has since stood as a good mental picture of why superconductors behave as they do. In 1972, Bardeen, Cooper, and Schrieffer received the Nobel Prize in Physics for their theory of superconductivity (for Bardeen it was the second Noble prize in Physics), which is now known as the BCS theory, after the initials of their last names.

The BCS theory explains superconductivity at temperatures close to absolute zero. Cooper realized that atomic lattice vibrations were directly responsible for unifying the entire current. They forced the electrons to pair up into teams that could pass all of the obstacles which caused resistance in the conductor. These teams of electrons are known as **Cooper pairs**. Cooper and his colleagues knew that electrons which normally repel one another must feel an overwhelming attraction in superconductors. The answer to this problem was found to be in phonons, packets of sound waves present in the lattice as it vibrates. Although this lattice vibration cannot be heard, its role as a moderator is indispensable.

According to the theory, as one negatively charged electron passes by positively charged ions in the lattice of the superconductor, the lattice gets distorted. This in turn causes phonons to be emitted which forms a trough of positive charges around the electron. Fig. 4.4.1 illustrates a wave of lattice distortion due to attraction to a moving electron. Before the electron passes by and before the lattice springs back to its normal position, a second electron is drawn into the trough. It is through this process that two electrons, which should repel one another, link up. The forces exerted by the phonons overcome the electrons' natural repulsion. The electron pairs are coherent with one another as they pass

Superconducting State
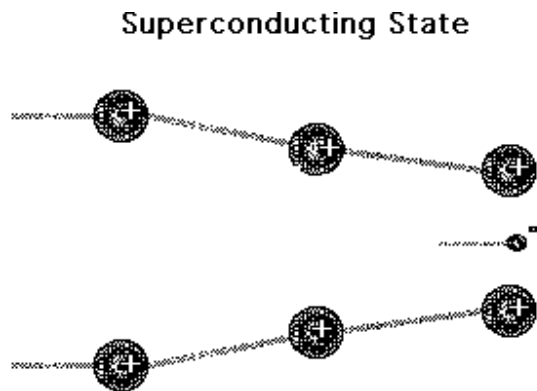
Fig. 4.4.1 As a negatively charged electron passes between the metal's positively charged atoms in the lattice, the atoms are attracted inward. This distortion of the lattice creates a region of enhanced positive charge which attracts another electron to the area.

through the conductor in unison. The electrons are screened by the phonons and are separated by some distance. When one of the electrons that make up a Cooper pair and passes close to an ion in the crystal lattice, the attraction between the negative electron and the positive ion cause a vibration to pass from ion to ion until the other electron of the pair absorbs the vibration. The net effect is that the electron has emitted a phonon and the other electron has absorbed the phonon. It is this exchange that keeps the Cooper pairs together. It is important to understand, however, that the pairs are constantly breaking and reforming. Because electrons are indistinguishable

Superconducting State

Area of distortion
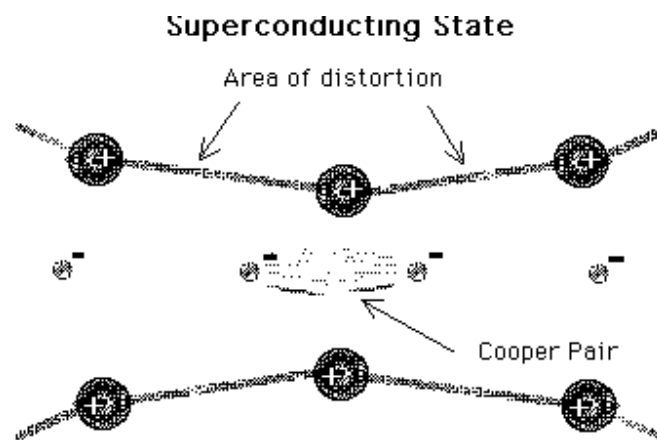
Cooper Pair

Fig. 4.4.2   The two electrons, called Cooper Pairs, become locked together and will travel through the lattice.

particles, it is easier to think of them as permanently paired. Fig. 4.4.2 illustrates how two electrons, called Cooper pairs, become locked together.

By pairing off two by two the electrons pass through the superconductor more smoothly. The electron may be thought of as a car racing down a highway. As it speeds along, the car cleaves the air in front of it. Trailing behind the car is a vacuum, a vacancy in the atmosphere quickly filled by inrushing air. A tailgating car would be drawn along with the returning air into this vacuum. The rear car is, effectively, attracted to the one in front. As the negatively charged electrons pass through the crystal lattice of a material they draw the surrounding positive ion cores toward them. As the distorted lattice returns to its normal state another electron passing

nearby will be attracted to the positive lattice in much the same way that a tailgater is drawn forward by the leading car.

The BCS theory successfully shows that electrons can be attracted to one another through interactions with the crystalline lattice. This occurs despite the fact that electrons have the same charge. When the atoms of the lattice oscillate as positive and negative regions, the electron pair is alternatively pulled together and pushed apart without a collision. The electron pairing is favorable because it has the effect of putting the material into a lower energy state. When electrons are linked together in pairs, they move through the superconductor in an orderly fashion.

As long as the superconductor is cooled to very low temperatures, the Cooper pairs stay intact, due to the reduced molecular motion. As the superconductor gains heat energy the vibrations in the lattice become more violent and break the pairs. As they break, superconductivity diminishes. Superconducting metals and alloys have characteristic transition temperatures from normal conductors to superconductors called Critical Temperature. Below the superconducting transition temperature, the resistivity of a material is exactly zero.

superconductors

The achievements of the BCS theory include:

1. An interaction between electrons can lead to ground state separated from excited states by an energy gap. The critical field, the thermal properties, electromagnetic properties etc consequences of the energy gap.
2. The electron-lattice-electron interaction leads to an energy gap of the observed magnitude. The indirect interaction proceeds when one electron interacts with

the lattice and deforms it; a second electrons sees the deformed lattice and adjusts itself to take advantage of the deformation to lower its energy. Thus the second electron interacts with the first electron via the lattice deformation.

3. The penetration depth and the coherence length emerge as natural consequences of the BCS theory. The London equation is obtained for magnetic field that vary slowly in space. Thus the central phenomenon in superconductivity, Meissner effect, is obtained in a natural way.

Ginzburg and Landau Theory and flux quantisation

In 1950 Ginzburg and Landau developed a macroscopic theory for superconducting phase transition based on a general thermodynamical approach to the theory of phase transition. They considered the long-range order as fundamental and introduced a complex wave function ψ as an order parameter to describe the superconducting state, where the density of the superconducting electrons $n_s \propto |\psi|^2$. For a given temperature, the order parameter ψ is a function of position in the material, i.e., it is not constant and vanishes above T_c. It is sometimes helpful to think of ψ as the wave function for a Cooper pair. Since all Cooper pairs are in the same two-electron state, a single wave function is sufficient.

Writing the wave function in terms the magnitude and a phase as

$$\psi = |\psi| \exp(I\varphi), \qquad\qquad\qquad \text{……………}(4.4.1)$$

then the current density ca be written as

$$\psi \quad \mathbf{J} = -(2e^2 \mathbf{A}/mc + eh\, \nabla\varphi/m)|\psi|^2 \quad \text{……………}(4.4.2)$$

where $\mathbf{A}$ is the vector potential.

Let us consider a superconducting material in the shape of a ring, we find in a closed path

$$\psi \quad \oint \mathbf{J}.dl = |\psi|^2 \oint (2e^2 \mathbf{A}/mc + eh\,\nabla\varphi/m).d\mathbf{l} = 0 \quad \text{……………}(4.4.3)$$

$$\psi \quad \oint J.dl = \iint \nabla X A.ds = \iint B.ds = \phi \qquad \text{……………}(4.4.4)$$

where ϕ is the flux enclosed by the ring. Since the order parameter is single valued, its phase change around the closed path must be zero or an integral multiple of 2π. Therefore,

$$\oint \nabla \phi . dl = 2\pi n \qquad \ldots\ldots\ldots\ldots (4.4.5)$$

where n is an integer.

Substituting eqn. (4.4.4) and (4.4.5) in eqn. (4.4.3) and solving for ϕ, we find that the magnetic flux enclosed in a ring must be quantized, i.e.

$$\phi = n \, h \, c \, / \, 2 \, e \; = n \, \phi_0$$

where $\phi_0 = h \, c \, / \, 2 \, e \; = \; 2.07 \text{ x } 10^{-7}$ gauss - cm^2 is known as flux quantum.

4.4.2 HIGH TEMPERATURE SUPERCONDUCTORS (HTS)

Extremely low critical temperatures of conventional superconductors (the low *Tc* type) put the most serious limitation on tQeir use in technological applications. Working with devices that have to be cooled to temperatures in the range of liquid helium temperature (4.2 K) is obviously not viable on any count. This has kept the scientists world over relentlessly trying to discover~uperconductivity near room temperat\lre. A decisive boost to this optimism came in 1986, when Bednorz and Muller synthesized metallic oxygen-deficient copper oxide compounds of La-Ba(Sr)-Cu~O system with the transition temperature of about 30 K. A vigorous activity towards the search for materials with higher critical temperatures ensued following this nobel prize winning announcement. It has resfilted in the development of a variety of materials with the highest critical tempe}ature *T* c in the vicinity of 135 K. The *Tc* values being so high compared to those of conventional superconductors, these materials are called *high temprtmture supe-reonduc-tors* or *high T* c *superconduct~(HTS).*

15.8.1 **Rare-Earth** Cup rates: **Structural Aspect**

Chu and Coworkers (1987) earned the distinction of raising *T* c to 90 K in ceramics of the Bal *-x* Y *x* CU03 *-y* system. With fastly improving methods of preparation of characterization, a ceramic alloy Y IBa2Cu3~ *-x* could be prepared even in single crystal form. In all respects including application

this has emerged as the most thoroughly studied and tested system, often referred to as YBCO. A ;

Isenes of this class of HTS has been produced with the Y atom being replaced by other rare-earth elements such as Eu and Gd. On the basis of their stoichiometry, these types of ceramics are

commonly called 123 systems. i

The crystal structure of the YBCO system is illustrated in Fig. 15.26(a). It can be represented by an orthorhombic primitive cell in the superconducting state. The structure is essentially an oxygen- defect modification of the perovskite structure with about one-third oxygen positions vacant. All members of this series are axial crystals with alternating CUO_2 planes [Cu(2), 0(2)] and oxygen atoms in both pyra.m-d-type and rectangular coordination along the c-axis. Oxygen chains are formed along the b-axis with the involvement of atoms in the rectangular planar structure. We will see a little later that the oxygen vacancies in this chain may be interpreted to be actively involved in the mechanism of superconductivity.

15.8.2 Bi-based and TI-based Cuprates: Structural Aspect

This class of HTS emerged within a year of the synthesis of 123 systems. These materials, typically represented by $Bi_2Sr_2Ca_2Cu_3O_{,o}$ and $Tl_2Ba_2Ca_2Cu_3O_{,o}$ systems, show still higher T c' The main classes

of ceramic superconductors with $T_c > 90$ K are compiled in Table 15.4. In accordance with their stoichiometry, Bi- and Tl-based HTS are named as 2212 and 2223 systems, respectively.

Similar to 123 systems, 2212 and 2223 systems too have a layered structure along the substantially larger c-axis. This layered structure is again considered to playa crucial role in the mechanism of superconductivity. The unit cell shown in Fig. 15.26(b) has two distinct regions, separated by two Bi-O (or Tl-O) planes. In the upper-half region, the copper atoms are located at centres while in the lower-half region they are at comers of the Cu-O planes. The T c value is strongly controlled by the number of CUO_2 layers in the unit cell. These ceramics differ from one another only in the number

of CUO_2 layers per unit cell.

15.8.3 Significant Properties of Cuprate HTS

Consider the example of YBCO which is the most thoroughly researched system. Its resistivity around 90 K falls most sharply to an immeasurable value for $x = 0$ -0.1, where x denotes oxygen deficiency. On increasing x, the transition temperature decreases. For $x > 0.7$, YBCO ceramics cease to be superconductors and behave as antiferromagnetic insulators. On account of their strongly anisotropic crystal structure, the ceramic superconductors show highly anisotropic electronic properties. There is a large difference in the resistivities of YBCO, measured along and perpendicular to the c-axis *(Pc* and *Pab* in Fig. 15.27). All the ceramic superconductors known to date show type II superconductivity for which *Bc* is usually less than 10 mT and the largest estimates of *Bc* are around 340 T.' 2

A few extraordinary features of these HTS that might provide clue to the mechanism of superconductivity are as under:

1. The resistivity in the normal state varies linearly with temperature.

2, A near zero oxygen isotope effect is observed *(a* -0-0.2). The vanishingly small isotope

: effect is considered an important evidence for non-phononic superconductivity in cuprates.

I

3i The observed energy gaps are large, nearly 20-30 meV, and *!!!:!!l* = 3 to 4, which is *kBTc* appreciably greater than the BCS estimate equalling 1.764.

4. The thermoelectric power shows a universal behaviour as a function of hole concentration.

5. The Hall coefficient is temperature dependent. ' 6, An inverted parabolic relation between *T* c and the hole concentration is observed.
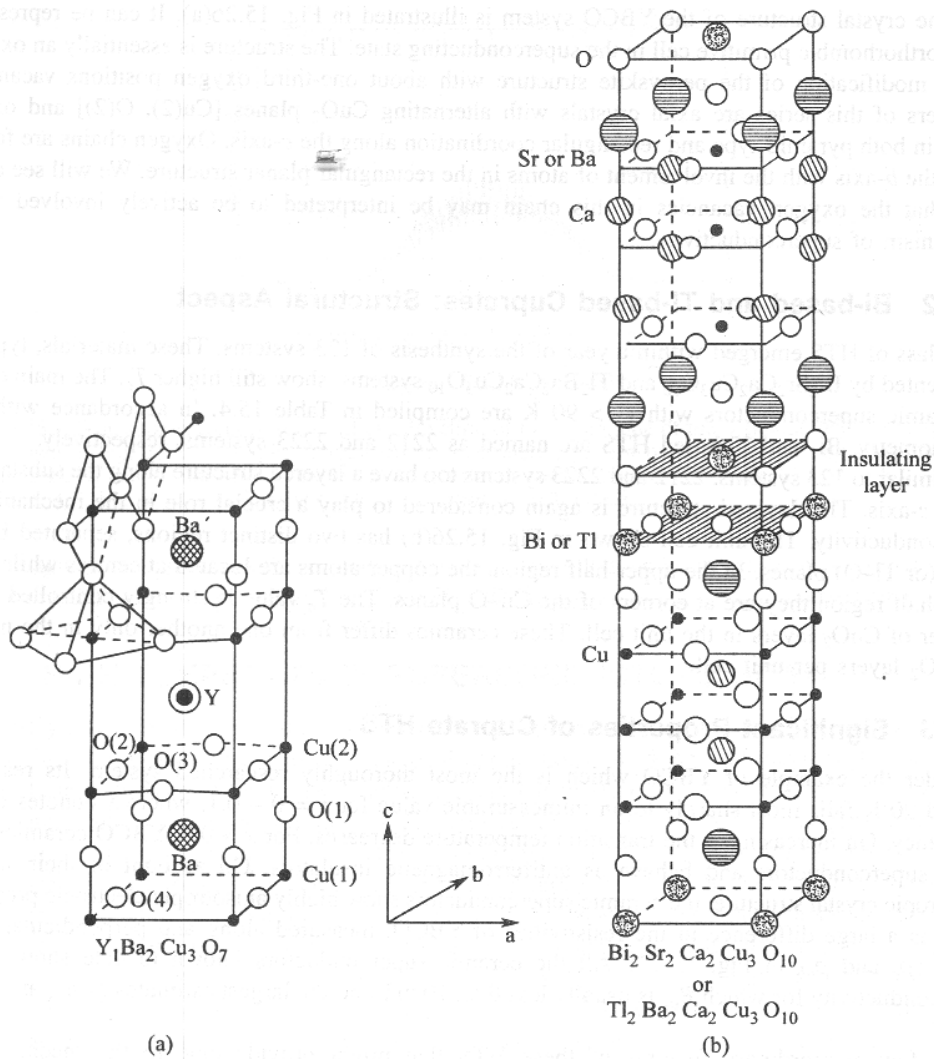
Fig. 15.26 (a) Unit cell structure of a Y .Ba2Cu307 crystal. The numbers in brackets represent the special sites jof oxygen and copper atoms in CUO2 layers. (b) Unit cell structure of Bi2Sr2Ca2Cu3010 or Tl2Ba2Ca2Cu3010 crystal.

~

From the data on Hall coefficient it is inferred that a Cooper pair in YBCO type and Bi- and 'n-based superconductors, is a pair of holes resulting in the *p-type* superconductivity in these materials. Because of their high electronegativity, oxygen atoms act as electron acceptors. For example, in YBCO, both Y and Ba ions contribute two electrons separately to the bonding in CUO2 layers where .

the oxygen atoms trap these electrons. For small x (i.e. for a less oxygen-deficient composition), there are enough oxygen atoms to swallow the electrons. This way more holes are made available in the CUO2 planes to get bound into hole Cooper pairs. These observations point to a quasi two-dimensional charge transport in CUO2 planes by means of holes 'bound in Cooper pairs. These ideas are also applicable to the Bi and Tl superconductors. Although most of the cuprates show *p-type*
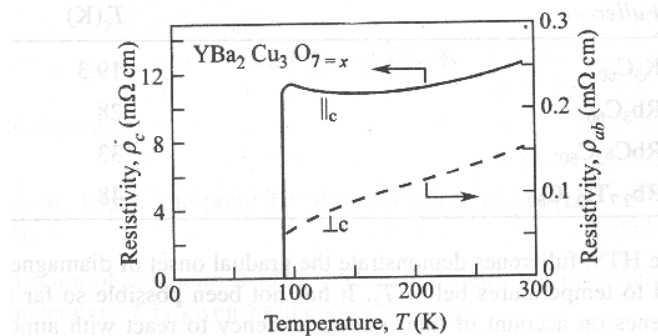

Fig. 15.27 Measured resistivity of YBCO along and perpendicular to the c-axis (Pa and Pab respectively) as a function of temperature. [After S.J. Hagen. T.W. Jing, Z.Z. Wang, J. Horvath, N.P. Ong, *Phys. Rev.,* B37,7928 (1988).]

superconductivity, there exist a couple of systems, namely NdzCuO4 and Ndz - xCexCuO4 in which the conventional n-type superconductivity has been confirmed.

15.8.4   Fulleranes

~

The novel superconductors added most recently (1991) to the list of HTS are fullerenes whose most prominent member is C6(). The transition temperatures of materials of this class range from 15 K to about 48 K. The structure of a single C6() molecule, as shown in Fig. 15.28, consists of 60 carbon atoms. It is a cluster of carbon atoms arranged in the shape of a truncated icosahedron with 20 hexagonal and 12 pentagonal faces (as in graphite, benzene and other organic molecules). The pentagons occur on account of the topological requirement for producing a closed structure that resembles a football.

4.4.3   Reference Books

1. Elementary Solid State Physics by M.A. Omar

2. Elements of Solid State Physics by J.P. Srivastava

3. Solid State Physics by Neil W. Ashcroft and N. David Mermin

4. Introduction to Solid State Physics by Charles Kittel
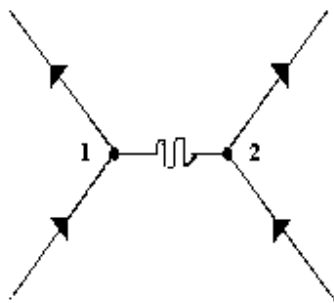
UNIT – IV

LESSON 2

ENERGY GAP AND RELATEED PROPERTIES OF SUPERCONDUCTORS

Objective of the lesson

To discuss thermodynamical properties of super conductors and the concept of energy gap

Structure of the lesson

4.2.1. Thermodynamic properties

4.2.2. Energy gap

4.2.3. Electodynamics of superconductors- London equations

4.2.1. Thermodynamic properties

The superconducting transitions are reversible in nature and hence we can apply thermodynamics for its study. By neglecting the volume changes and considering only the magnetic work term, the Gibbs free energy can be written as

$$G = U - TS - M. B_a \qquad \text{..........(4.2.1)}$$

A small change in applied field B_a at a constant temperature produces a small change in the free energy given by

$$dG = - M. dB_a \qquad \text{..........(4.2.2)}$$

where all extensive quantities are defined for a unit volume.

After substituting $M = - B_a / \mu_0$ and integrating (4.2.2), we get

$$\int_{T,0}^{T,B_a} dG = \int_0^{B_a} \left(\frac{B_a}{\mu_0} \right) . dB_a$$

or $\qquad G_s(B_a,T) = G_s(0,T) + \dfrac{B_a^2}{2\mu_0} \qquad \text{..........(4.2.3)}$

At the critical field B_c, where the normal and superconducting states are in equilibrium:

$$G_n(T) = G_s(B_c,T)$$

Here, we ignore any weak magnetism in the normal state and assume that the free energy G_n is independent of field. Then, from (4.2.3)

$$G_n(T) - G_s(0,T) = \frac{B_a^2}{2\mu_0} \qquad \qquad ....(4.2.4)$$

The above relation shows that in zero field the superconducting state is lower in free energy by $B_c^2/2\mu_0$ per unit volume. For a typical field of 0.1 -1.0 kG, this is 10^3 J m^{-3}. In the presence of weak fields below $T_{c'}$ the specimen has to choose between gaining in energy by forcing all the magnetic flux out (retaining superconductivity) and gaining in energy by letting the flux in (going to the normal state). The superconducting state is found to be energetically favoured for small fields, but not for large fields. The experimental behaviour of free energy as a function of temperature in the two states is shown in Fig. 4.2.1.. Making use of (4.2.3), we can estimate the critical field $B_c(T)$ from this graph.
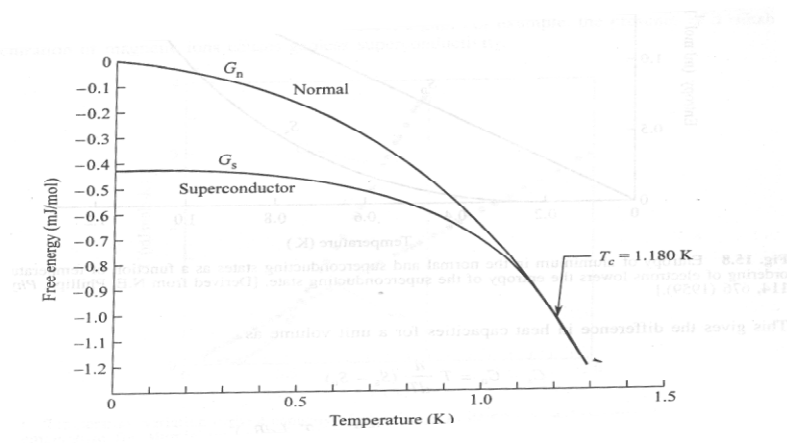

Fig. 4.2.1. Behaviour of Gibbs energy as a function of temperature in the superconducting and normal states of a superconducting material.

The difference of entropies is determined from (4.2.) with entropy S defined as $S = -\left(\partial G / \partial T\right)$:

$$\Rightarrow S_n\text{-}S_s = -\frac{B_c}{\mu_0}\frac{dB_c}{dT} \qquad\qquad \ldots\ldots\ldots(4.2.4)$$

Since the slope dB_c/dT of the critical field curve is negative, $S_n \geq S_{S,}$ revealing that the superconducting state is a 'more ordered state' than the normal state. Also, the slope dB_c/dT approaches zero at absolute zero, leading to the result $S_n \to S_s$ as $T \to 0$, which is consistent with the requirement of the third law of thermodynamics. Figure 4.2.2 presents a view of the variation of entropy in the two states.

If U_n and U_s denote the internal energy in the normal and superconducting states respectively, then

$$U_n\text{-}U_s = T(S_n\text{-}S_s) \qquad\qquad \ldots\ldots\ldots(4.2.5)$$
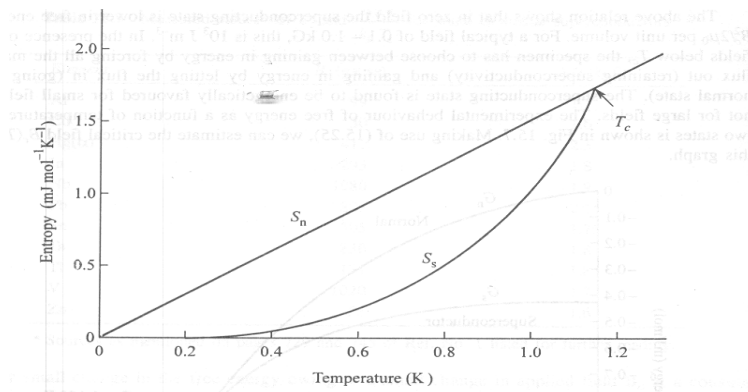

Fig.4.2.2. Entropy of a superconducting material in the normal and superconducting states as a function of temperature.

This gives the difference in heat capacities for a unit volume as

$$C_s - C_n = T\frac{d}{dT}(S_s - S_n)$$

$$= \frac{TB_c}{\mu_0} \cdot \frac{d^2 B_c}{dT^2} + \frac{T}{\mu_0} \left(\frac{dB_c}{dT} \right)^2 \qquad\qquad \text{……….(4.2.6)}$$

at T= T_c, B_c=0 , and then the above relation reduces to

$$C_s - C_n = \frac{T_c}{\mu_0} \left(\frac{dB_c}{dT} \right)^2_{T=T_c} \qquad\qquad \text{……….(4.2.7)}$$

This relation is known as the Rugers formula.

4.2.2. Energy gap

The energy gap in superconductors is entirely different nature from the energy gap in insulators. In an insulator the gap is related to the lattice and in the superconductor the gap tied to the Fermi gas. In superconductors the energy gap separates superconducting electron states lying below the normal electron states. This gap decreases continuously to zero as the temperature is increased to the critical temperature T_c. The energy gap in insulators on the other hand separates filled valence band and vacant conduction band and is almost independent of temperature.

The heat capacity below T_c gave evidence for forbidden energy gap between normal super conducting state.
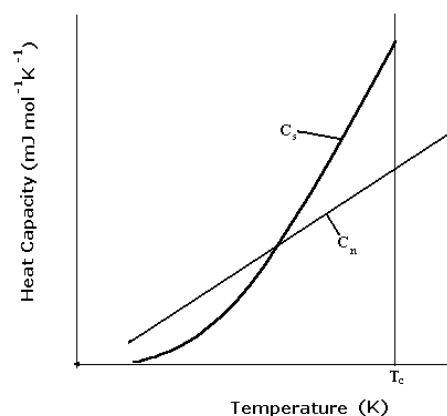

Fig. 4.2.3. The variation of specific heat with temperature for a superconductor.

Experiments at very low temperatures indicate that the specific heat of the electrons in that region decreases exponentially, i.e.

$$C_v = a \exp[-b(T/T_c)]. \qquad\qquad \ldots\ldots(4.2.8)$$

This exponential behaviour implies the presence of an energy gap in the energy spectrum of the electrons. This gap which lies just at Fermi level (Fig. 4.1.4) prevents the electrons from being readily excitable.   It also leads to a very small specific heat.   The
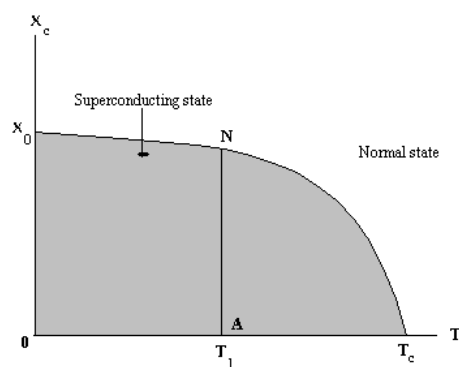

Fig. 4.2.4   The density of states versus E for a superconductor, illustrating the gap

(magnified) at the Fermi level

width of the gap Δ is of the order of kT_c, because when the substance is raised to T_c, it becomes normal and its electrons are then readily excited.   Thus

$$\Delta \approx k\, T_c. \qquad\qquad \ldots\ldots(4.2.9)$$

Substituting $T_c = 5$ K one finds that $\Delta \approx 10^{-4}$ eV. This energy gap is very small compared with the gaps compared with the gaps of insulators or semiconductors and it is for this reason that superconductivity appears only at very low temperatures.   The critical field H_c versus temperature curve is given in Fig 4.2.4 .   The curve divides the H_c and T plane into two regions: the normal and the superconducting.   Suppose the substance is at temperature $T_1 < T_c$.   When substance starts at point A and follows the vertical path AN, i.e., gradually increasing the filed, it becomes normal at the point N. Thus the condensation energy is

$$\Delta E = E_N - E_A \qquad\qquad ....(4.2.10)$$

Since the substance acts as a perfect diamagnet along the path AN, ΔE is equal to the demagnetization energy,

$$\Delta E = -\oint H_c \, B dM = -\mu_0 \int H(-dH) = 1/2\mu_0 H_c^2 \qquad ....(4.2.11)$$

per unit volume. This is the amount of energy needed to convert a system from the superconducting into the normal state or it is the amount lost by the system when it makes the transition from normal to the superconducting state. The maximum amount of condensation energy is

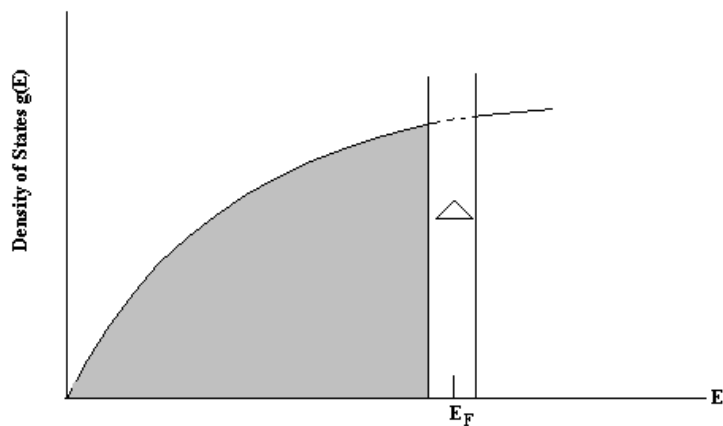$$\Delta E = \tfrac{1}{2}\ \mu_0\ H_c^{\,2}(0), \qquad\qquad ....(4.2.12)$$

Fig. 4.2.5   Calculation of the superconducting condensation energy

which occurs at $T = 0$ K. Let us obtain a useful relation between the critical filed and the critical temperature.   The only fraction of the electrons, those lying within a shell kT_c of the Fermi surface, is affected by the superconducting transition.   This is because those electrons lying deep inside the Fermi sphere require much greater energy for excitation.   Thus the concentration of effective electrons is

$$n_{eff} \approx n\ (kT_c/E_F), \qquad\qquad ....(4.2.13)$$

where n is the total concentration of conduction electrons. Each of the effective electrons acquires an additional energy of about kT_c in order to be excited across the gap. Therefore

$$\Delta E \approx n_{eff}\, kT_c = n[\,(kT_c)^2/E_F\,], \qquad\qquad \text{.........(4.2.14)}$$

which is the same as the energy calculated in eqn (4.2.8). Equating these energies, one finds that

$$H_c(0) \approx (2nk^2/\mu_0 E_F)^{1/2}\, T_c \qquad\qquad \text{.........(4.2.15)}$$

That is, the critical field is proportional to the critical temperature. Thus the higher the transition temperature, the greater the field required to destroy superconductivity. The eqn (4.2.15) can be used to estimate $H_c(0)$ if T_c is given or vice versa.

4.2.3. Electodynamics of superconductors- London equations

The Meissner effect did not account for the flux penetration observed in thin films. To explain this phenomenon F. London and H. London, in 1935, modified the conventional equations of electrodynamics.

The equation of motion for a superelectron in the presence of an electric field is

$$m\frac{dv_s}{dt} = -\,e\,E \qquad\qquad \text{.........(4.2.16)}$$

The density of the supercurrent $\mathbf{J}_s$ is given by

$$\mathbf{J}_s = -\,e\,n_s\,\mathbf{v}_s \qquad\qquad \text{.........(4.2.17)}$$

Taking the time differential both sides we get

$$\frac{dJ_s}{dt} = -en_s\frac{dv_s}{dt} \qquad\qquad \text{.........(4.2.18)}$$

from eqns (4.2.16) and (4.2.18), we can write

$$\frac{dJ_s}{dt} = (n_s e^2/m)E \qquad\qquad \text{.........(4.2.19)}$$

In the steady state, the current in a superconductor is constant, i.e.,

$$\frac{dJ_s}{dt} = 0 \qquad \qquad \text{……….(4.2.20)}$$

It means in the steady state the electric field inside a superconductor vanishes or the voltage drop across a superconductor is zero.

Combining eqn. (4.2.20) with the Maxwell equation,

$$\frac{\partial B}{\partial t} = -\nabla \times E , \qquad \qquad \text{……….(4.2.21)}$$

gives, $\dfrac{\partial B}{\partial t} = 0.$

This states that the magnetic field is constant regardless of the temperature. But we know that the flux suddenly penetrates when temperature is increased toward T_c .   So the above formalism requires some modification.   For this, let us substitute for E from eqn. (4.2.19)   into eqn. (4.2.21), which yields

$$\frac{\partial B}{\partial t} = -(\frac{m}{n_s e^2}) \nabla \text{ x } \frac{dJ_s}{dt} \qquad \qquad \text{……….(4.2.22)}$$

Since this equation is invalid, because it predicts that $\dfrac{\partial B}{\partial t} = 0$, London postulated the relation as

$$\mathbf{B} = -\left(\frac{m}{n_s e^2}\right) \nabla \text{ x } \mathbf{J}_s \qquad \qquad \text{……….(4.2.23)}$$

and is called as the London equation.   This equation is in agreement with the experimental results. We can express it in another way by using the Maxwell equation,

$$\nabla \text{ x } \mathbf{B} = \mu_0 \mathbf{J}_s$$

and taking the curl on both sides, we get

$$\nabla \text{ x } \nabla \text{x } \mathbf{B} = \nabla(\nabla . \mathbf{B}) - \nabla^2 \mathbf{B} = \text{ - } \nabla^2 \mathbf{B} = \mu_0 \nabla \text{ x } \mathbf{J}_s \qquad \qquad \text{……….(4.2.24)}$$

substituting for $\nabla \times \mathbf{J}_s$ from eqn (4.2.23), we obtain

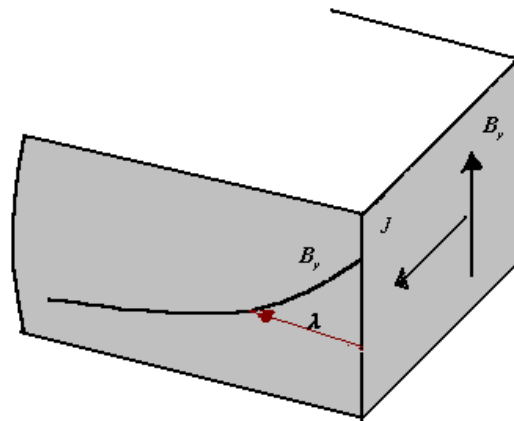$$\nabla^2 \mathbf{B} = (\mu_0 \ n_s \ e^2/m) \ \mathbf{B}. \qquad \qquad ……….(4.2.25)$$

Fig. 4.2.6.

Let us apply it to a simple geometry (see Fig. 4.2.6). The specimen surface is lying in the yz-plane and the filed is applied in the y-direction. For this geometry, the eqn . (4.2.25) reduces to

$$\frac{\partial^2 B_y}{\partial x^2} = (\mu_0 \ n_s \ e^2/m) \ B_y \qquad \qquad ……….(4.2.26)$$

The solution of this equation is

$$B_y(x) = B_y(0) \ e^{-x/\lambda_L} \qquad \qquad ……….(4.2.27)$$

$$\text{where} \qquad \lambda = (\mu_0 \ n_s \ e^2/m)^{1/2} \qquad \qquad ……….(4.2.28)$$

Eqn (4.2.28) shows that the field decreases exponentially as one goes from the surface into the superconductor. Thus the magnetic field vanishes inside the bulk specimen, this is in agreement with the Meissner effect. The parameter λ known as the London penetration

depth, which represents the distance of the field penetration into the specimen.   This has been verified experimentally.

4.2.4   Summary of the lesson

The variation of entropy with the temperature of superconductor and its comparison with the normal conductors is discussed. The origin of the energy gap and its related properties of the superconductor are explained in detail. The equation for the London penetration depth is derived.

4.2.5   Key Terminology

Entropy– specific heat – Gibbs free energy – energy gap.

4.2.6   Self – Assessment questions

1. Obtain the expression for Gibbs free energy of a super conductor .
2. Discuss variation of specific heat with temperature and the prediction of the energy gap of a superconductor
3. Derive the London equation and explain the term London penetration depth.

4.2.7   Reference Books

1. Elementary Solid State Physics by M.A. Omar
2. Elements of Solid State Physics by J.P. Srivastava
3. Solid State Physics by Neil W. Ashcroft and N. David Mermin
4. Introduction to Solid State Physics by Charles Kittel

UNIT – IV

LESSON 3

Josephson effect and its consequences

Objective of the lesson

To discuss concept of Josephson effect,

Structure of the lesson

4.3.1.Tunneling and Josephson effect

4.3.2 Supercurrent quantum interference

4.3.1.Tunneling and Josephson effect

When a thin insulating layer (about 30 A^0) is sandwiched between two metals (Example, Al-Al_2O_3-Pb) , it acts as potential barrier as far as the flow of conduction electrons is concerned. Quantum mechanically electrons can tunnel across a thin potential barrier and in thermal equilibrium they continue to do so until the potential of electrons in both the metals become equal. When both the metals are normal conductors (Fig.4.3.1 a) and if a potential difference is applied across them, the potential of one them increases with respect to other. As a result electrons tunnel through the insulating layer. The current-voltage relation across tunneling junction is observed to obey Ohm's law at low voltages(Fig.4.3.1 b). However, when one of the metals is a superconductor (Fig.4.3.1 c), no current is observed to flow across the junction until the potential reaches a threshold value, $eV = \Delta/2$ (half of the energy gap). It is because the energy states lying horizontally below E_F in the normal metal are already occupied. Further, since the Fermi level F_F is the same
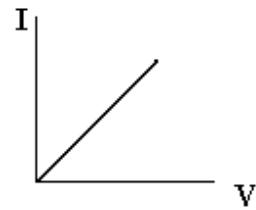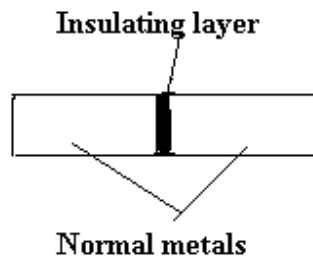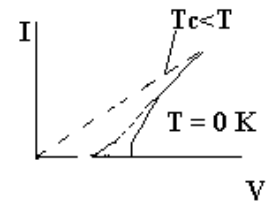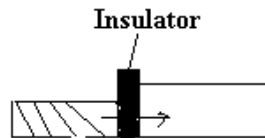
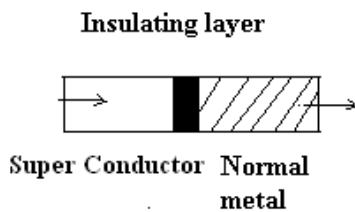Fig.4.3.1 a   Fig.4.3.1. b

Fig.4.3.1 c   Fig.4.3.1 d   Fig.4.3.1 e

throughout the system and lie in the middle of the energy gap of the superconductor, the knowledge of the threshold voltage helps in determining the energy gap of the superconductor. As the temperature is increased towards T_c , the threshold voltage decreases.   The current-voltage relations across the tunnelling junctions at different temperatures are shown in Fig.4.3.1e. This tunnelling is called single electron tunnelling (or normal tunnelling) , where electrons tunnel in singles through the insulated layer. When both the materials are superconductors (Fig.4.3.1 d), Josephson predicted that in addition to single electron tunnelling , Cooper pairs not only can tunnel through the insulating layer from one superconductor to another without dissociation, even at zero potential difference across the junction, but also their wave functions on both sides would be highly correlated. This is known as Josephson effect. The introduction of the insulating layer between two superconductors develops a phase difference.   Josephson showed that the tunnelling current is given by

$$I = I_0 \, Sin \, \varphi_0 \qquad\qquad\qquad\qquad ……….(4.3.1)$$

Where I_0 is the maximum current that the junction can carry without a potential difference across it and depends on the temperature. With no applied voltage, a dc current will flow across the junction. This is called **dc Josephson effect.** A dc magnetic field applied through a superconducting circuit containing two junctions causes the maximum supercurrent to show interference effects as a function of magnetic field intensity. This effect can be utilized in sensitive magnetometers.

Ac Josephson effect : A dc voltage applied across the junction causes rf current oscillations across the junction. This effect has been utilized in a precision determination of the value of $\hbar/e$. Further, an rf voltage applied with the dc voltage can then cause a dc current across the junction.

The detailed theory concerning this tunnelling phenomenon is discussed below.

a) **Dc Josephson effect.**

Our discussion of Josephson junction phenomena follows the discussion of flux quantization. Let ψ_1 be the probability amplitude of electron pairs on one side of a junction, and let ψ_2 be the amplitude on the other side. Let both superconductors be identical and we assume that they are both at zero potential. The time-dependent Schrodinger equation $i\hbar\,\partial\psi/\partial t = H\psi$ applied to the two amplitudes gives

$$i\hbar\frac{\partial\psi_1}{\partial t} = \hbar T\psi_2 \qquad\qquad i\hbar\frac{\partial\psi_2}{\partial t} = \hbar T\psi_1 \qquad\qquad \ldots\ldots\ldots.(4.3.2)$$

Here $\hbar T$ represents the effect of the electron-pair coupling or transfer interaction across the insulator; T has the dimensions of a rate or frequency. It is a measure of leakage of ψ_1 into the region 2 and of ψ_2 into the region 1. If the insulator is very thick, T is zero and there is no pair tunnelling.

Let $\psi_1 = n_1^{1/2}\,e^{i\theta_1}$ and $\psi_2 = n_2^{1/2}\,e^{i\theta_2}$ $\qquad\qquad \ldots\ldots\ldots.(4.3.3)$

$$\frac{\partial\psi_1}{\partial t} = \tfrac{1}{2}n_1^{-1/2}\,e^{i\theta_1}\frac{\partial n_1}{\partial t} + i\psi_1\frac{\partial\theta_1}{\partial t} = -iT\psi_2 \qquad\qquad \ldots\ldots\ldots.(4.3.4)$$

$$\frac{\partial \psi_2}{\partial t} = \tfrac{1}{2} n_2^{-1/2} \, e^{i\theta_2} \frac{\partial n_2}{\partial t} + i\psi_2 \frac{\partial \theta_2}{\partial t} = -iT\psi_1 \qquad \ldots\ldots(4.3.5)$$

Multiplying equn. (4.3.4) by $n_1^{1/2} \, e^{-i\theta_1}$ and equn.(4.3.5) by $n_2^{1/2} \, e^{-i\theta_2}$, we obtain,

$$\frac{1}{2}\frac{\partial n_1}{\partial t} + in_1 \frac{\partial \theta_1}{\partial t} = -iT(n_1 n_2)^{\frac{1}{2}} e^{i\delta} \qquad \ldots\ldots(4.3.6)$$

$$\frac{1}{2}\frac{\partial n_2}{\partial t} + in_2 \frac{\partial \theta_2}{\partial t} = -iT(n_1 n_2)^{\frac{1}{2}} e^{-i\delta} \qquad \ldots\ldots(4.3.7)$$

where $\delta \equiv \theta_2 - \theta_1$

Equating the real and imaginary parts of (4.3.6) and (4.3. 7), we get

$$\frac{\partial n_1}{\partial t} = 2T(n_1 n_2)^{\frac{1}{2}} \sin\delta \; ; \qquad \frac{\partial n_2}{\partial t} = -2T(n_1 n_2)^{\frac{1}{2}} \sin\delta \qquad \ldots\ldots(4.3.8)$$

$$\frac{\partial \theta_1}{\partial t} = -T\left(\frac{n_2}{n_1}\right)^{\frac{1}{2}} \cos\delta \; ; \qquad \frac{\partial \theta_2}{\partial t} = -T\left(\frac{n_1}{n_2}\right)^{\frac{1}{2}} \cos\delta \qquad \ldots\ldots(4.3.9)$$

If $n_1 \cong n_2$ as for identical superconductors 1 and 2, we have from (4.3. 9) that

$$\frac{\partial \theta_1}{\partial t} = \frac{\partial \theta_2}{\partial t} \quad \Rightarrow \quad \frac{\partial}{\partial t}(\theta_2 - \theta_1) = 0 \qquad \ldots\ldots(4.3.10)$$

From (4.3. 8) we see that

$$\frac{\partial n_2}{\partial t} = -\frac{\partial n_1}{\partial t} \qquad \ldots\ldots(4.3.11)$$

The current flow from region 1 to region 2 is proportional to $\partial n_2 / \partial t$ or, the same thing, $-\partial n_1 / \partial t$. We therefore conclude from (4.3.11) that the current J of superconductor pairs across the junction depends on the phase difference δ as

$$J = J_0 \sin \delta = J_0 \sin(\theta_2 - \theta_1) \qquad \text{.........(4.3.12)}$$

where J_0 is proportional to the transfer interaction T. The current J_0 is the maximum zero-voltage current that can be passed by the junction. With no applied voltage a dc current will flow across the junction (Fig. 4.3.2), with a value between J_0 and $-J_0$ according to the value of the phase difference $\theta_2-\theta_1$. This is the dc Josephson effect.
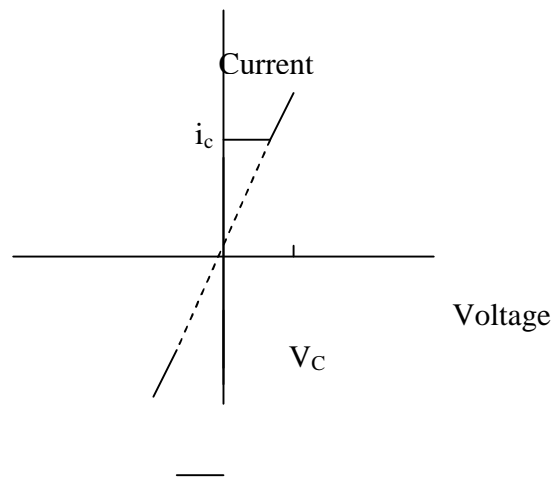

Fig.4.3.3. Current voltage characteristics of Josephson junction

Ac Josephson effect

Let a dc voltage V be applied across the junction. We can do this because the junction is an insulator. An electron pair experiences a potential energy difference qV on passing across the junction, where q=-2e. We can say that a pair on one side is at potential energy –eV and a pair on the other side is at eV. The equations of motion are

$$i\hbar \, \partial \psi_1 / \partial t = \hbar T \psi_2 - eV \psi_1 ; \quad i\hbar \, \partial \psi_2 / \partial t = \hbar T \psi_1 + eV \psi_2 \quad \text{.........(4.3.12)}$$

Adopting the similar procedure as in the case of dc Josephson effect , we get

$$\frac{1}{2}\frac{\partial n_1}{\partial t} + i n_1 \frac{\partial \theta_1}{\partial t} = ieVn_1\hbar^{-1} - iT(n_1 n_2)^{\frac{1}{2}} e^{i\delta} \quad \ldots\ldots\ldots(4.3.13)$$

the real part of the equation (4.3.13) gives

$$\frac{\partial n_1}{\partial t} = 2T(n_1 n_2)^{\frac{1}{2}} \sin\delta \qquad\qquad \ldots\ldots\ldots(4.3.14)$$

and the imaginary part gives,

$$\frac{\partial \theta_1}{\partial t} = (eV/\hbar) - T(n_2/n_1)^{\frac{1}{2}} \cos\delta \qquad\qquad \ldots\ldots\ldots(4.3.15)$$

which differs from (4.3.8   ) by the term $eV/\hbar$

Further, by a extension of (4.3.7), we have

$$\frac{1}{2}\frac{\partial n_2}{\partial t} + i n_2 \frac{\partial \theta_2}{\partial t} = ieVn_2\hbar^{-1} - iT(n_1 n_2)^{\frac{1}{2}} e^{-i\delta} \quad \ldots\ldots\ldots(4.3.16)$$

whence

$$\partial n_2/\partial t = -2T(n_1 n_2)^{\frac{1}{2}} \sin\delta \qquad\qquad \ldots\ldots\ldots(4.3.17)$$

$$\frac{\partial \theta_2}{\partial t} = -(eV/\hbar) - T(n_1/n_2)^{\frac{1}{2}} \cos\delta \quad \ldots\ldots\ldots(4.3.18)$$

From (4.3.17) and (4.3.18) with $n_1 \cong n_2,$ we have

$$\frac{\partial}{\partial t}(\theta_2 - \theta_1) = \frac{\partial \delta}{\partial t} = -2eV/\hbar \;\ldots\ldots\ldots(4.3.19)$$

By integrating eqn.(4.3.19) that with a dc voltage across the junction the relative phase of the probability amplitudes vary as

$$\delta(t) = \delta(0) - (2eVt/\hbar) \qquad \ldots\ldots\ldots(4.3.20)$$

The current is now given by

$$J = J_0 \sin[\delta(0) - 2eVt/\hbar] \qquad \ldots\ldots\ldots(4.3.21)$$

The current oscillates with frequency

$$\omega = 2eV/\hbar \qquad \ldots\ldots\ldots(4.3.22)$$

This is the ac Josephson effect. A dc voltage of 1 micro voltage produced a frequency of 483.6 MHz. Further the equ.4.3.11 says that a photon of energy 2 eV is emitted or observed when an electron crosses the barrier by measuring V and ω , we can obtain the precise values of e/$\hbar$.

The physical explanation of this tunnelling can be explained as follows. For the two superconductors having different gaps, the Fermi level is in the middle of the gap. The energy level diagram at thermal equilibrium is aw shown in Fig. 4.3.4 a. . There are some electrons above the gap and holes below the gap in superconductor I . Such charge carriers can hardly be found in superconductor II, because of its large energy gap.
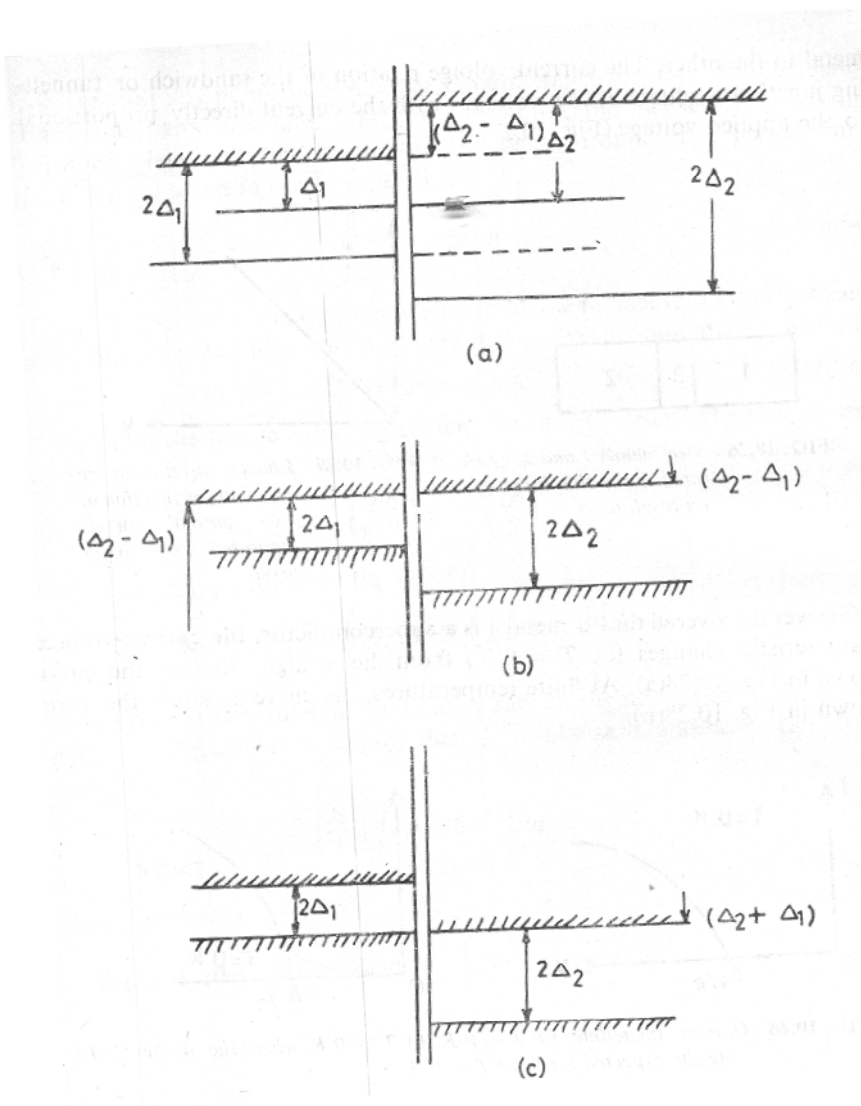
Figure 4.3.4. Energy diagram for two different superconductors separated by a thin
insulator (a) V=0,   (b) V = $(\Delta_2 - \Delta_1)/e$ (c) V=$(\Delta_1 + \Delta_2)/e$

When a voltage is applied, a current will flow and will increase with voltage(Fig.4.3.5) .Since more and more number of thermally excited electrons in superconductor I can tunnel through the insulator into the available states of superconductor II . When the applied voltage reaches $\Delta_2 - \Delta_1$ (Fig.4.3.4b) . It is energetically possible for all thermally excited electrons to tunnel across. It the voltage is increased further the current decreases, because the number of electrons capable of tunnelling is unchanged. But they now face a
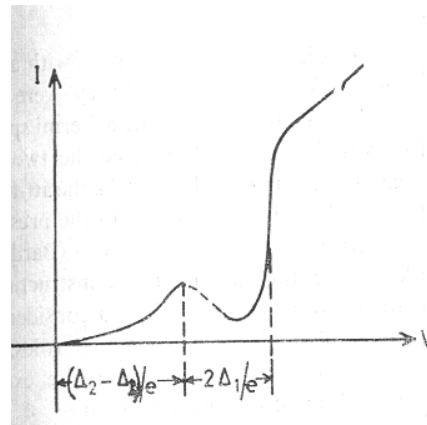
Figure 4.3.5 Current-voltage characteristics of a Josephson junction. There is a negative

resistance $(\Delta_2 - \Delta_1)/e < V < (\Delta_1 + \Delta_2)/e$

lower density of states. When the voltage becomes greater than $\Delta_2 + \Delta_1$, the current increases rapidly because the electrons below the gap begins to flow(Fig.4.3.4c). Basing on these explanations dc Josephson effect can now be defined as the phenomenon in which the junction permits the flow of current without any net loss of energy, even if the potential difference across it is zero, which is a familiar one in quantum mechanics. But the new thing is that as explained above, if we apply a dc voltage V across the junction the result is an alternating current-the constant voltage generates an oscillating current with a frequency $\omega = 2eV/\hbar$ as explained above. This is the ac Josephson effeect

4.3.2 Supercurrent quantum interference

The Josephson tunneling in the presence of a magnetic field provides strong evidence for the highly coherent nature of the superconducting state. Two Josephson junctions arranged in a parallel combination are placed in a region which a magnetic field B is impressed as shown in Fig. 4.3.6. A supercurrent starting in region I if divided into two parts

and made to flow along parallel paths, each of which contains a tunnel junction. The currents I_a and I_b crossing the tunnel barriers 'a' and 'b', respectively, reunite in region II. The combined current shows oscillations characteristic of an interference pattern produced by two coherent sources. By analogy with the interference of light, I_a and I_b are regarded as two coherent sources of current whose disturbances, when superposed by the way of recombination, produce an interference pattern.
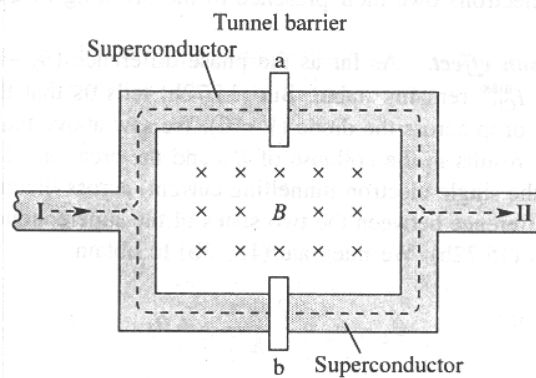

Fig. 4.3.6. Experimental geometry for producing supercurrent quantum interference.

As seen in the ac Josephson effect the tunnelling of Cooper pairs causes a phase shift of the total wavefunction of the superconducting state in region II relative to that in region I. The phase difference $\theta_2 - \theta_1$ around a closed curve which encompasses the total magnetic flux is given by

$$\theta_2 - \theta_1 = \frac{2e}{\hbar} \phi = \frac{2e}{\hbar} \int B.dS \qquad \ldots\ldots\ldots \qquad (4.3.28)$$

Let the phase difference between points I & II taken on a path through junction a be δ_a When taken on a path through junction b, the phase difference is δ_b. in the absence of magnetic field these two phases must be equal. Now let the flux ϕ pass through the interior of the circuit than from the eqn. (4.3.28), we have and The above relation states that the total phase difference around the loop can be controlled by varying the magnetic field. The general expressions for δ_a and δ_b in (4.3.24) may, however, be put as

$$\delta_a = \delta_0 - \left(\frac{2e}{\hbar c}\right)\phi \qquad \ldots\ldots\ldots(4.3.29a)$$

$$\delta_b = \delta_0 + \left(\frac{2e}{\hbar c}\right)\phi \qquad\qquad \text{………(4.3.29b)}$$

the total current is some of J_a and J_b. The current through each junction is

$$\text{`}J_{Total} = J_0 \left[\sin\left(\delta_0 + \left(\frac{e}{\hbar c}\right)\phi + \sin\left(\delta_0 - \left(\frac{e}{\hbar c}\right)\phi\right.\right] = 2 J_0 \sin \delta_0 \cos\left(\frac{e}{\hbar c}\phi\right) \quad \text{….(4.3.30)}$$

The cosine interference term characterizes the total current. This phenomenon is called the **supercurrent quantum** interference. Its maxima are determined by the condition,

$$\frac{e}{\hbar c}\phi = s\,\phi, \quad \text{….(4.3.31)}$$

where s is equal to integer

This condition states that for every addition of a flux quantum to the enclosed flux, a new maximum appears. The total supercurrent is plotted as a function of magnetic field in Fig. 4.3.6 to demonstrate the quantum interference where each oscillation corresponds to a change of flux quantum. Based on this principle, extremely sensitive magnetometers have been developed. Even extremely weak magnetic fields such as those produced by currents in human brain can be measured with these magnetometers. This magnetometer is called a SQUID (Superconducting Quantum Interference Device).
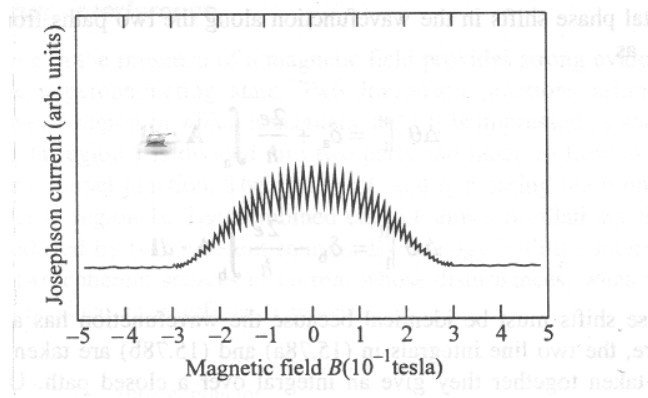

Fig. 4.3.6 Total supercurrent in region II as a function of magnetic field

4.3.3   Summary of the lesson

The phenomena of D.C and A.C Josephson effects have been discussed in detail. The concept of quantum interference as a consequence of Josephson Effect has also been described.

4.3.4   Key Terminology

Josephson junction- D.C and A.C Josephson effects –supercurrent quantum interference

4.3.5   Self – Assessment questions

1. What is Josephson effect? Discuss in detail D.C and A.C Josephson effects.
2. Write a note on supercurrent quantum interference.

4.3.6   Reference Books :

1. Elementary Solid State Physics by M.A. Omar
2. Elements of Solid State Physics by J.P. Srivastava
3. Solid State Physics by Neil W. Ashcroft and N. David Mermin
4. Introduction to Solid State Physics by Charles Kittel.